SIMULATION OF HYDRODYNAMICS AND SOLUTE TRANSPORT IN THE NEUSE RIVER ESTUARY, NORTH CAROLINA

By Jeanne C. Robbins and Jerad D. Bales

U.S. GEOLOGICAL SURVEY

Open-File Report 94-511

Albemarle-Pamlico Estuarine Study Report No. 94-11

Prepared in cooperation with the

ALBEMARLE-PAMLICO ESTUARINE STUDY and the

DIVISION OF ENVIRONMENTAL MANAGEMENT of the

NORTH CAROLINA DEPARTMENT OF ENVIRONMENT, HEALTH, AND NATURAL RESOURCES

Raleigh, North Carolina

1995

U.S. DEPARTMENT OF THE INTERIOR
BRUCE BABBITT, Secretary

U.S. GEOLOGICAL SURVEY
Gordon P. Eaton, Director

Any use of trade, product, or firm names is for descriptive purposes only and does not imply endorsement by the U.S. Geological Survey or the State of North Carolina.

For additional information write to:

District Chief
U.S. Geological Survey
3916 Sunset Ridge Road
Raleigh, North Carolina 27607

Copies of this report may be purchased from:

U.S. Geological Survey
Earth Science Information Center
Open-File Reports Section
Denver Federal Center, Box 25286, MS 517
Denver, Colorado 80225

CONVERSION FACTORS, TEMPERATURE, VERTICAL DATUM, AND ABBREVIATIONS

Multiply	By	To obtain
	Length	
centimeter (cm)	0.3937	inch
meter (m)	3.281	foot
kilometer (km)	0.6214	mile
	Area	
square meter (m^2)	10.76	square foot
square kilometer (km^2)	0.3861	square mile
	Volume	
cubic meter (m^3)	35.31	cubic foot
	Mass	
gram (g)	0.03527	ounce avoirdupois
kilogram (kg)	2.205	pound avoirdupois

Temperature: In this report, temperature is given in degrees Celsius (°C), which can be converted to degrees Fahrenheit (°F) by the following equation:

$$°F = 1.8\,(°C) + 32$$

Sea level: In this report, "sea level" refers to the National Geodetic Vertical Datum of 1929 (NGVD of 1929)—a geodetic datum derived from a general adjustment of the first-order level nets of both the United States and Canada, formerly called Sea Level Datum of 1929.

Abbreviations and acronyms used in this report in addition to those shown above:

cm/s	centimeter per second
m/s	meter per second
m^2/s	square meter per second
m^3/s	cubic meter per second
ppt	parts per thousand
ppt/km	parts per thousand per kilometer

CONTENTS

ILLUSTRATIONS

ILLUSTRATIONS (Continued)

ILLUSTRATIONS (Continued)

TABLES

SIMULATION OF HYDRODYNAMICS AND SOLUTE TRANSPORT IN THE NEUSE RIVER ESTUARY, NORTH CAROLINA

By Jeanne C. Robbins *and* Jerad D. Bales

ABSTRACT

An investigation was conducted to characterize flow, circulation, and solute transport in the Neuse River estuary. The study included a detailed field-measurement program and calibration, validation, and application of a physically realistic numerical model of hydrodynamics and transport to a 40-kilometer reach of the estuary.

Water level, salinity, water temperature, wind speed and direction, current velocity, and bathymetric data were collected during the study period March 1988 through September 1992. Additional data from pre-existing continuous-record streamflow gaging stations and meteorological stations also were used in the study. During the study period, the mean daily water-level range was 0.292 meter at the upstream end of the study reach and 0.186 meter at the downstream end. Mean near-surface salinities ranged from 0.9 part per thousand near New Bern, North Carolina, at the upstream end of the study reach, to 11.4 parts per thousand at the downstream end of the study reach, and mean near-bottom salinities ranged from 4.9 parts per thousand near New Bern to 12.9 parts per thousand at the downstream end of the study reach. Daily variations in salinity were generally less than 3 parts per thousand. Wind speeds usually were greatest during the winter months, when winds were from the west, northwest, and north. Current meters deployed for an 18-day period recorded velocities ranging from a maximum downstream velocity of 48 centimeters per second to a maximum upstream velocity of 52 centimeters per second, with a marked difference in velocity direction and magnitude across the estuary.

A two-dimensional, vertically averaged hydrodynamic and solute-transport model was applied to the study reach. The model domain was discretized into 5,801 computational cells, 200 x 200 meters each, bounded by the estuary shoreline. Model calibration was achieved through adjustment of model parameters for June 1-24, 1991. The calibrated model used a resistance coefficient of 0.028; wind-stress coefficient of 0.001; unadjusted, horizontal, momentum-mixing coefficient of 10 square meters per second; isotropic mass-dispersion coefficient of 20 square meters per second; and coefficient relating mass dispersion to flow properties of 14 square meters per second.

Additional simulations for October 24-November 3, 1989, when recording current meters were in place, and for September 1-30, 1991, were used to validate the model. The model was calibrated and validated for water levels ranging from -0.104 to 0.908 meter, for salinities ranging from 2.8 to 22.0 parts per thousand, and for wind speeds from calm to 9 meters per second. The model was tested for stratified and unstratified conditions. The mean difference between simulated and observed water levels was less than 3 centimeters. The mean difference between simulated and observed salinities at the interior checkpoint was less than 1 part per thousand.

Simulated results were sensitive to the downstream water level and the value of the wind-stress coefficient, but were relatively insensitive to changes in other model parameters. Model boundary forcing conditions were varied to characterize the effects on simulated model results. The presence of baroclinic forcing, varied wind speeds, and gage height played key roles in simulated mean transports.

Simulated flow for the model calibration period ranged from 960 cubic meters per second in the upstream direction to 1,260 cubic meters per second in the downstream direction at the upper end of the study reach, and from 6,360 cubic meters per second in the

upstream direction to 6,180 cubic meters per second in the downstream direction at the lower end of the study reach.

Vector plots displayed strong recirculation eddies and lateral differences in velocity, including concurrent upstream and downstream flow. Particle tracks showed that under some hydrologic conditions, particles released at several locations might not exit the estuary during a 30-day simulation period. A simulated conservative solute released at mid-estuary was present across the estuary within 3 days of continuous release and was present at 500 times dilution throughout an 18-kilometer reach after 17 days.

Comparisons of simulated results for a period in June 1991 were made between the Neuse and Pamlico models to characterize differences between the two systems. Greater observed water-level ranges in the Neuse River estuary were reflected in the flow and circulation patterns. Range in simulated transport was greater in the Neuse River estuary than in the Pamlico River estuary, and simulated currents generally were much greater throughout most of the Neuse River for similar points in the tide cycle. Particle tracks also indicated greater overall movement in the Neuse River than in the Pamlico River.

INTRODUCTION

The physical, chemical, and biological characteristics of the Neuse River estuary, which extends from about 12 kilometers (km) upstream from New Bern to Pamlico Sound, exhibit extreme spatial and temporal variability. The hydrodynamic processes in the estuary are key components of this complex aquatic ecosystem. Water movements at different scales and of different types govern the distribution of salt, dissolved gases, nutrients, and sediment, as well as the aggregation and distribution of microorganisms and plankton. The proper description of flow and circulation is critical to the understanding and management of water quality, productivity, and distribution and abundance of biota in this and in other estuaries.

Because of the complexities of estuaries, field measurements and numerical models are needed to better understand and describe circulation processes. Field observations provide necessary information for characterizing and understanding local physical and biochemical processes and for detecting trends. However, the expense of field measurements and the extreme heterogeneity of the estuarine environment limit the extent to which measurements can be extrapolated over space and time. Moreover, the generalization of field measurements must be qualified by the specific conditions under which the data are collected (Signell and Butman, 1992).

Numerical models make it possible to describe physical and biochemical processes with high spatial resolution throughout the entire estuary. Numerical models also can be used to conduct experiments by evaluating estuarine response to a wide range of imposed tidal, inflow, meteorological, and chemical loading conditions. The design of field-measurement programs can sometimes be improved by the application of a numerical model to identify important locations or processes that should be measured. However, the accuracy of numerical model simulation results are limited by (1) the manner in which physical processes are represented by the model, (2) the assumptions and simplifications included in the model, (3) the numerical scheme used to solve the governing equations, and (4) the availability of reliable field observations. Scientifically credible and effective modeling requires carefully collected field measurements for use in model calibration, validation, and application.

The development of numerical models to characterize water circulation was identified as a high-priority goal of the Albemarle-Pamlico Estuarine Study (North Carolina Department of Natural Resources and Community Development, 1987). Successful implementation of North Carolina's innovative basinwide approach to water-quality management requires the development and application of sophisticated numerical models to assist in wasteload allocation (Creager and others, 1991). In fact, the Neuse River basinwide water-quality management plan (North Carolina Division of Environmental Management, 1993) recommends that a multidimensional water-quality model be developed for the Neuse River estuary as a cooperative effort between dischargers, the Division of Environmental Management (DEM), and the U.S. Geological Survey (USGS). Such issues as the origin of depressed dissolved-oxygen levels, resuspension and movement of contaminated sediments, residence times of nutrients, and flushing of pollutants cannot be addressed fully without an understanding and documentation of water and solute movement in the estuary.

To address the specific need for a reliable numerical model of flow and solute transport in the Neuse River estuary, the USGS, in cooperation with the Albemarle-Pamlico Estuarine Study and the Division of Environmental Management of the North Carolina Department of Environment, Health, and Natural Resources, conducted an investigation of hydrodynamics and transport in a reach of the Neuse River estuary. The investigation included a detailed field-measurement program and the calibration, validation, and application of a physically realistic numerical model of hydrodynamics and solute transport. The objectives of the modeling were to (1) provide a spatially detailed description of circulation and solute transport in the estuary, (2) develop the capability to compute bulk-flow rates, and (3) characterize the movement of passive materials in the estuary.

Purpose and Scope

This report documents development and application of a two-dimensional, unsteady hydrodynamic and solute-transport model for a reach of the Neuse River estuary that extends 40 km downstream (approximately east) from the U.S. Highway 17 bridge at New Bern, North Carolina. The model is based on the vertically integrated equations of motion and transport solved by using the alternating-difference implicit numerical scheme on a finite-difference grid. The governing equations solved within the model are nonlinear, time-dependent, and retain coupling of motion and transport. This report is the third in a series of reports describing flow and transport models in North Carolina estuaries (Strickland and Bales, 1993; Bales and Robbins, 1995).

A general description of the study area and an overview of previous investigations is followed by a summary of the data collection. Data collected during 1988-92 are used to provide a general characterization of the hydrologic conditions in and around the Neuse River estuary. Conditions in the Neuse River estuary are compared with those measured in the Pamlico River during the same period (Bales and Robbins, 1995). The numerical model, including the governing equations, numerical solution scheme, and input requirements, was described in detail by Bales and Robbins (1995) to document model capabilities and limitations; only an overview of the model is given in this report. Model construction, calibration, and validation are documented, along with the results of an analysis of model sensitivity to changes in various parameters. The model is then applied to the study reach to characterize flow, circulation patterns, and solute transport for different sets of hydrologic conditions. Simulations also are made for the Neuse River estuary and the Pamlico River estuary using concurrently observed boundary data, and circulation and transport conditions in the two estuaries are compared.

Approach

The approach leading to the development and implementation of the hydrodynamic and solute-transport model consisted of data collection to characterize conditions in the study area and to implement and operate the model; calibration, validation, and sensitivity testing; and model application. Data collection included measurements of water level, salinity, wind speed and direction, inflow from tributary streams, currents, and channel bathymetry.

Model calibration is accomplished by adjusting model parameters until model results agree with observations (Ditmars and others, 1987). The model is considered to be validated if model results agree with observations distinct from those used for model calibration without further adjustment of model parameters (Ditmars and others, 1987). The model is assumed to be valid over the range of conditions used in the calibration and validation process. Sensitivity testing is the determination of the effects of small changes in model parameters or input data on model results.

The validated model was applied to the study reach to compute flow, circulation patterns, and solute transport for different hydrologic conditions. Model simulations also were used to track the movement of materials released at different locations within the study reach under different flow conditions, and to compare circulation and transport in the Neuse River estuary and the Pamlico River estuary for the same time period.

Description of Study Area

The Neuse River estuary lies within the Coastal Plain physiographic province of North Carolina

(fig. 1). Much of the shoreline surrounding the estuary is composed of marshes, particularly near the mouth of the estuary, although high bluffs predominate along the south shore of the estuary between New Bern and Cherry Point (Bellis and others, 1975). The land-surface elevation in the area is generally less than 8 meters (m) above sea level. Streams that drain to the Neuse River estuary have small drainage basins with little topographic relief, low sediment loads, and fairly acidic waters.

The climate of the region is mild and moderately moist. The annual mean temperature is more than 16 degrees Celsius (°C), and the mean annual precipitation is about 142 centimeters (cm) (Hardy and Hardy, 1971). Interannual variability in precipitation is large, ranging from 80 to 200 cm; but on the average, precipitation is relatively uniform throughout the year, although slightly higher rainfall amounts typically occur in July, August, and September. Evapotranspiration rates average about 85 cm per year and exhibit much less variability from year to year than precipitation (Wilder and others, 1978).

Upstream from New Bern, the Neuse River drains an 11,600-square-kilometer (km^2) area in the Piedmont and Coastal Plain Provinces (fig. 1). The Piedmont part of the basin is characterized by urban areas, including Raleigh, parts of Durham, and outlying communities; whereas, land use in the Coastal Plain part of the basin is primarily agricultural and silvicultural (North Carolina Division of Environmental Management, 1993). Downstream from New Bern, an additional area of 2,950 km^2 drains directly to the Neuse River estuary. The drainage area for the entire Neuse River Basin is 14,550 km^2 (fig. 1). (The Neuse River Basin as defined by the North Carolina Division of Environmental Management (1993) includes an additional area of 1,590 km^2 which drains to Bay River, West Bay, and Pamlico Sound.)

The Neuse River estuary is somewhat deeper than the Pamlico River estuary. Maximum depths range from about 3 m at New Bern to about 8 m near Oriental (fig. 2); maximum depths near the mouth of the Pamlico River are about 6 m. The bottom material near New Bern is primarily organic-rich mud. In the lower reaches of the estuary, fine-grained materials occur mostly along the channel axis, and sand predominates near the shoreline (Wells, 1989).

The numerical model was developed for the reach of the Neuse River estuary bounded on the west by the U.S. Highway 17 bridge at New Bern and on the east by a section which extends from near Oriental on the north to a point approximately 4 km downstream from Adams Creek on the south side of the estuary (figs. 1 and 2). The study reach is 40 km long, 1.5 km wide at the western (upstream) end, and 6 km wide at the eastern (downstream) end. Some data collection for the investigation occurred outside of this reach.

Previous Studies

There have been many investigations of the hydrology, characteristics, and water quality of the Neuse River estuary (Bales and Nelson, 1988). Pertinent information from some of these investigations is presented in the Hydrologic Conditions section of this report. However, very little data or information are available on hydrodynamic and transport processes in the Neuse River estuary. Woods (1969) measured the movement of dye in a 59-km reach of the Neuse River estuary following two separate dye releases. One release was made near New Bern, and the dye was tracked for 12 days. The second release was made about 3 km west of the mouth of Adams Creek, and the dye was tracked for 6 days.

Knowles (1975) measured currents at seven locations in the Neuse River estuary for 38 days. Cross-channel, upstream, and downstream currents were measured at all stations. Fluctuations between upstream and downstream currents occurred at approximately the M2 tidal period (12.4 hours). Hence, Knowles (1975) concluded that lunar tides are the "driving mechanism for the observed circulation" in the Neuse River estuary. Knowles (1975) also concluded that winds generally enhanced the estuary circulation.

Lung (1988) developed a tidally averaged, two-layer model of the Neuse River between Kinston and New Bern to simulate seasonal variations in nutrients, salinity, chlorophyll *a*, and dissolved-oxygen concentrations. The study reach was divided into 13 longitudinal segments, and the model contained 11 water-quality constituents, including 4 algal groups. Although overall seasonal trends were reproduced by the model, agreement between simulation results and data was generally poor for any given time. No information on the performance of the hydrodynamic component of the model was given.

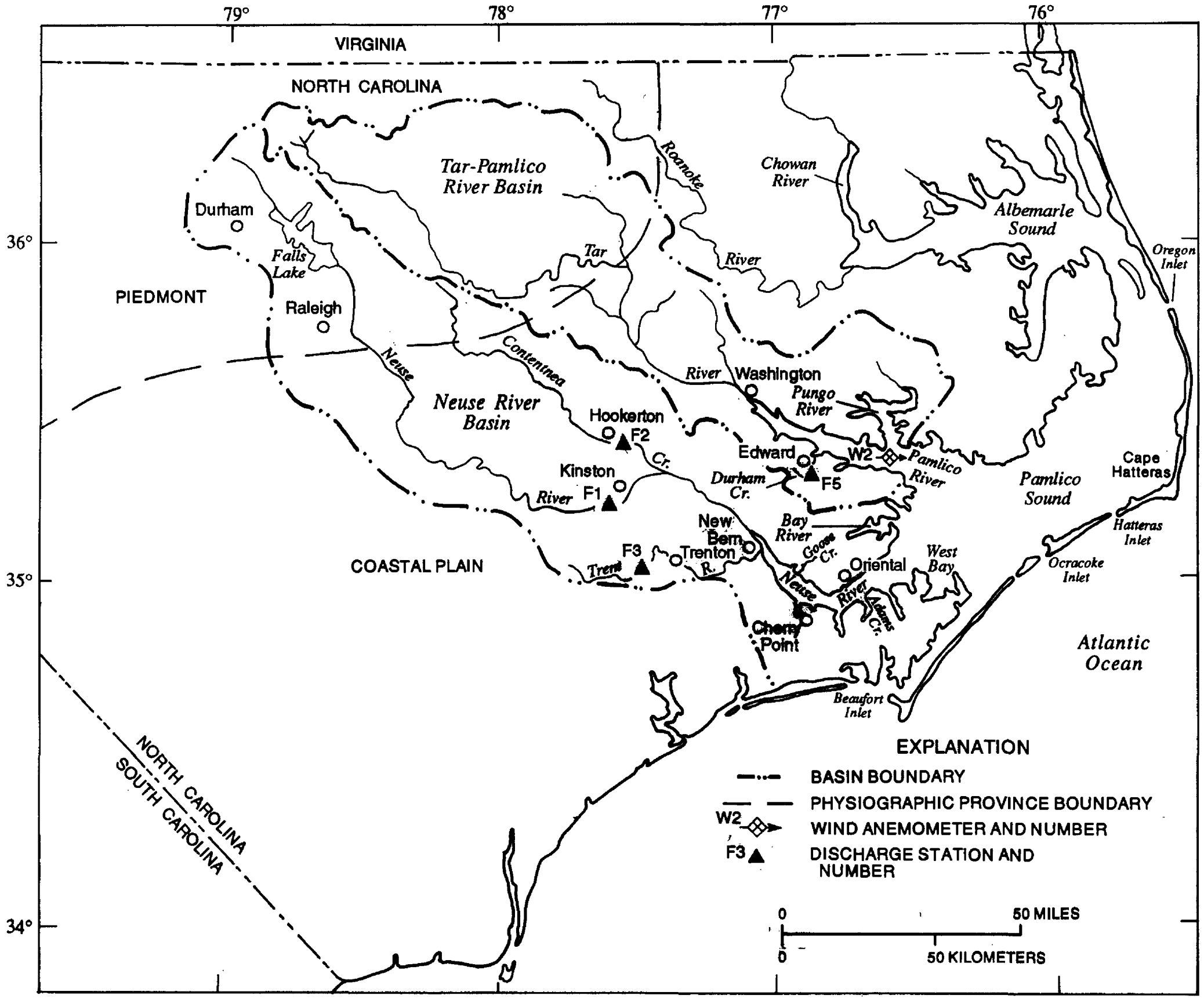

Figure 1. Location of the Neuse River Basin and estuary, North Carolina, and wind and discharge data-collection sites outside of study reach.

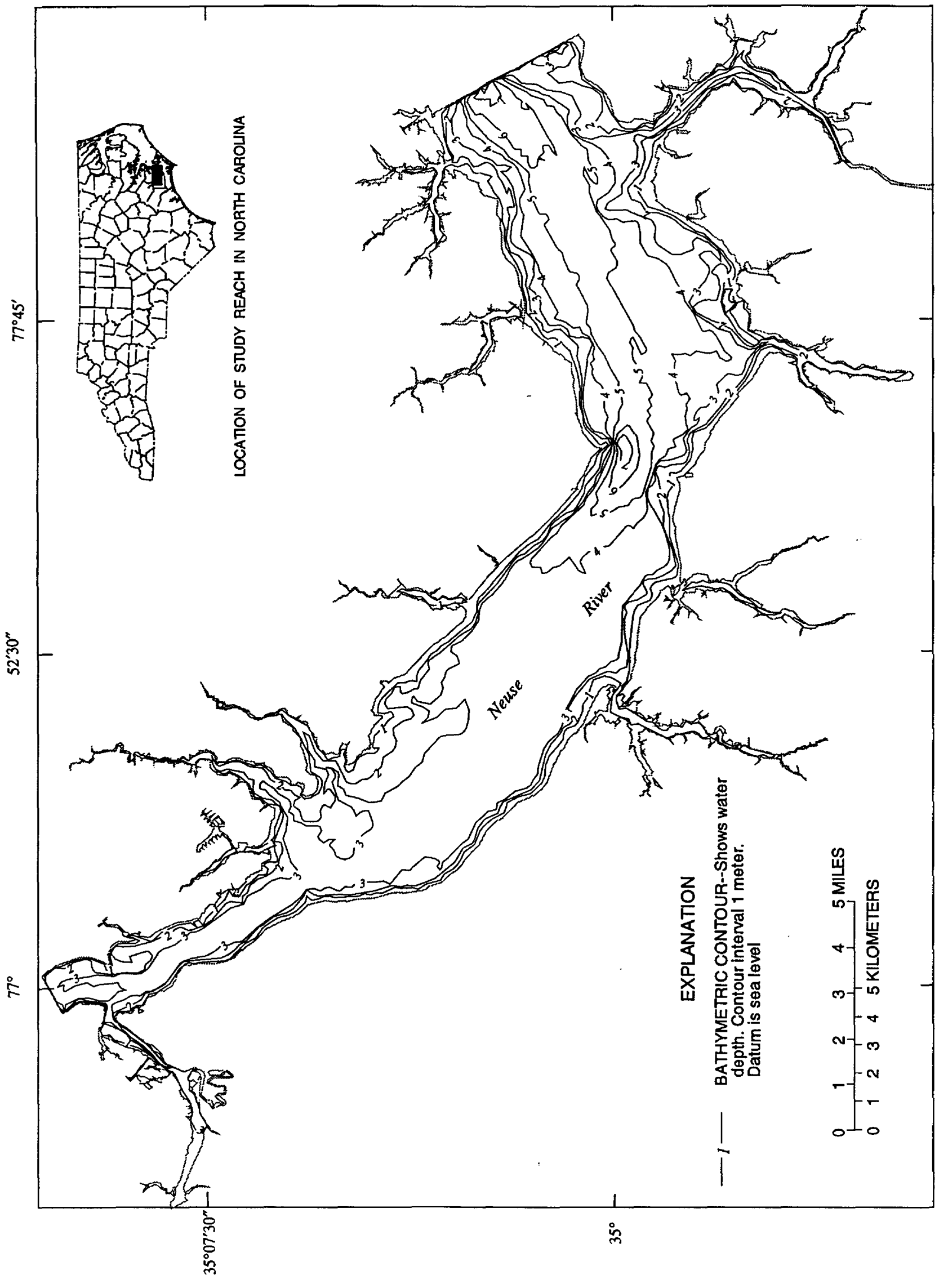

Figure 2. Neuse River study reach showing bathymetry.

During a 2-year period, Wells and Kim (1991) made monthly measurements of salinity, temperature, and current speed and direction at 15 stations in the 30-km reach of the Neuse River upstream from the mouth of Goose Creek. Upstream and downstream current velocities were typically between 10 and 20 centimeters per second (cm/s), but speeds as high as 30 cm/s were measured. East of the mouth of the Trent River, upstream flows were typically present in the bottom 1 m of water during these monthly measurements, with the strongest flows occurring during the fall and winter months. At least two hydrodynamic models of Pamlico Sound have been published (Amein and Airan, 1976; Pietrafesa and others, 1986), but these models did not include the Neuse River estuary.

Acknowledgments

This study was conducted in cooperation with the Albemarle-Pamlico (A-P) Estuarine Study and the Division of Environmental Management of the North Carolina Department of Environment, Health, and Natural Resources. The support and assistance of former A-P Study directors D.N. Rader, R.E. Holman, and R.G. Waite are greatly appreciated. Staff from the North Carolina Division of Environmental Management and Division of Marine Fisheries assisted with the design of the data-collection network and with the collection of some data. The U.S. Coast Guard granted permission for the installation of instrumentation on Neuse River multipile channel markers. The assistance of the U.S. Coast Guard in installing data-collection instrumentation on channel markers and in deploying and recovering current meters is also gratefully acknowledged. The cooperation of the following landowners, who allowed water-level recorders to be installed on their property, is appreciated: the North Carolina Department of Transportation; Mr. Jack Jones, Fairfield Harbor; Mr. Art Bailey, Oriental; and Mr. Tom Tosto, South River.

DATA COLLECTION AND HYDROLOGIC CONDITIONS

Scientifically credible and effective modeling requires carefully collected, continuous records of boundary data for model application and short-term records for model calibration and validation. To provide the required information for the Neuse River estuary hydrodynamic model and to better define the physics of flow in the estuary, water level, salinity and water temperature, wind speed and direction, current velocity, and bathymetric data were collected during March 1988 through September 1992. Data from pre-existing, continuous-record streamflow gaging stations and meteorological stations also were available during this period.

Water Level

Water-level data were recorded at 15-minute intervals at five locations in the study reach (fig. 3; table 1) and were referenced to sea level. Water-level records from sites WL1 and WL4 were used for model boundary data, and records from sites WL2 and WL3 were used for model calibration and validation. Site WL5 was outside of the model domain and could not be used for model calibration; additionally, analysis of the data indicated that hydrologic conditions at the site were sufficiently different from conditions within the model domain. Data collection began in March 1988 and continued at some stations through September 1992 (fig. 4).

Because of the relatively small water-level gradients in the estuary and the importance of these gradients in affecting hydrodynamic conditions, efforts were made to ensure the accuracy of gage datums. The North Carolina Geodetic Survey conducted a ground survey in which all gage datums were tied to the national first-order network. Second-order vertical accuracy (for example, between 4.2 and 5.7 cm in 50 km) was achieved during this survey. However, a difference in elevation of 5 cm over a 50-km distance is approximately equal to the typical water-surface slope in the Neuse River estuary; therefore, small errors in gage datums have significant effects on computed water-surface slope and, thus, on simulated flow.

Water-level fluctuations in Pamlico Sound east of the study reach have been extensively examined by Jarrett (1966) and Pietrafesa and others (1986) who also collected and analyzed data from a site near site WL3. For periods of 1 to 7 days, the water level in the northern part of the sound was typically coherent and

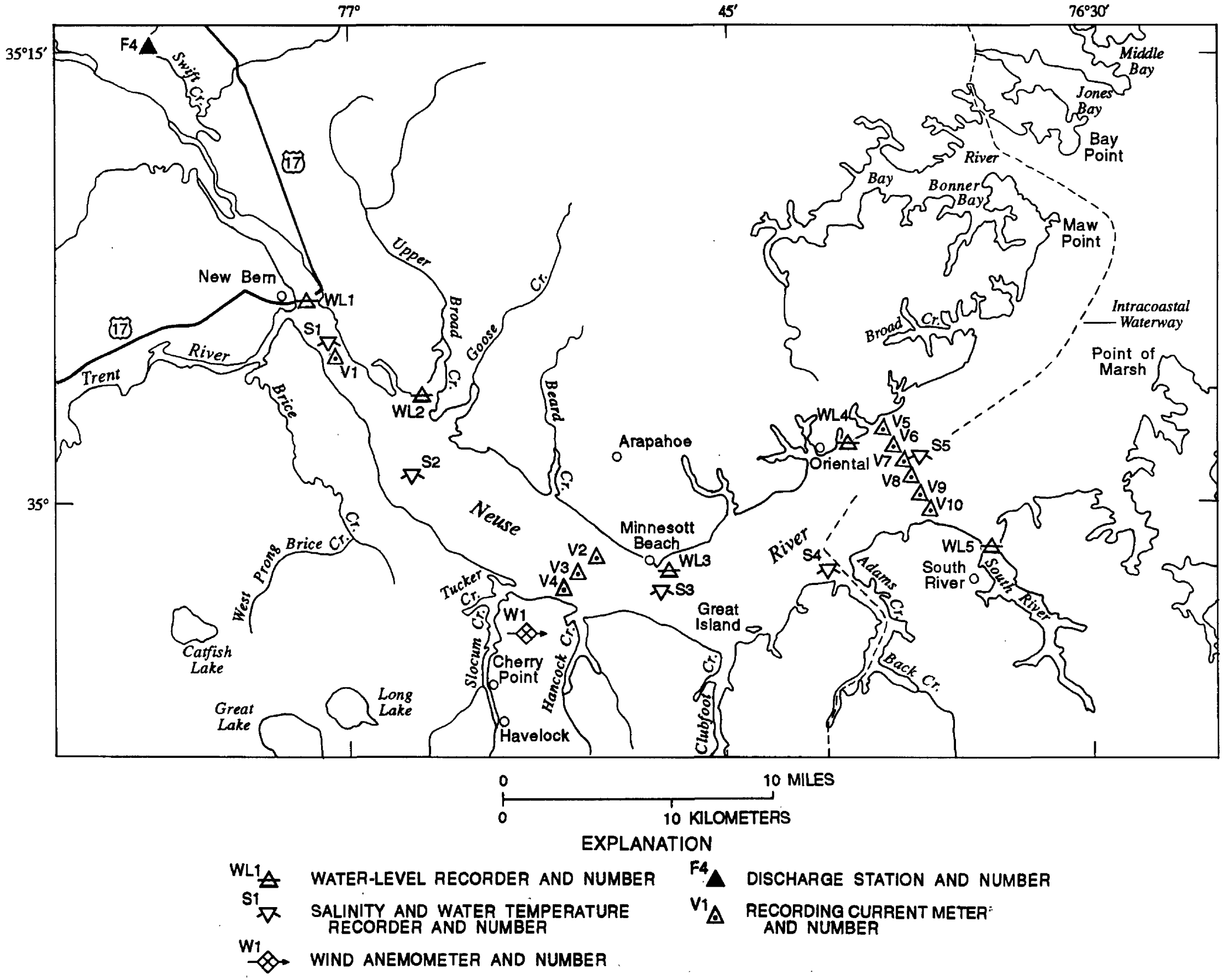

Figure 3. Location of Neuse River data-collection sites, North Carolina.

Table 1. Description of Neuse River data-collection sites
[USGS, U.S. Geological Survey; ---, no number assigned]

Site no.	USGS station number	Latitude	Longitude	Measurement interval (minutes)
Water-level data (fig. 3)				
WL1	02092162	35°06'42"	77°01'37"	15
WL2	0209259278	35°03'24"	76°57'23"	15
WL3	02092658	34°57'58"	76°48'20"	15
WL4	02092675	35°01'26"	76°41'35"	15
WL5	02092678	34°57'12"	76°35'02"	15
Salinity and temperature data[1] (fig. 3)				
S1	0209258400	35°04'48"	77°00'24"	15
S2	0209262905	34°59'56"	76°56'36"	15
S3	0209265810	34°56'54"	76°48'36"	15
S4	0209266925	34°57'24"	76°40'54"	15
S5	0209267575	35°00'30"	76°39'42"	15
Wind speed and direction data (fig. 3)				
W1	---	34°54'	76°53'	60
W2	---	35°22'42"	76°33'24"	15
Flow data (figs. 1 and 3)				
F1	02089500	35°15'29"	77°35'09"	60
F2	02091500	35°25'44"	77°34'59"	60
F3	02092500	35°03'54"	77°27'24"	30
F4	02092000	35°20'42"	77°11'45"	60
F5	02084540	35°19'25"	76°52'26"	60
Velocity, salinity, and temperature data[2] (fig. 3)				
V1	---	35°04'48"	77°00'24"	5
V2	---	34°56'24"	76°47'16"	5
V3	---	34°57'05"	76°47'11"	5
V4	---	34°57'36"	76°47'05"	5
V5	---	35°01'30"	76°40'06"	5
V6	---	35°01'07"	76°39'57"	5
V7	---	35°00'43"	76°39'34"	5
V8	---	35°00'19"	76°39'17"	5
V9	---	34°59'54"	76°38'59"	5
V10	---	34°59'30"	76°38'43"	5

[1]Salinity measured near the water surface and near the channel bottom; water temperature measured near the water surface.

[2]Data collected at a point about 1.5 meters above the channel bottom; salinity, water temperature, and current speed and direction recorded.

180° out of phase with water-level oscillations in the southern part of the sound (Pietrafesa and others, 1986). Coherent wind fields for all periods greater than 1 day were generally aligned in the north-northeast to south-southwest direction, or along the major topographic axis of the sound (Pietrafesa and others, 1986). Hence, for all periods of 1 to 7 days, predominant winds that blow along the axis of the sound result in a rise in water level at one end of the sound and an associated lowering of water level at the other end. When the wind relaxes, a seiching (water-level oscillation in a closed basin) motion results. In this respect, the lower Neuse River estuary (east of site WL3), which is aligned with the axis of Pamlico Sound, is an extension of the sound, rather than a separate system. Pietrafesa and others (1986) also detected a strong sea breeze effect at periods of 24 hours. However, water levels in the sound responded relatively uniformly to the sea breeze, in contrast to the 1- to 7-day winds.

Characteristics of water-level fluctuations in the Neuse River estuary have not been documented as thoroughly as have characteristics of Pamlico Sound. It generally has been assumed that wind is primarily responsible for water-level fluctuations in the Neuse River estuary. Jarrett (1966) analyzed 5 months of water-level data collected at 6-hour intervals at a location near Cherry Point and concluded that the semi-diurnal tidal component, which has a period of 12.42 hours (M2 tide), accounted for about 1.5 percent of the variance in the water-level record. This result could be questionable, however, because of the data-collection interval (one-half of the M2 period) and the relatively short period of record. Pietrafesa and others (1986) analyzed 1 year of water-level data collected near site WL3 and reported no evidence of an M2 tidal signal.

Although the analysis of Jarrett (1966) and Pietrafesa and others (1986) demonstrated that water-level fluctuations in the Neuse River estuary are probably not driven by astronomical tides, there is often a marked periodicity in the water-level fluctuations (fig. 5). The mechanisms driving the water-level fluctuations in the Neuse River estuary, as well as in the Pamlico River, have not been fully explained. As shown by Pietrafesa and others (1986), the lower frequency water-level fluctuations (for example, the generally increasing water level during July 20-26, 1991, [fig. 5]) is likely caused by Pamlico

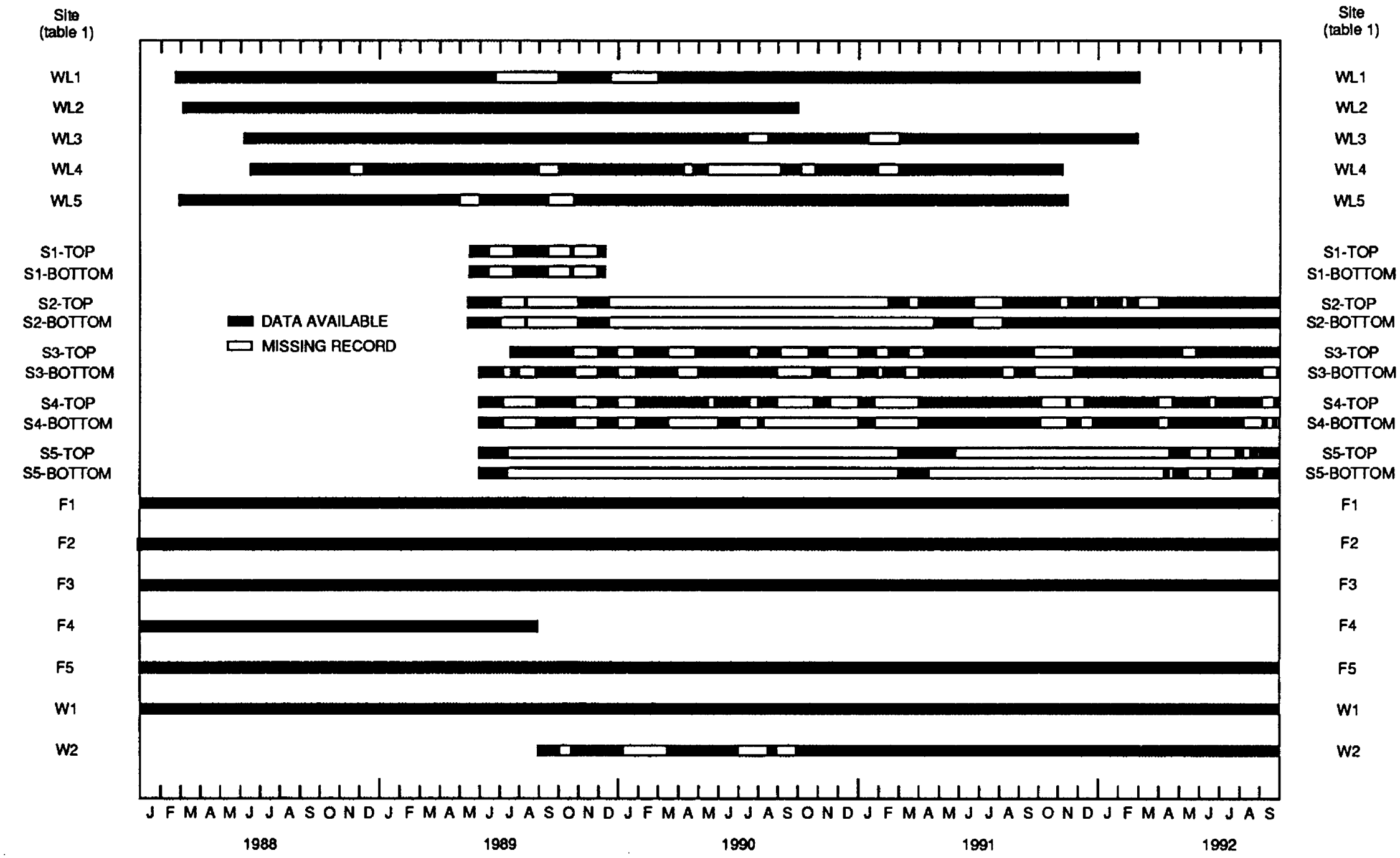

Figure 4. Period of record at selected data-collection sites in the Neuse River estuary.

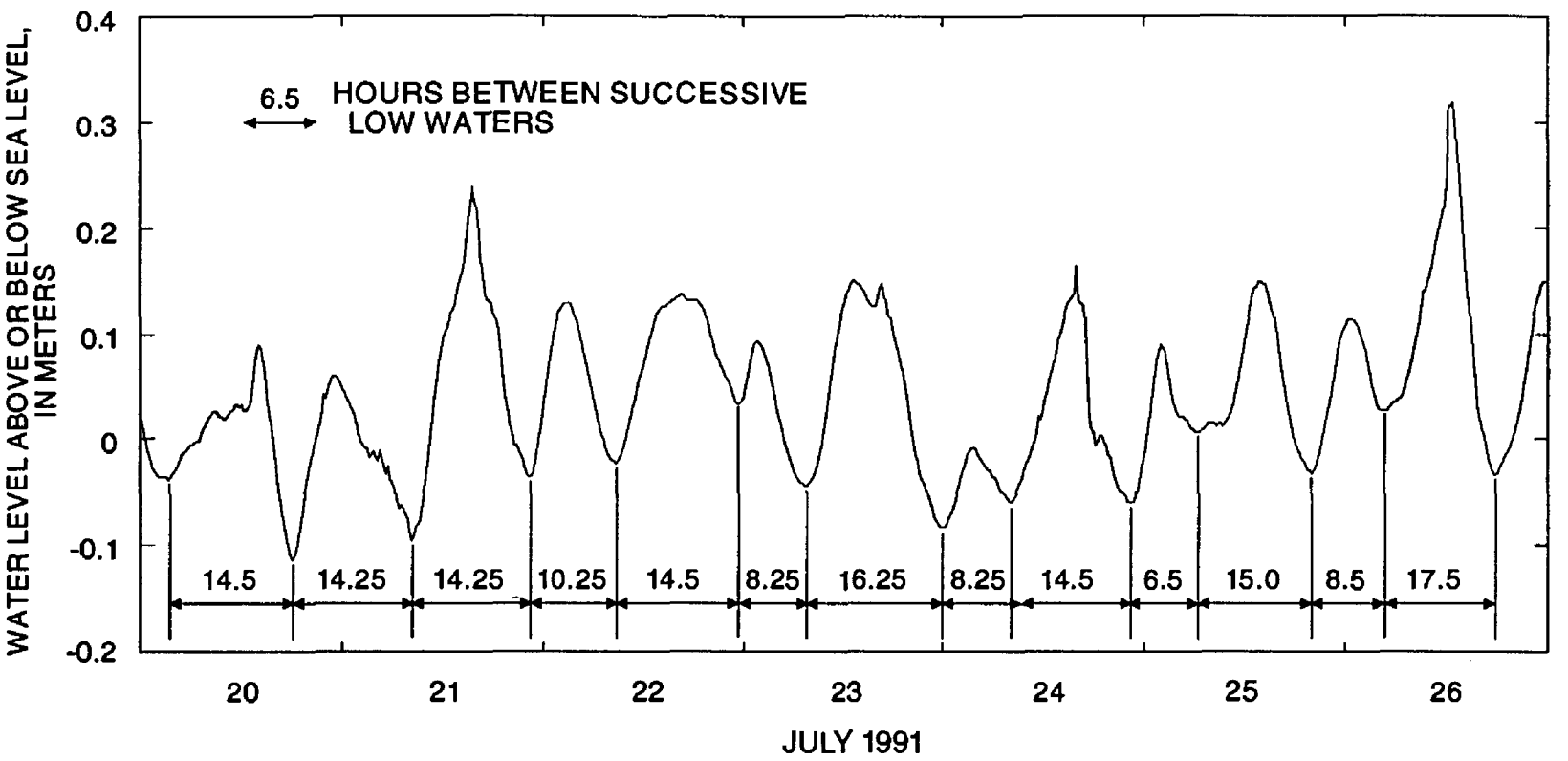

Figure 5. Water level at site WL1 in the Neuse River during July 20-26, 1991, showing near-periodic fluctuations in water level.

Sound water-level fluctuations which generally occur in response to wind. The higher frequency fluctuations (periods of 6.25 to 16.25 hours in figure 5) could be caused by a combination of the sea-breeze effect and a Pamlico Sound seiche, or by other mechanisms. A simplified formula for a seiche in a long, narrow rectangular basin (Ippen and Harleman, 1966) that has a length of 140 km (the approximate length of Pamlico Sound), gives a seiche period of 8.3 hours, which is within the range of the typical fluctuations shown in figure 5. Additional, more sophisticated analyses are needed to identify the mechanisms responsible for water-level fluctuations in the Neuse River estuary.

During the study period, the mean water level in the Neuse River estuary ranged from 0.195 m at site WL2 to 0.249 m at site WL3 (table 2). (Mean values are computed from available data, and for some months there are periods of missing data, as shown in figure 4.) The largest daily water-level fluctuations occurred at the upstream end of the estuary.

Water levels generally were highest in the late summer and early fall (August-October) and lowest during the winter (December-February) (table 3). As noted by Pietrafesa and others (1986), the water level in the coastal ocean is at a minimum during January and February when water temperature is lowest and water density is greatest. Likewise, water levels in the coastal ocean increase in the spring and summer as water temperature increases. The water level in the Neuse River estuary responds to these changes in the coastal ocean water level.

Table 2. Observed water-level characteristics in the Neuse River estuary, 1988-92

Water-level characteristic	Site (fig. 3)				
	WL1	WL2	WL3	WL4	WL5
Mean water level[1]	0.243	0.195	0.249	0.244	0.204
Mean daily maximum[1]	.387	.329	.366	.336	.295
Maximum observed[1]	1.469	1.329	1.463	1.097	1.493
Mean daily minimum[1]	.095	.057	.138	.147	.109
Minimum observed[1]	-.735	-.533	-.488	-.445	-.463
Mean daily range[2]	.292	.272	.228	.189	.186
Total range[2]	2.204	1.862	1.951	1.542	1.956
Days of record	1,510	928	1,503	1,049	1,272

[1]Values are in meters above or below sea level.
[2]Values are in meters.

Table 3. Observed monthly mean water level and monthly mean of the daily water-level range at five Neuse River water-level gages, 1988-92

Site (fig. 3)	Jan.	Feb.	Mar.	Apr.	May	June	July	Aug.	Sept.	Oct.	Nov.	Dec.
	Monthly mean water level (meters above sea level)											
WL1	0.221	0.192	0.223	0.250	0.266	0.237	0.146	0.271	0.351	0.328	0.261	0.123
WL2	.081	.125	.234	.239	.191	.151	.118	.225	.348	.301	.173	.118
WL3	.185	.198	.263	.236	.262	.242	.151	.285	.375	.326	.277	.149
WL4	.179	.162	.256	.212	.228	.210	.170	.270	.375	.347	.270	.193
WL5	.140	.137	.262	.215	.194	.183	.117	.220	.311	.276	.240	.135
	Monthly mean daily water-level range (meters)											
WL1	0.286	0.297	0.324	0.341	0.325	0.305	0.275	0.269	0.258	0.241	0.270	0.281
WL2	.254	.309	.284	.321	.318	.294	.254	.226	.256	.198	.264	.271
WL3	.221	.271	.279	.261	.263	.237	.218	.213	.216	.138	.212	.229
WL4	.180	.210	.221	.216	.214	.203	.171	.165	.184	.159	.170	.196
WL5	.176	.215	.202	.227	.216	.193	.164	.158	.169	.146	.178	.196
	Days of record											
WL1	93	92	155	150	155	145	124	124	121	124	120	107
WL2	62	56	91	90	93	90	93	93	90	62	60	62
WL3	108	82	122	120	124	141	145	145	150	124	120	122
WL4	88	84	93	72	74	75	93	93	96	115	84	82
WL5	93	88	124	120	101	120	119	120	110	85	104	88

The observed difference in mean water levels between the upstream and downstream boundaries of the study reach was very small (tables 2 and 3). Although instantaneous differences in water level of as much as 0.3 m were observed throughout the study reach, the water-surface slope in the Neuse River estuary was generally small, on the order of 10^{-6}. Mean water-level data suggest that there could have been some small errors in recorded water levels. For example, the long-term mean water level at site WL4, a downstream site, slightly exceeded that at site WL1, the upstream site (table 2). If this condition indeed existed, it would suggest that the long-term mean flow is in the upstream direction, which, of course, is untrue. There are three possible sources for inconsistencies in the water-level records: (1) The period of record at site WL1 was greater than at site WL4 (table 2); however, comparison of records for shorter periods of time, when records were available at all water-level gages, indicates similar inconsistencies. (2) The datums at the two gages were not internally consistent. As previously noted in this section, internal inconsistencies in datum elevation of as much as 5 cm could be present at the two gages because of the distance between the gages. (3) The gage at site WL4 shifted or settled because of wave action, and adjustments made for these effects were not accurate. Field notes indicate that adjustments of as much as 6 cm were made in the record; these adjustments were based on readings made during fluctuating water levels. Thus, an accurate determination of water level was difficult.

The daily water-level range (difference between daily maximum and daily minimum water level) generally was greatest during the late winter and spring, and at a seasonal minimum during October. Increased water-level fluctuations corresponded to increased energy available for mixing and transport processes.

Salinity and Water Temperature

Continuous records of specific conductance and water temperature were collected at five sites in the

Neuse River estuary (fig. 3; table 1). Salinity was computed from specific-conductance values standardized to 25 °C using the conversion given by Miller and others (1988). Salinity data from sites S2 and S4 were used for model boundary conditions; data from site S1 were available for only a short time; and data from site S5 were limited during the study period (fig. 4). Data from site S3 were used for model calibration and validation. These data, as well as data-collection procedures, were summarized by Garrett and Bales (1991) for April 1989 through September 1990, and by Garrett (1992) for October 1990 through September 1991.

Water-quality monitors were located on U.S. Coast Guard channel markers. Water temperature was measured near the water surface. Specific conductance was monitored near the surface and about 1 m above the channel bottom. Exact placement of sensors in the water column at each site was summarized by Garrett and Bales (1991). The underwater sensors were controlled by a single above-water unit, and data were electronically recorded at 15-minute intervals. Monitors were typically serviced once every 3 weeks.

Vertical profiles (measured at 0.3-m intervals) of salinity and water temperature were recorded each time the monitors were serviced. The difference between near-surface and near-bottom water temperatures was typically less than 1 °C. However, top-to-bottom differences in salinity of more than 8 parts per thousand (ppt) sometimes were observed.

Although some information on salinity in the Neuse River estuary is available, data usually consist of measurements made at biweekly or monthly intervals. At least two hydrographic atlases of the Neuse River estuary have been published. Data collected in North Carolina estuarine waters by the University of North Carolina Institute of Marine Sciences were summarized by Williams and others (1967) for 1948 through 1966. Data collected near the water surface and near the channel bottom at six sites in the Neuse River estuary as well as three sites at the mouth of the estuary were tabulated, and figures were presented showing monthly mean surface and bottom isotherms and surface and bottom isohalines. The total number of observations for each month at a site varied between 0 and 28, but was usually less than 15. According to the somewhat limited data, salinity in the estuary is typically at a minimum in April and a maximum in November, which is the same general pattern found in the Pamlico River. Isohalines presented by Williams and others (1967) depicted the presence of a lateral salinity gradient. In the lower part of the estuary (east of Cherry Point), salinity is typically higher on the south side of the estuary. West of Cherry Point, higher salinity generally occurs on the north side of the estuary, which was the condition observed in the Pamlico River. During summer months, the lateral difference for near-bottom measurements was as much as 5 ppt; highest lateral differences generally occurred during winter months in the Pamlico River. The smallest lateral gradients were for near-surface conditions during the late spring and early summer. Schwartz and Chestnut (1973) presented data collected monthly during 1972 at six sites in the Neuse River estuary. These data also seemed to indicate the presence of a lateral salinity gradient, with the largest gradient occurring during summer months.

Giese and others (1985) analyzed daily salinity observations made near site WL1 during 1957-67. Daily observations of surface salinity at site WL1 were less than 0.2 ppt more than 50 percent of the time between 1957 and 1967. Near-surface salinity was greater than 4.5 ppt and near-bottom salinity was greater than 8.7 ppt about 5 percent of the time at site WL1 between 1957 and 1967. Salinity at site WL1 was generally higher than salinity measured in the Pamlico River near Washington during the same period. Continuous measurements of salinity at site WL1 for a 2-year period, when daily observations also were made, indicate that daily salinity variations were small. The ratio of near-surface to near-bottom salinity at site WL1 was 0.8 or greater, indicating generally weak stratification. Finally, results of the salinity surveys indicate that salinities were higher on the north side of the estuary than on the south side, which agrees with the conclusions of Williams and others (1967) and Schwartz and Chestnut (1973).

Harned and Davenport (1990) compiled available salinity data collected in the Neuse River estuary between 1970 and 1988. The estuary, from New Bern to the mouth, was subdivided into five zones to expedite data analysis. The number of observations per zone ranged from 406 to 1,100. No distinction was made in the analysis between near-surface and near-bottom salinity. The median salinity ranged from about 2 ppt in the upstream zone to 13 ppt in the downstream zone. However, the difference between the minimum and maximum observed

salinity in each zone was between 12 and 20 ppt. Twenty-five percent of the observations were greater than 6 ppt in the upstream zone, and 25 percent were greater than 16 ppt in the downstream zone.

Near-surface and near-bottom salinities were recorded at sites S1-S5 for the period 1989-92 (tables 4 and 5). The number of days of record for sites S1 and S5 was significantly less than at other sites. The channel marker on which site S1 was mounted was destroyed by ice in December 1989 and was never rebuilt by the Coast Guard, and site S5 was damaged by boats and storms several times during the study period. Consequently, results for sites S1 and S5 in tables 4 and 5 are not directly comparable to results for other sites.

Mean near-surface salinity values ranged from 0.9 ppt at site S1 to 11.4 ppt at site S5, and mean near-bottom salinity values ranged from 4.9 ppt at site S1 to 12.9 ppt at site S5 (table 4). The difference between maximum observed and minimum observed salinity at each site ranged from 9.2 ppt at site S1 to 32.5 ppt at site S4, which is somewhat higher than the range reported by Harned and Davenport (1990). High salinity was observed at site S1 (9.2 ppt near the surface and 12.0 ppt near the bottom). Likewise, low salinity was observed at the downstream end of the estuary (1.3 ppt near the surface at site S5). Mean and maximum salinities were higher in the Neuse River estuary than in the Pamlico River for the same period (Bales and Robbins, 1995).

Although overall observed variations in salinity were large at each site, daily variations were generally less than 3 ppt. Larger daily variations were observed near the bottom than near the surface at each site (table 4). Daily variations in salinity were also somewhat greater in the Neuse River estuary than in the Pamlico River, where mean daily salinity ranges were generally less than 2 ppt (Bales and Robbins, 1995).

Because of the presence of the Intracoastal Waterway (fig. 3), Adams Creek is directly connected to the Atlantic Ocean through Beaufort Inlet. The distance from site S4 to Beaufort Inlet is about 35 km, which is less than the length of the Neuse River estuary. Adams Creek appears to be a source of high-salinity water to the Neuse River estuary. Maximum observed salinity at site S4 was higher than at site S5, the downstream monitoring site (table 4). Moreover, a strong tidal signal was often present in the site S4 salinity record, but at the same time was less apparent at the other Neuse River estuary monitoring sites (fig. 6), which further demonstrates the influence of ocean inflows through Adams Creek on the estuary.

At sites S2, S3, and S4, minimum monthly mean salinity generally occurred in March or April

Table 4. Observed salinity characteristics in the Neuse River estuary, 1989-92
[<, less than]

Site (fig. 3)	Salinity (in parts per thousand)							Complete days of record
	Mean	Mean daily maximum	Maximum observed	Mean daily minimum	Minimum observed	Mean daily range	Total range	
				Near surface				
S1	0.9	1.5	9.2	0.6	<0.1	0.9	9.2	106
S2	5.7	6.6	14.4	4.9	<.1	1.7	14.4	568
S3	8.1	9.1	16.5	7.4	.3	1.7	16.2	820
S4	10.2	12.0	32.8	8.9	.3	3.1	32.5	784
S5	11.4	12.4	30.5	10.5	1.3	1.9	29.2	222
				Near bottom				
S1	4.9	6.2	12.0	3.2	<0.1	3.0	12.0	110
S2	8.9	10.1	20.8	7.7	.1	2.4	20.7	568
S3	9.4	10.8	18.3	8.2	.5	2.6	17.8	820
S4	11.5	13.5	31.5	9.7	3.5	3.8	28.0	784
S5	12.9	14.4	31.5	11.5	7.2	2.9	24.3	222

Table 5. Observed monthly mean salinity, in parts per thousand, for near-surface and near-bottom conditions at five salinity monitors in the Neuse River estuary, 1989-92
[ND, no data; ---, fewer than 20 days of data]

Site (fig. 3)	Jan.	Feb.	Mar.	Apr.	May	Juna	July	Aug.	Sept.	Oct.	Nov.	Dec.
						Near surface						
S1	ND	ND	ND	ND	0.2	---	---	1.8	---	---	---	---
S2	6.3	---	---	3.9	5.1	5.5	6.6	4.6	6.4	5.8	5.3	9.0
S3	8.7	7.1	6.4	6.9	7.1	8.6	10.0	8.3	7.7	7.2	11.6	8.9
S4	10.7	8.7	8.6	8.0	10.7	10.3	12.0	11.5	10.5	9.8	---	9.6
S5	ND	---	11.4	10.6	---	10.5	---	11.8	12.0	ND	ND	ND
						Near bottom						
S1	ND	ND	ND	ND	3.0	---	---	8.6	---	---	---	---
S2	10.3	---	---	8.2	7.5	7.9	11.8	12.0	9.2	7.5	7.6	10.2
S3	10.1	7.9	7.7	8.4	8.1	9.7	11.0	10.5	8.6	8.2	13.2	9.6
S4	11.2	10.1	8.5	11.0	12.1	12.5	14.5	11.0	10.8	9.7	---	10.9
S5	ND	---	14.3	12.1	---	10.5	---	15.0	13.9	ND	ND	ND
						Days of record						
S1	0	0	0	0	20	10	11	29	17	5	1	13
S2	28	18	7	34	82	79	38	60	59	36	46	32
S3	71	75	61	58	70	90	87	93	61	28	24	62
S4	62	57	42	44	68	107	70	40	91	31	5	46
S5	0	1	31	34	15	33	16	24	30	0	0	0

(table 5); minimum monthly mean salinity generally occurred during April or May in the Pamlico River (Bales and Robbins, 1995). Maximum monthly mean salinity at sites S2, S3, and S4 was generally in November or December (table 5). At a particular site, the difference between the maximum and minimum monthly mean salinities at these three sites ranged from 4.0 ppt at site S4 (near surface) to 6.0 ppt at site S4 (near bottom).

The difference between simultaneously observed near-surface and near-bottom salinities was computed for all observations at each site. Monthly means of the differences were then determined (table 6). The smallest top-to-bottom differences in salinity generally occurred at site S3, and the largest differences occurred at site S2. Because of the sparseness of the data, seasonal trends are difficult to detect, but it appears that the greatest top-to-bottom salinity difference in the Neuse River estuary is typically during the summer months. However, monthly mean values mask much of the dynamics of the stratification process in the Neuse River estuary, and short-term variations in flow and wind conditions can have major effects on vertical salinity distributions. Finally, stratification appears to be greater in the Neuse River estuary than in the Pamlico River.

Wind

Wind speed and direction were recorded at two locations. Wind data were manually recorded at hourly intervals by personnel at the Cherry Point Marine Corps Air Station (site W1, fig. 3). Wind direction was recorded to the nearest 22.5 degrees at this site (for example, north, north-northeast, northeast, and so on). At a site near the mouth of the Pungo River (site W2, fig. 1), wind data were measured at 5-minute intervals; every 30 minutes, the 5-minute data were averaged and automatically recorded. The recording wind anemometer at site W2 was located at an elevation of 10 m above the water surface, and direction was recorded to the nearest degree. The anemometer was serviced at approximately monthly intervals. At site W1, wind speeds less than about 1.0 meter per second

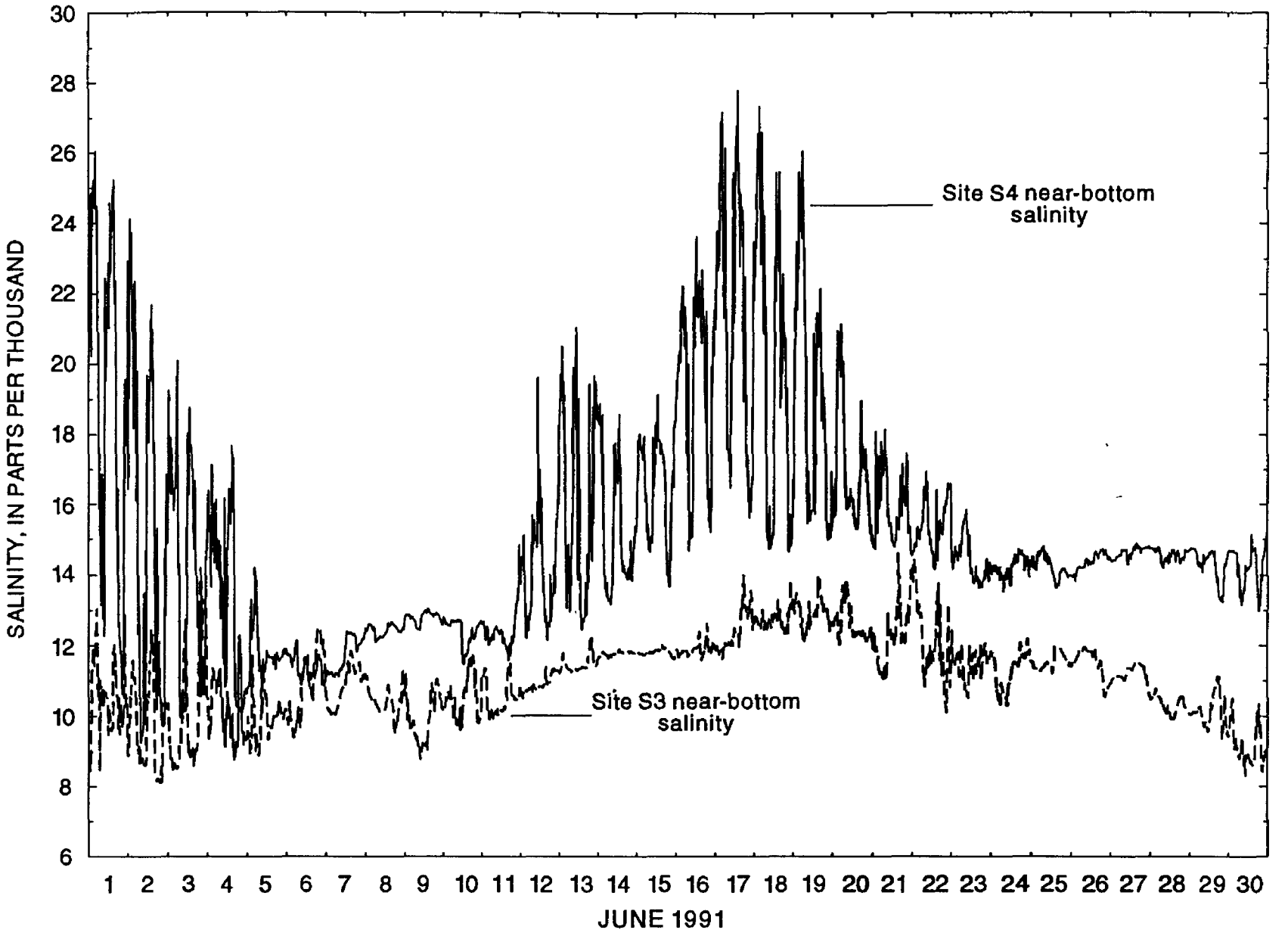

Figure 6. Typical salinity variations at site S4 at the Intracoastal Waterway and at site S3 in the Neuse River estuary.

Table 6. Monthly mean of the difference between simultaneously measured near-bottom and near-surface salinity at five sites in the Neuse River, 1989-92
[---, fewer than 20 days of record, no mean computed]

Site (fig. 3)	Monthly mean of the difference between simultaneously measured near-bottom and near-surface salinity (in parts per thousand)											
	Jan.	Feb.	Mar.	Apr.	May	June	July	Aug.	Sept.	Oct.	Nov.	Dec.
S1	---	---	---	---	2.8	---	---	7.1	---	---	---	---
S2	4.5	---	---	3.0	2.4	2.6	5.3	7.4	2.8	1.7	1.5	0.6
S3	1.4	0.8	1.3	1.5	1.2	1.3	1.1	1.4	.8	.9	1.5	.7
S4	.6	1.4	.3	1.3	.9	2.2	2.9	.2	.3	1.7	---	1.0
S5	---	---	2.9	1.0	---	1.1	---	2.5	1.8	---	---	---

(m/s) were recorded as "calm" (or 0.0 m/s), whereas the anemometer at site W2 recorded wind speed to the nearest 0.1 m/s.

Wind data from the two sites were compared, and there was a marked difference in the number of non-zero wind speeds recorded at the two sites. For example, during June 14-24, 1991, 22 percent of the wind speeds at site W1 were recorded as calm, whereas all of the wind speeds at site W2 were greater than zero. During September 1-17, 1991, 64 percent of the observations at site W1 were non-zero, whereas 98 percent of the wind speeds at site W2 were greater than zero. Consequently, only observations with speeds greater than zero were included in the comparison shown in table 7.

Measured wind directions at the two sites were in general agreement (table 7), particularly considering the difference in recording precision at the two sites (22.5 degrees at site W1 compared to 1 degree at site W2). Wind speeds at site W2, however, were 2 to 3 times greater than those recorded at site W1 (table 7). Because site W2 is located over the open water, wind speeds measured at this site are likely more representative of wind conditions over the Neuse River estuary than those measured at site W1. However, because of its proximity to the Neuse River, data from site W1 were applied in the model.

Winds measured at site W2 during 1989-92 were generally from the south-southwest-west in the late spring and summer months. Winds were typically from the northwest-north-northeast during the fall and shifted to the west, northwest, and north during the winter. There was a general progression of winds back to the south until about June, when winds slowly began to rotate back to the north. Wind speeds were greatest during the winter months; during December through May, wind speeds were greater than 9 m/s at least 10 percent of the time. Winds generally were light during June through August, when wind speeds were less than 4.5 m/s about 37 percent of the time. Additional details on wind conditions at site W2 are given by Bales and Robbins (1995).

According to Weisberg and Pietrafesa (1983), annual vector-average wind direction over the coastal ocean east of Pamlico Sound is from the northeast. Weisberg and Pietrafesa (1983) also noted that the maximum mean and maximum variance in wind speeds occurred during the winter months in the coastal ocean, east of the study area; minimum mean and minimum variance in wind speeds occurred during summer months.

Pietrafesa and others (1986) analyzed the frequency characteristics of winds measured at New Bern and Cape Hatteras during a 340-day period in 1978. A well-defined sea breeze oriented approximately north-northwest to south-southeast was detected. At periods greater than about 2 days, winds tended to be aligned in the northeast-southwest direction, or along the major topographic axis of Pamlico Sound, and approximately perpendicular to the axis of the Pamlico River.

Freshwater Inflow

The flow of the Neuse River has been regulated by Falls Lake Dam (about 200 km upstream) since

Table 7. Wind statistics at Neuse River sites W1 and W2 during June 14-24, 1991, and September 1-17, 1991

[m/s, meter per second. Site W1 is shown in figure 3. Site W2 is shown in figure 1. Statistics shown are for observations with recorded wind speeds greater than zero]

Statistic	June 14-24, 1991				September 1-17, 1991			
	Wind speed (m/s)		Wind direction (degrees)		Wind speed (m/s)		Wind direction (degrees)	
	Site W1	Site W2	Site W1	Site W2	Site W1	Site W2	Site W1	Site W2
Mean	2.3	4.9	180	171	3.4	4.8	125	135
Minimum	.5	.2	0	1	.6	.4	10	2
25th percentile	1.0	3.1	180	104	2.1	3.6	30	49
Median	2.1	4.8	180	188	3.1	4.9	70	132
75th percentile	3.1	6.6	202	223	4.4	6.0	200	224
Maximum	4.6	12.8	338	356	8.7	12.5	360	358

January 1983. The Neuse River drains an area of 2,010 km^2 at the dam, which represents 17 percent of the Neuse River Basin upstream from New Bern, where the drainage area is 11,600 km^2. The downstream-most gaging station on the mainstem of the Neuse River is at Kinston (site F1, fig. 1; table 1), where the drainage area is 7,000 km^2. Two tributaries of the Neuse River downstream from Kinston, Contentnea Creek (site F2) and the Trent River (site F3), are also gaged, and Swift Creek (site F4) was gaged until October 1989. The flow of 64 percent of the entire 14,550-km^2 Neuse River Basin is gaged.

With the exception of site F3 (fig. 1) on the Trent River, none of the streams which drain directly to the study reach are gaged. The gaging station nearest the study reach is on Durham Creek (site F5), which is on the north side of the Neuse River estuary but drains to the Pamlico River. Much of the land around the Neuse River estuary consists of altered wetlands that have been ditched and drained to accommodate agriculture and other land uses. Water-control structures are widely used in these agricultural drainage ditches and may alter the natural seasonal distribution as well as the volume of runoff. Hydrologic characteristics of streams that drain these lands are not well documented; however, Treece and Bales (1992) and Treece (1993) reported data from three small agricultural drainage canals in Beaufort County on the south side of the Pamlico River.

The flow of the Neuse River at site F1 (fig. 1) generally was less than average between September 1988 and February 1989 (fig. 7). Average flow was

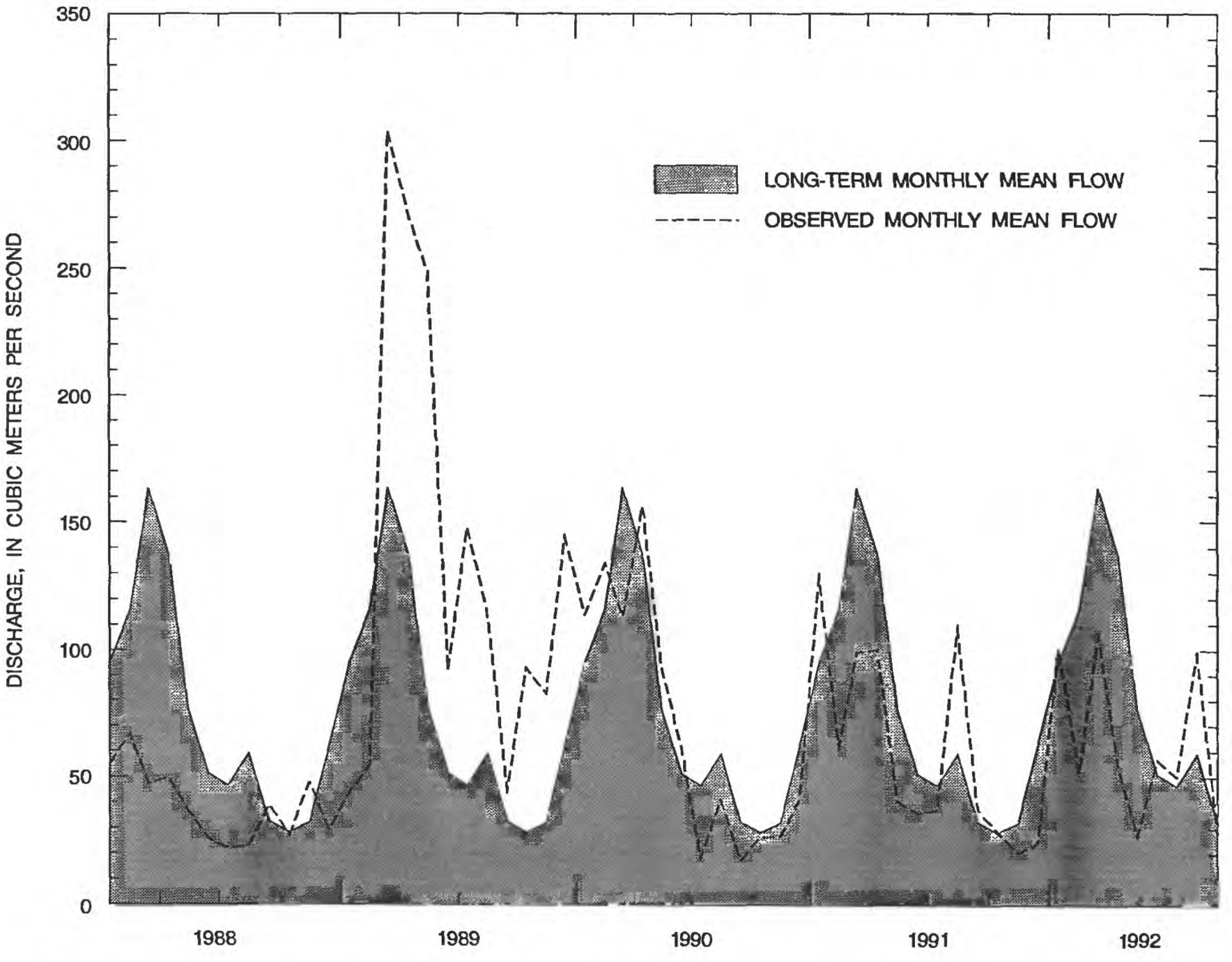

Figure 7. Long-term monthly mean flow during 1983-92, and observed monthly mean flow during January 1988 through September 1992 at Neuse River site F1.

based on water years 1983, when Falls Lake Dam began affecting flow, through 1992. A water year is the period from October 1 through September 30, determined by the calendar year in which the water year ends. With the exception of March 1990, the monthly mean flow values at site F1 were greater than average between March 1989 and June 1990. July 1990 through September 1992 was another low-flow period, when monthly means were less than average for 20 of the 27 months.

The average annual flow at site F1 (fig. 1) during 1983-92 was 74.9 cubic meters per second (m^3/s). By applying a drainage area ratio of 1.66 (11,600-km^2 drainage area at New Bern divided by 7,000-km^2 drainage area at site F1), an estimated average annual freshwater inflow of 124 m^3/s at New Bern is obtained. Using observed annual average flow at site F1 and the drainage area ratio, estimated annual average freshwater inflows at New Bern during the study period were 57 m^3/s in 1988; 198 m^3/s in 1989; 147 m^3/s in 1990; 103 m^3/s in 1991; and 90 m^3/s in 1992. Annual averages are based on the water year.

Flow data from sites F3, F4, and F5 (fig. 1) were used to estimate freshwater inflow from the 2,950-km^2 area that drains directly to the study reach. For each month between January 1988 and September 1992 when data were available, measured monthly mean flow at each of the three sites was converted to mean flow per square kilometer of drainage area; the three (or two) values were averaged, and the result was multiplied by the local inflow drainage area of 2,950 km^2 (table 8). Site F3 drains an area of 435 km^2, site F4 drains a 471-km^2 area, and site F5 drains a 67-km^2 area.

Estimated monthly mean inflow from the 2,950-km^2 area ranged from 2.4 m^3/s to 96 m^3/s, which is 86 percent of the estimated average annual freshwater inflow at New Bern. Estimated monthly mean freshwater inflows were less than 10 m^3/s 21 percent of the time, and less than or equal to 25 m^3/s about half of the time. The monthly mean flow per square kilometer of drainage area was higher 58 percent of the time at site F5 than at site F4. The estimated long-term annual mean inflow from the 2,950-km^2 area to the Neuse River estuary is 40 m^3/s, or about one-third of the estimated annual average freshwater inflow at New Bern.

Table 8. Estimated monthly mean freshwater inflow from the 2,950-square-kilometer area draining directly to the Neuse River Basin, 1988-92
[---, no data available]

Month	Flow, in cubic meters per second				
	1988	1989	1990	1991	1992
January	58	11	67	68	70
February	29	26	29	39	26
March	32	27	39	53	21
April	44	75	47	73	18
May	20	68	18	34	11
June	9.7	18	12	27	25
July	3.3	28	2.4	12	12
August	6.0	23	18	92	96
September	2.6	38	9.4	15	28
October	5.1	53	6.5	8.0	---
November	3.6	20	26	8.0	---
December	3.0	80	22	13	---

Currents

Measurements of time of travel and of currents have been made in the Neuse River estuary. Woods (1969) made two dye releases in the estuary during the summer of 1967. Dye from the July release, which was made about 4 km west of site S4 (fig. 3), was tracked for 6 days. At the end of the 6-day period, the dye cloud was 7.1 km long, with more dye on the north than on the south side of the estuary. Woods (1969) estimated an average dye transport rate of 5.4 cm/s during the period. Dye from the August release, which was made 4.2 km downstream from site WL1 (fig. 3), was tracked for 18 days. Ten days after the release, the dye cloud was 15.5 km long, and the estimated dye transport rate was 3.1 cm/s.

In August 1973, Knowles (1975) deployed nine current meters at sites located from approximately site S1 (fig. 3) to the mouth of the estuary at Pamlico Sound; the meters were in place for 38 days. At five sites, currents were measured near the channel bottom, and at two sites, currents were measured near the bottom and near the top of the water column. Knowles (1975) observed a complicated flow pattern, with strong lateral currents, circular flow across the estuary, and the presence of upstream and downstream currents. Mean longitudinal currents ranged from -2.2 cm/s (upstream) to 4.8 cm/s, but only one current

meter (located near site S5) showed a net upstream current during the deployment period. Knowles (1975) estimated that the mean net velocity in the Neuse River estuary during the 38-day period was 1.8 cm/s, giving a transit time from New Bern to Pamlico Sound of 32 days. Woods (1969) estimated the transit time during his studies to be about 27 days. However, Knowles (1975) cautioned that, "because of the complicated cross-stream, upstream flow *** materials could remain in a local area for a time considerably longer than that predicted by the *** transit time." The presence of a fairly strong M2 tidal signal (lunar, semi-diurnal) was detected in the record of seven of the nine meters. Knowles concluded that the primary effect of winds on circulation in the Neuse River estuary was diurnal and indirect through oscillations in Pamlico Sound, although winds seemed to directly affect surface currents in the estuary during the afternoon hours.

During this study, 10 Aanderaa RCM4 current meters were deployed on October 17, 1989, and recovered on November 3, 1989 (fig. 3; table 1). At each of the 10 sites, current speed and direction, water temperature, and specific conductance were recorded at 5-minute intervals at a location about 1.5 m above the channel bottom. One meter (site V1, fig. 3) was located near the upstream end of the study reach, three meters were placed across the channel near Cherry Point (sites V2, V3, and V4; fig. 3), and the remaining six meters were deployed across the channel near the downstream boundary of the study reach at Oriental (sites V5, V6, V7, V8, V9, and V10; fig. 3).

Locations for meter deployment were selected and identified on topographic maps and nautical charts. The latitude, longitude, and horizontal distance from the shore were determined from the charts for each location. The compass heading for the line along which the meters were to be deployed (fig. 3) also was determined from the charts. In the field, locations for meter deployment were identified by starting near the shore at a predetermined landmark, cruising along the proper compass heading, and using radar to determine the distance from the shore. Loran-C was insufficiently accurate for identifying meter location, so exact independent field determinations of meter latitude and longitude were unavailable. The latitude and longitude values given for each meter in table 1 are the values determined from the charts.

Near the upstream end of the study reach, the longitudinal axis of the Neuse River is oriented downstream at an angle of 146° (fig. 8). Near Cherry Point, the longitudinal axis is oriented downstream at an angle of about 103° east of north (fig. 8). In the eastern part of the study reach, the longitudinal axis of the estuary is oriented downstream at an angle of 56° east of north (fig. 8). Consequently, in subsequent discussions, downstream velocity at site V1 is defined as having a direction between 57° and 236° east of north, and upstream velocity is defined as having a direction of between 237° and 56° east of north. At sites V2-V4, downstream currents are those oriented between 13° and 192° east of north. Similarly, at sites V5-V10, downstream currents are those having a direction of between 327° and 146° east of north, and upstream currents are those oriented between 147° and 326° east of north.

During the meter deployment period, velocity ranged from a maximum downstream velocity of 48 cm/s at site V9 to a maximum upstream velocity of 52 cm/s at site V6 (table 9; fig. 3). These values were much higher than those measured by Knowles (1975) in the Neuse River in 1973, and were also higher than currents measured in the Pamlico River during August-September 1989 when the maximum downstream velocity was 31 cm/s and the maximum upstream velocity was 34 cm/s (Bales and Robbins, 1995). The highest mean velocity at the mid-estuary section occurred at site V4 near the south bank at the downstream section. The highest mean velocity was near the north shore of the estuary at site V6 (table 9). Median values of velocity at each meter were, with three exceptions, less than or equal to 7 cm/s and were less than mean velocity, indicating the presence of very low currents for much of the time during the deployment period.

The mean upstream and downstream currents measured at 9 of the 10 current meters during October 24-November 3, 1989, are depicted in figure 9. (Note: Data were collected at site V1 for only 6 days because of meter malfunction.) The orientation of the longitudinal axis of the estuary at each meter site is also included in the figure to show the mean direction of the currents relative to the estuary axis. The length of each vector is proportional to the velocity magnitude.

Even at the relatively narrow section of the estuary where meters V2, V3, and V4 were deployed (fig. 3), there was a marked difference in currents across the estuary (fig. 9). Velocities were generally lower on the north side (site V2) of the estuary than at

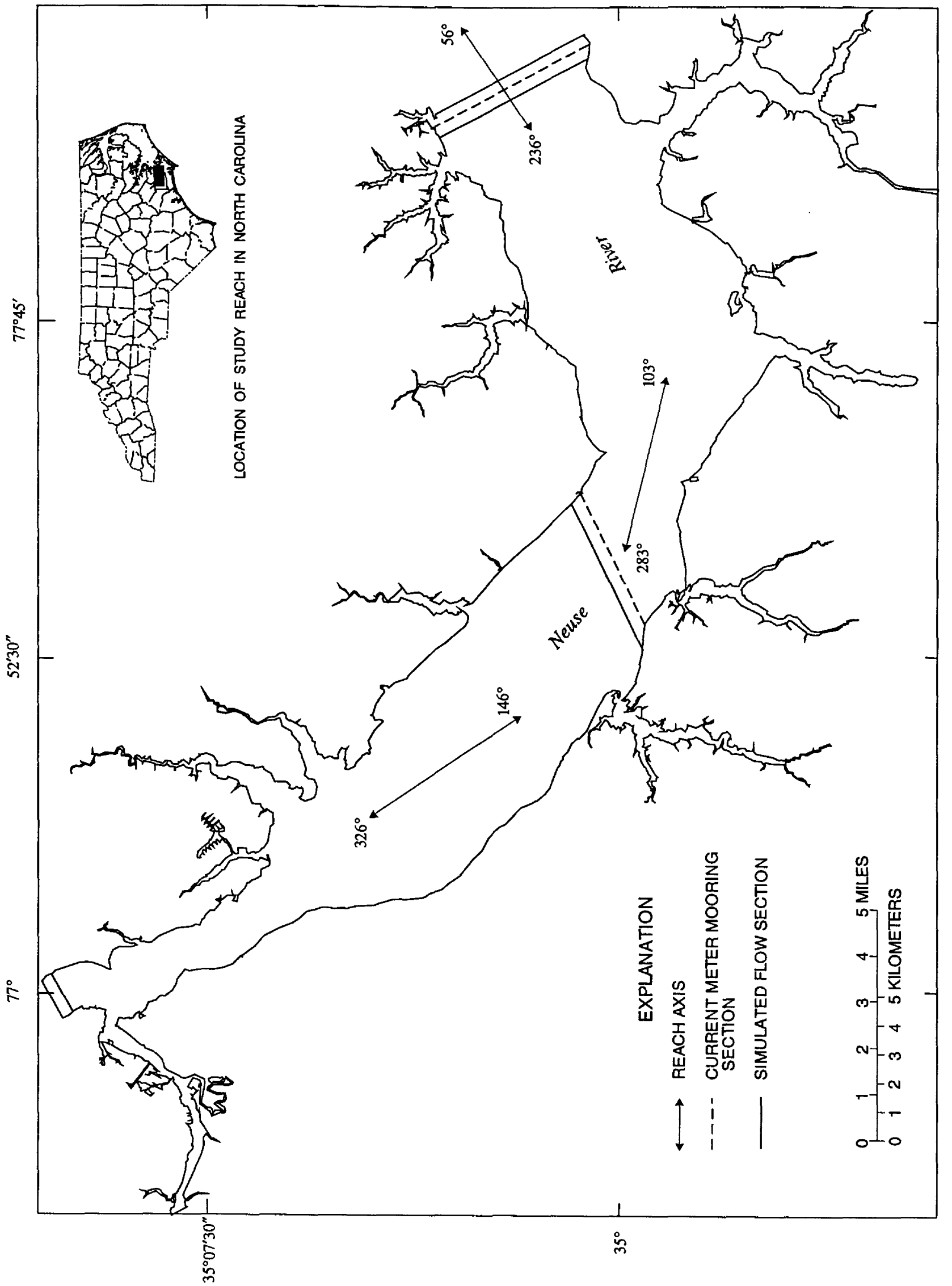

Figure 8. Orientation of longitudinal axis upstream reach, mid-estuary, and downstream reach, current meter mooring sections, and simulated flow sections.

sites V3 and V4 on the south side (table 9; fig. 9). Upstream currents were more frequent at sites V2 and V3, but downstream currents predominated at site V4, although the mean downstream currents exceeded mean upstream currents at sites V3 and V4. Downstream currents at sites V3 and V4 were directed more nearly along the longitudinal axis of the lower reach of the estuary than the axis of the mid-estuary reach (fig. 9).

Table 9. Summary of current velocities measured during October 17-November 3, 1989, at moored current meters in the Neuse River estuary
[cm/s, centimeters per second]

Site (fig. 3)	Downstream velocities			Upstream velocities		
	Mean (cm/s)	Median (cm/s)	Maximum (cm/s)	Mean (cm/s)	Median (cm/s)	Maximum (cm/s)
V1[a]	6.8	5	26	10.1	5	32
V2	7.5	6	30	6.4	6	19
V3	8.7	7	36	7.8	7	42
V4	9.6	9	38	9.1	7	38
V5	5.9	5	22	8.1	6	37
V6	11.0	10	30	13.2	12	52
V7	6.9	5	38	7.8	6	44
V8	5.6	4	38	7.6	5	50
V9[b]	5.6	3	48	7.3	5	37
V10	5.3	5	22	6.0	6	29

[a]Data collected October 17-22, 1989.
[b]Data collected October 13-30, 1989.

The presence of the relatively deep channel near the north shore (fig. 10) at the downstream measurement section (sites V5-V10, fig. 3) apparently affects the distribution of currents in the lower reach of the estuary. Velocities were greatest at site V6, which was located in the deepest part of the cross section. Currents were generally downstream during the measurement period at sites V5, V6, V7, and V8. At all meters, the mean upstream currents were directed toward the north shore, particularly on the south side of the estuary. It is possible that outflow from South River (fig. 3) could have resulted in the northwesterly mean upstream currents. Mean downstream currents generally were aligned with the axis of the estuary.

The measured velocity vectors (magnitude and direction) were reformatted in terms of north-south and east-west components to further illustrate the characteristics of the velocity. Each point in figure 11A represents the north-south and east-west components of one velocity measurement. Points falling on the longitudinal axis indicate currents in the upstream or downstream direction. Currents at site V2 were in the upstream direction the majority of the time (fig. 11A and B), but downstream currents were greater than upstream currents. The direction of upstream currents at site V2 varied widely (fig. 11A and B), whereas downstream currents were generally along, or slightly to the south of, the longitudinal axis of the estuary. Downstream currents at site V2 were typically parallel to the north shore near the site. Current directions at site V6 were focused fairly tightly around the longitudinal axis (fig. 11B), with fewer cross-channel currents than at site V2. At site V6, currents also were distributed fairly evenly between the upstream and downstream direction.

Bathymetry

Bathymetric data for the Neuse River estuary were obtained from the National Ocean Survey (NOS). Approximately one million soundings were recorded for the study reach. Additional depth points were digitized from the 1:40,000-scale NOS chart for the Neuse River (chart number 11552). NOS data, which were referenced to mean low water, were adjusted to the sea level datum.

The 0-, 1.5-, and 3.0-m (0-, 5-, and 10-foot [ft]) elevation contours around the study reach were digitized from 1:24,000-scale USGS topographic maps. Spot elevations which were below the 3.0-m (10-ft) contour were also digitized from the topographic maps to complete the bathymetric data base.

At a level water-surface elevation of 0.0 m, the total water volume in the study reach is 7.313×10^8 cubic meters (m^3), and the surface area is 2.320×10^8 square meters (m^2). Assuming a long-term freshwater inflow of 124 m^3/s (see Freshwater Inflow section), the ratio of the study reach volume to the inflow rate is about 68 days (retention or residence time has no precise meaning for estuaries). During the 1988-92 study period, this ratio varied between 43 days (1989) and 148 days (1988).

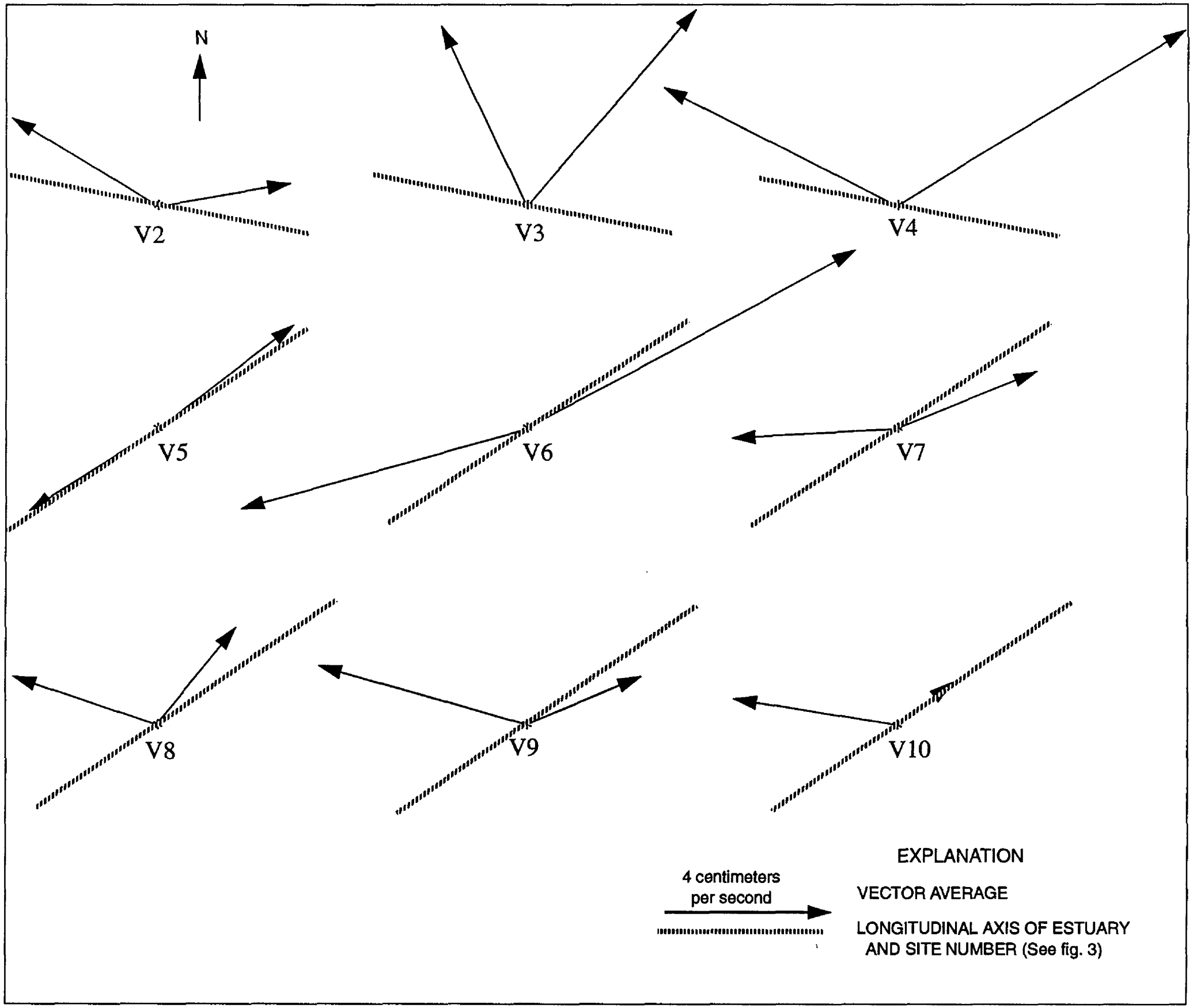

Figure 9. Upstream and downstream vector averages of observed current meter data at each meter location in the Neuse River for October 24-November 3, 1989.

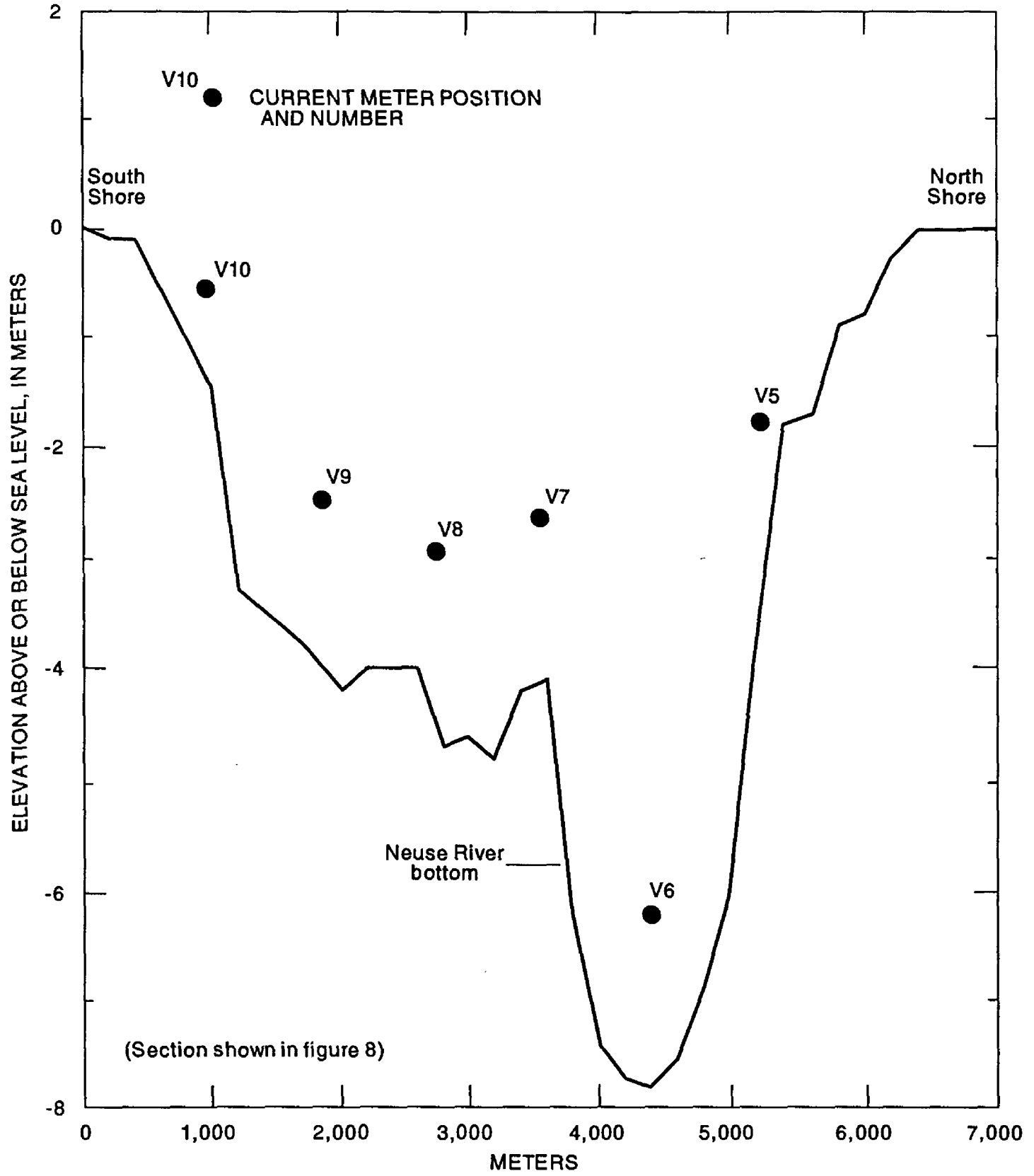

Figure 10. Cross section showing position of current meters at downstream measurement section of the Neuse River.

MODELING APPROACH

The modeling approach chosen for the Neuse River estuary was based on the objectives of the investigation, the observed physical characteristics of the estuary, and the time and funding constraints of the study. Pertinent physical characteristics of the estuary included water-level fluctuations, wind effects, freshwater inflow, and salinity regime. The amplitude of astronomical tides in the estuary and Pamlico Sound is small, and wind has a significant effect on water levels in the sound. The daily water-level range in the Neuse River estuary is typically less than 0.3 m, and the daily salinity range is about 3 ppt. Although the estuary is shallow, stratification does occur; however, the stratification is relatively weak and does not generally persist for extended periods of time. Lateral water-level and salinity gradients exist in the estuary, and large differences in velocity magnitude

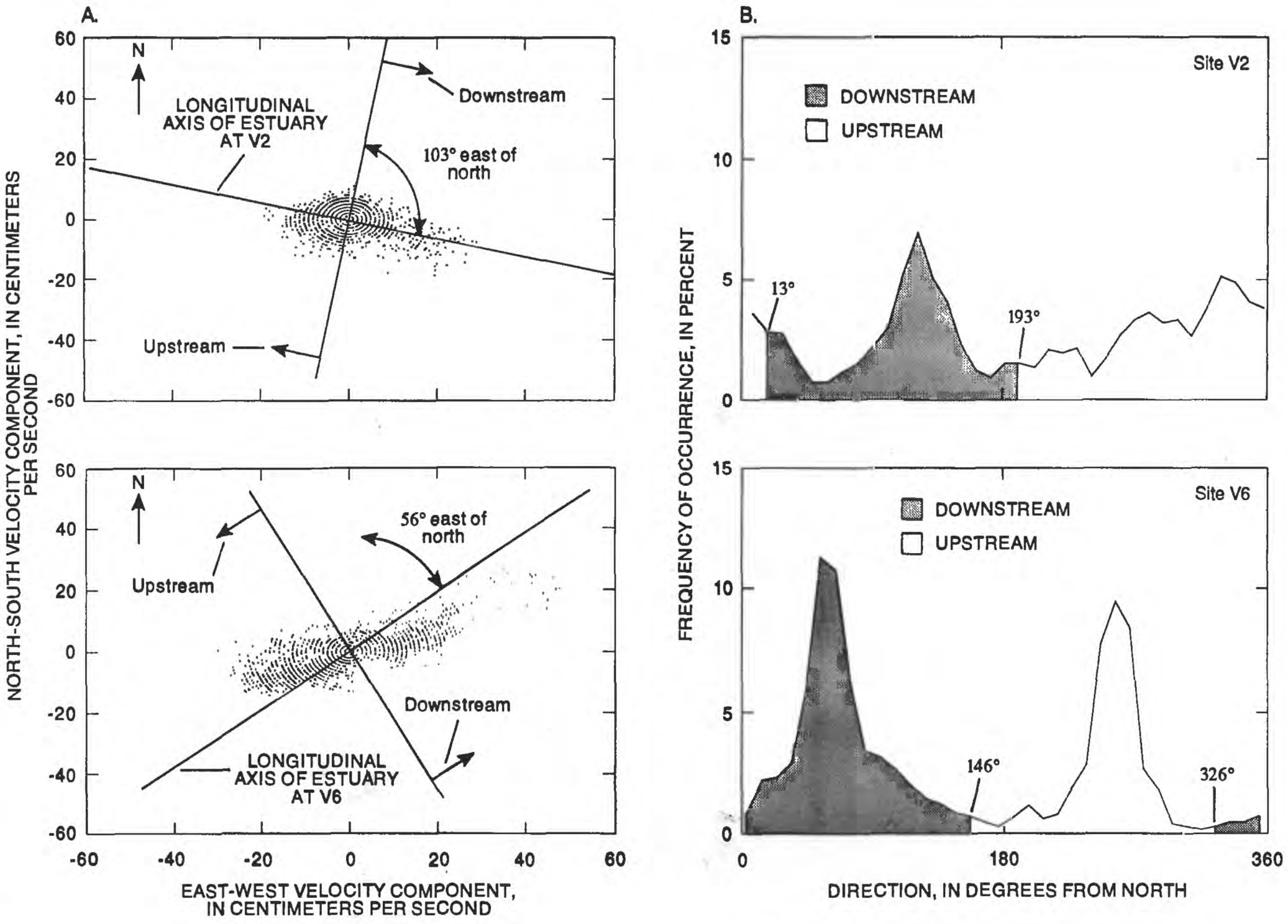

Figure 11. (A) Longitudinal and lateral velocity components and (B) frequency of occurrence of observed velocity direction at sites V2 and V6 in the Neuse River during October 24-November 3, 1989.

and direction occur across the estuary. Because of the weak astronomical tides and low inflow-to-volume ratio, flow velocity values are usually small.

Previous investigations provide useful insight in selecting the modeling approach. Hunter and Hearn (1987) evaluated lateral and vertical variations in the wind-driven circulation of long shallow lakes and concluded that for most natural bathymetries, lateral circulation is predominant over vertical circulation. Signell (1992) also noted that estuarine flushing by wind is often adequately represented by using a depth-averaged model, particularly when variations in bathymetry exist. Garvine (1985) investigated the effects of local and remote wind forcing on estuarine circulation. He concluded that (1) water-level and barotropic current variations are dominated by remote wind forcing, and (2) the water-surface slope is generated in response to local wind and is in phase with the local wind stress. As previously discussed, water-level fluctuations at the downstream boundary of the study reach appear to be primarily the result of wind-induced water-level fluctuations in Pamlico Sound. Consequently, water-level fluctuations in the Neuse River are likely dominated by barotropic wind forcing in Pamlico Sound.

With regard to spatial averaging, available modeling options included (1) one-dimensional, (2) two-dimensional, vertically averaged, (3) two-dimensional, laterally averaged, and (4) three-dimensional approaches. Each of these approaches could include time-varying (unsteady) conditions or steady flow. Moreover, complete nonlinear governing equations could be simplified to include only linear partial differential terms.

Steady-flow and linear models were judged to be too simplistic to realistically characterize the circulation and transport regime of the estuary. Likewise, one-dimensional approaches would provide information only on the longitudinal variation in flow and transport, and would not adequately characterize circulation. At the time the investigation began (1988), nonlinear, unsteady three-dimensional models, which included coupled flow and transport equations, were not widely used to provide spatially detailed simulations of estuarine circulation and transport. In addition, computing power at that time made long-term simulations of flow and transport with such models somewhat impractical. Since 1988, improvements in computer hardware, enhanced visualization techniques, and declining costs, as well as additional experience with nonlinear, unsteady three-dimensional models which include barotropic and baroclinic forcing, have resulted in increased application of these models for simulation of estuarine circulation and transport. Nevertheless, spatially detailed, nonlinear, unsteady three-dimensional modeling continues to require significant computing resources.

A two-dimensional, vertically averaged modeling approach was selected. This approach allowed discretization of the estuary into small computational cells so that spatially detailed information on velocity, circulation, and transport could be simulated. Longitudinal and lateral movement of materials within the estuary can be simulated, including the mixing across and along the estuary of substances discharged at one shoreline. The vertically averaged approach, however, does not permit the direct simulation of vertical salinity gradients or the effects of these gradients on flow and transport. Additionally, gravitational circulation, which is the long-term net movement of water upstream along the channel bottom in response to the longitudinal salinity gradient, is not directly simulated by the vertically averaged approach, although the gravitational circulation can be included using empirical methods. Recognition of these assumptions inherent in the modeling approach is important for interpretation of model results, as well as to maintain scientific credibility of the investigation.

NUMERICAL MODEL DESCRIPTION AND IMPLEMENTATION

The two-dimensional, vertically integrated, unsteady flow and transport model SIMSYS2D (Leendertse, 1987) was applied to the Neuse River estuary study reach. The model was first developed for applications in Jamaica Bay, New York (Leendertse and Gritton, 1971). Since that time, the model has undergone numerous revisions and updates and is now probably the most widely used,

best-documented model of vertically integrated hydrodynamics in the world. Among its many applications, the model was used to investigate flooding and drying of tidal flats in Port Royal Sound, South Carolina (Schaffranek and Baltzer, 1988), to quantify the effects of dredge and fill on circulation in Tampa Bay, Florida (Goodwin, 1987), and to aid in the design of the Dutch Delta Works (Leendertse and others, 1981). In an application of the model to Puget Sound, Chu and others (1989) reported that the model was capable of reproducing the major tide and current characteristics in the sound. A modified version of the model was used by Ridderinkhof and Zimmerman (1992) to evaluate mixing and chaotic stirring in the Dutch Wadden Sea.

Westerink and Gray (1991) described the model as "a very comprehensive modeling package which is based on a staggered ADI [alternating-direction implicit] solution *** and includes many features such as various time stepping options, advective term discretization options, transport of passive tracers, coupled salinity transport, flooding and drying, the ability to include hydraulic structures, two forms of the bottom friction term including a form based on the sub-grid scale energy level, a parametric expression for turbulence effects, various formulations for horizontal dispersion, and reactions and local inputs for transport." This section includes a general description of the numerical model, followed by a more detailed discussion of model implementation. Implementation of the model for the Neuse River estuary included (1) development of the computational grid, (2) specification of boundary and initial conditions, and (3) selection of model parameters.

Model Description

The numerical model is based on the full three-dimensional equations of motion which are reduced to a set of two-dimensional equations by assuming that vertical accelerations are negligibly small and by integrating the equations throughout the depth of flow. The resulting equations are nonlinear, time-dependent, and retain coupling of motion and transport so that time-varying horizontal density gradients are included in the equations of motion. Because the nonlinear advective and bottom stress terms are retained in the governing equations, the presence of eddies can be simulated and residual circulation can be computed. The governing equations are applied at specified, equally spaced computational points within the study reach and are solved at successive time steps to provide a close approximation of the time history of water level, current velocity, and constituent transport in the estuary. This section summarizes the governing equations, the numerical procedures to solve the equations in the model, and the model input requirements. Bales and Robbins (1995) provide a more complete description of the governing equations than is given in this report.

Governing Equations

Estuarine flows are unsteady, nonuniform, and turbulent. Unsteady flows are those in which velocity at a point varies with time. Nonuniform flows vary spatially. In turbulent flows, the instantaneous value of velocity varies randomly with respect to space and time about some mean value.

The basic equations of unsteady, nonuniform, turbulent fluid motion are formulations of the law of conservation of mass and of Newton's second law of motion. Conservation of mass for the fluid is given by the equation of continuity, and mass conservation for dissolved or suspended substances is expressed by a transport equation. The law of conservation of momentum is given by the Navier-Stokes equation, which is the basic relation expressing Newton's second law for a viscous fluid. These equations apply to the turbulent flow of a minute parcel of fluid at an instant in time.

A deterministic description of turbulent flow at all points in time and space is not feasible. Consequently, following the original idea of Osborne Reynolds, the governing equations are simplified by decomposing quantities (velocity, pressure, and mass) into mean components and turbulent fluctuations. The equations are then averaged throughout a time interval, which is long relative to the time scale of the turbulent fluctuations. The mean quantity can also vary slowly with time, in which case the flow is characterized as unsteady turbulent flow.

The equations solved by the numerical model are as follows. The vertically integrated continuity equation is:

$$\frac{\partial z_1}{\partial t} + \frac{\partial (HU)}{\partial x} + \frac{\partial (HV)}{\partial y} = 0 \qquad (1)$$

where z_1 = water-surface elevation relative to a horizontal reference plane;
t = time;
x = longitudinal coordinate direction;
y = lateral coordinate direction;
H = $(z_1 + h)$, where h = distance from the channel bottom to the reference plane;
U = vertically integrated longitudinal velocity =

$$\frac{1}{H}\int_h^{z_1} u\,dz \qquad (2)$$

where u = point velocity in the longitudinal, or x-, direction; and
V = vertically integrated lateral velocity =

$$\frac{1}{H}\int_h^{z_1} v\,dz \qquad (3)$$

where v = point velocity in the lateral, or y-, direction.

The vertically integrated equation for conservation of longitudinal momentum is:

$$\frac{\partial U}{\partial t} + U\frac{\partial U}{\partial x} + V\frac{\partial U}{\partial y} - fV = -g\frac{\partial z_1}{\partial x} - \frac{g}{2}\frac{H}{\rho}\frac{\partial \rho}{\partial x} - RU$$

$$+ \frac{C_d \rho_a W^2 \sin\theta}{\rho H} + k_x\left[\frac{\partial^2 U}{\partial x^2} + \frac{\partial^2 U}{\partial y^2}\right] \qquad (4)$$

and the vertically integrated equation for conservation of lateral momentum is:

$$\frac{\partial V}{\partial t} + U\frac{\partial V}{\partial x} + V\frac{\partial V}{\partial y} - fU = -g\frac{\partial z_1}{\partial y} - \frac{g}{2}\frac{H}{\rho}\frac{\partial \rho}{\partial y} - RV$$

$$+ \frac{C_d \rho_a W^2 \cos\theta}{\rho H} + k_y\left[\frac{\partial^2 V}{\partial x^2} + \frac{\partial^2 V}{\partial y^2}\right] \qquad (5)$$

where f = Coriolis parameter, which is computed from the latitude of the estuary,
g = acceleration of gravity,
ρ = density of water,
R = bottom stress term,
ρ_a = density of air,
W = wind speed,
C_d = wind-stress coefficient,
θ = angle between wind direction and the positive y-direction,
k_x = longitudinal mixing coefficient, and
k_y = lateral mixing coefficient.

Because of the dependence of the momentum balance on salinity, the horizontal density gradient terms couple the momentum equations to the transport equation. Consequently, salinity distribution within the estuary affects the flow field through the presence of the horizontal density gradient, and the flow field affects the salinity distribution by transporting mass. The horizontal gradient of atmospheric pressure is not included in the model, which is a reasonable assumption for the 40-km length of the Neuse River estuary study reach.

Bottom stress (R) is related to the flow velocity using a quadratic formulation which is essentially a depth-dependent friction relation based on the assumption of a vertical logarithmic profile of horizontal velocity in a steady flow. In this case, the equivalent drag coefficient increases with decreasing depth, and the correct vorticity is produced at land

boundaries if the shoreline is adequately resolved by the computational grid (Signell and Butman, 1992). Parameters required in the computation of R include η, a resistance coefficient analogous to the Manning coefficient for steady flow; and α, which is an empirical value relating bottom stress to the time-varying horizontal-density and velocity gradients. Because the magnitude of bottom stress is a function of the direction of the current and the strength of the horizontal-density gradient, the term α increases the effects of bottom stress during flood flows and decreases the effects of bottom stress during ebb flows as a function of the horizontal-density gradient.

The last term in equations 4 and 5, which Leendertse (1987) calls a horizontal diffusion term, is the sum of viscous stresses, turbulent stresses, the horizontal gradient of the cross product of vertical deviations from the vertical mean, and the subgrid-scale momentum transfer. Viscous stresses oppose relative movement between adjacent fluid particles, but are small compared to turbulent stresses in estuarine flows. Turbulent stresses result from the Reynolds decomposition of the nonlinear Navier-Stokes equation and represent a turbulent momentum flux. The unsteadiness of the tidal flow affects turbulence mechanisms and structure (Gordon and Dohne, 1973; Anwar and Atkins, 1980). Partch and Smith (1978), in studies in a salt-wedge estuary, and Anwar (1983), in studies in well-mixed and stratified estuaries, reported turbulent mixing to be highly time dependent, with the most intense turbulent exchange occurring at the time of maximum current during ebb flow. Consequently, methods of predicting turbulent momentum flux should include temporal variability.

The third component of the so-called horizontal diffusion term results from vertical integration of the advection terms in three-dimensional horizontal momentum equations. For the longitudinal direction, the velocity at any point in the vertical ($u(z)$) is equal to the sum of the vertically integrated velocity (U) and the deviation of the point velocity from the vertically integrated value ($u_d(z)$). When three-dimensional horizontal momentum equations are vertically integrated, horizontal gradients of the cross products of $u_d(z)$ and $v_d(z)$ result. These gradients have been included in the horizontal diffusion term, as is the normal procedure for models in which dimensionality has been reduced by integration over the depth of flow, across the channel, or through a cross section.

Momentum (or energy) transfers that occur at horizontal scales greater than the model computational grid length are resolved by the model through computation of the velocity field. However, momentum transfers that occur at the subgrid scale must be described empirically and also are included in the horizontal mixing term. Within the model, subgrid-scale turbulent energy is computed as a constituent using the transport equation (eq 6). The subgrid-scale energy source is the energy loss from the main flow resulting from bottom stress, and energy sink is the decay of turbulent energy. Using this model of turbulent energy, vertically integrated energy is (1) dependent on previous conditions (the system has memory), (2) related to the square of the velocity, and (3) inversely related to the resistance coefficient. It also generally follows that prediction of subgrid-scale energy transfer becomes less important as the spatial resolution increases (the size of the computational grid decreases).

Various procedures have been used to compute the horizontal mixing coefficients, k_x and k_y (for example, Rodi, 1978; Rodi, 1987; and van Dam, 1988). In this model, horizontal mixing coefficients are computed as a function of the coefficient of kinematic viscosity, ν; an unadjusted horizontal mixing coefficient, k'; the horizontal gradient of the vertical vorticity; and the subgrid-scale energy (Leendertse, 1987; Bales and Robbins, 1995). One value of viscosity, ν, is assigned to the entire model domain. Likewise, one value of k' is assigned to the entire domain. The mixing coefficient for each computational cell is then computed at each time step from the vorticity and the subgrid-scale energy in the cell at that time.

The vertically integrated transport equation is:

$$\frac{\partial (HS)}{\partial t} + \frac{\partial (HUS)}{\partial x} + \frac{\partial (HVS)}{\partial y} + \frac{\partial}{\partial x}\left(HD_x \frac{\partial S}{\partial x}\right)$$

$$+ \frac{\partial}{\partial y}\left(HD_y \frac{\partial S}{\partial y}\right) + G = 0 \qquad (6)$$

where

S = constituent concentration,
D_x = longitudinal dispersion coefficient,
D_y = lateral dispersion coefficient, and
G = combined effect of sources, sinks, generation, and decay of S within the model domain.

The dispersion coefficient in each horizontal coordinate direction is assumed to equal the sum of a dispersion in the direction of flow (D_f) and an isotropic dispersion (D_i). The isotropic dispersion coefficient combines the effects of wind and waves, as well as molecular diffusion, residual terms from the vertical integration of the transport equation (as described above for the momentum equation), and subgrid-scale effects. D_i is specified by the model user. D_f is computed from the relation developed by Elder (1959) as a function of the depth of flow and flow velocity.

The final equation required by the model is an equation of state relating water density to water temperature and salinity. The equation of state used in the model is the relation derived by Eckert (1958):

$$\rho = \frac{\left[(5{,}890 + 38T) - (0.375T^2 + 3S_s)\right]}{\left[(1{,}779.5 + 11.25T - 0.0745T^2) - (3.8 + 0.01T)S_s + 0.698\,(5{,}890 + 38T - 0.375T^2 + 35S_s)\right]} \qquad (7)$$

where

T = water temperature in degrees Celsius, and
S_s = salinity in grams per kilogram (or parts per thousand).

Because density varies only slightly with temperature, temperature is assumed to be uniform throughout the model domain. Density and the horizontal density gradients are computed at every computational point and for every time step during a simulation.

In summary, the governing equations are (1) vertically integrated continuity equation (eq 1), (2) vertically integrated longitudinal momentum equation (eq 4), (3) vertically integrated lateral momentum equation (eq 5), (4) vertically integrated transport equation (eq 6), and (5) equation of state (eq 7). These five equations are solved simultaneously for the unknown water level (z_l), vertically integrated longitudinal velocity (U), vertically integrated lateral velocity (V), vertically integrated constituent concentration (S), and vertically integrated density (ρ).

Numerical Solution Scheme

The governing differential equations (eqs 1, 4, 5, and 6) cannot be solved analytically for the complex conditions that exist in the Neuse River estuary. Instead, these equations are solved using a procedure which replaces the continuous differentials in the equations by finite differences. Hence, each differential equation is reduced to an algebraic equation which can be solved for values at defined locations within the model domain.

The finite-difference equations are formulated on a space-staggered grid (fig. 12). According to Leendertse (1987), the space-staggered grid results in an efficient solution because velocity points are located between depth points on the grid for solution of the momentum equations (eqs 4 and 5), and because velocity points are located between water-level points for solution of the continuity equation (eq 1). A complete description of the finite-difference formulation of the continuity, momentum, and transport equations on the space-staggered finite-difference grid is given by Leendertse (1987).

The alternating-direction implicit (ADI) finite-difference method is used to solve the governing equations. The ADI method was first introduced by Douglas (1955) and Peaceman and Rachford (1955), and uses a splitting of the time step to obtain a multi-dimensional implicit method which provides second-order accuracy. The longitudinal momentum equation is solved during the first half of the time step, and the lateral momentum equation is solved during the second half of the time step. The advantage of the ADI method over other implicit schemes is that solution of each set of algebraic finite-difference equations requires only the inversion of a tridiagonal matrix (Roache, 1982). The stability and convergence characteristics of the ADI technique as applied to the governing equations were discussed by Leendertse

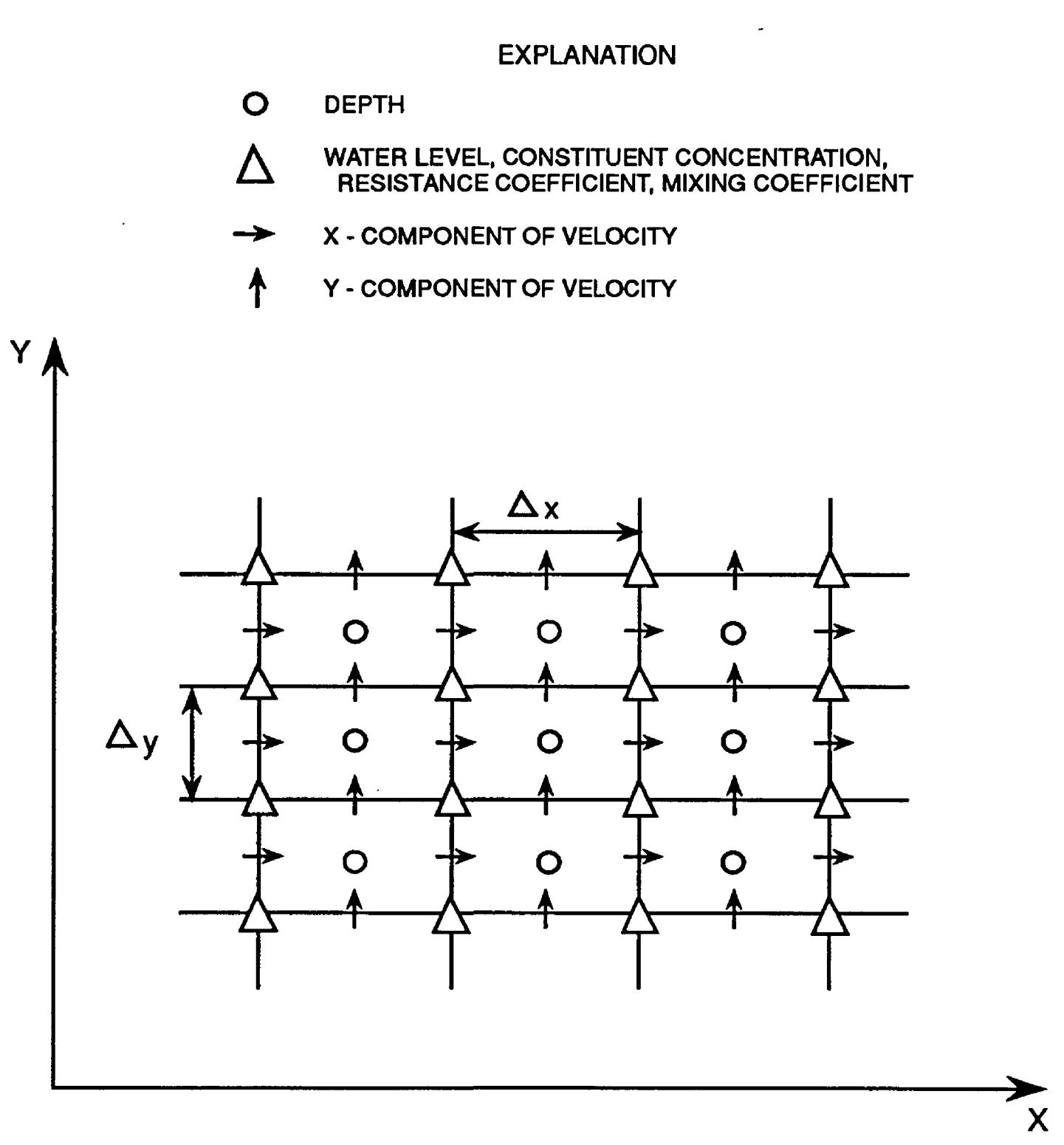

Figure 12. Location of variables on staggered finite-difference grid.

(1987). Although the method is theoretically and unconditionally stable, there are some practical limitations to the magnitude of the time step (Roache, 1982), particularly for model domains having irregular boundaries (Weare, 1979) or complex bathymetries (Benque and others, 1982).

Model Implementation

Implementation of the hydrodynamic and transport model for the Neuse River estuary included (1) development of the computational grid, (2) specification of model boundary conditions, (3) identification of initial conditions, and (4) selection of model options and parameters. In this section, the model domain, computational grid, and results of convergence tests for the computational grid are described. Procedures and associated assumptions for specification of boundary and initial conditions are given, and model parameters are identified.

Computational Grid and Time Step

The model domain extends from New Bern downstream to a section of the estuary just east of Oriental (fig. 13). The domain encompasses segments of most of the major tributary streams, including Upper Broad Creek, Goose Creek, Beard Creek, the Green-Kershaw-Smith Creek embayment near Oriental, Adams Creek, Clubfoot Creek, Hancock Creek, Slocum Creek, and the mouth of the Trent River.

A finite-difference solution to a partial-differential equation, such as is used in this model, is convergent if the numerical solution approaches the true solution of the differential equation as the finite-difference mesh size and the time step approach zero (Roache, 1982). Spatial convergency can be tested by repeatedly running the model with a fixed set of boundary conditions for successively smaller computational grid sizes. The model is convergent if no further change in model results is observed as the grid size is refined (Thompson, 1992). To determine the effects of grid size on model results, convergence testing should be included in modeling investigations and be conducted prior to model calibration.

Simulations of flow and transport in the Neuse River estuary were performed for three computational grid sizes: (1) 100 m x 100 m, (2) 200 m x 200 m, and (3) 400 m x 400 m. The model was run using the same set of boundary conditions for a 6-day period in June 1989. Initial conditions and model parameters for each of the three grid sizes were identical. Water level, salinity, transport, and circulation patterns from each simulation were compared to determine if model results were significantly different for the three grid sizes.

Simulated water levels were only slightly affected by changes in grid size. The simulated time of occurrence of maximum and minimum water levels also was generally unaffected by the grid size. Likewise, the mean and maximum simulated salinity at sites S1, S2, S3, S4, and S5 (fig. 3) did not change appreciably with grid size. However, changes in the distribution of salinity within the estuary were noted (fig. 14). For example, the 5 ppt line of equal salinity was at approximately the same location within the estuary for the 100-m and the 200-m grid simulation results, but was about 2 km farther downstream for the 400-m grid (fig. 14). The lines of equal simulated salinity for the 100-m and 200-m grids were generally in agreement with each other but differed from the results for the 400-m grid simulation, particularly in the reach of the estuary east of Minnesott Beach.

Differences also were evident in the simulated flow rates for the three grid sizes. The simulated mean flow for the 6-day period increased in magnitude with a decrease in grid size. The simulated mean flow at New Bern for the 200-m grid was 7 percent less than that for the 100-m grid, but was 14 percent more than that for the 400-m grid. Differences in simulated mean flows among the three grids were greater at the downstream boundary, where the simulated mean flow for the 200-m grid was 5 percent less than that for the 100-m grid, but 30 percent greater than that for the 400-m grid.

All hydrodynamic components of the natural system having a wave length less than twice the selected grid size cannot be resolved by the model. Components which cannot be resolved by the grid are essentially filtered (or aliased into lower frequency components) from the description of the hydrodynamics of the estuary (Abbott and others, 1981). Processes which occur at length scales smaller than the size of the grid spacing, or at the subgrid scale, must be described empirically in the model, so that increased spatial resolution results in more direct simulation of hydrodynamic processes and less empiricism in the model. In addition, small-scale flow features, which may be important for mixing and

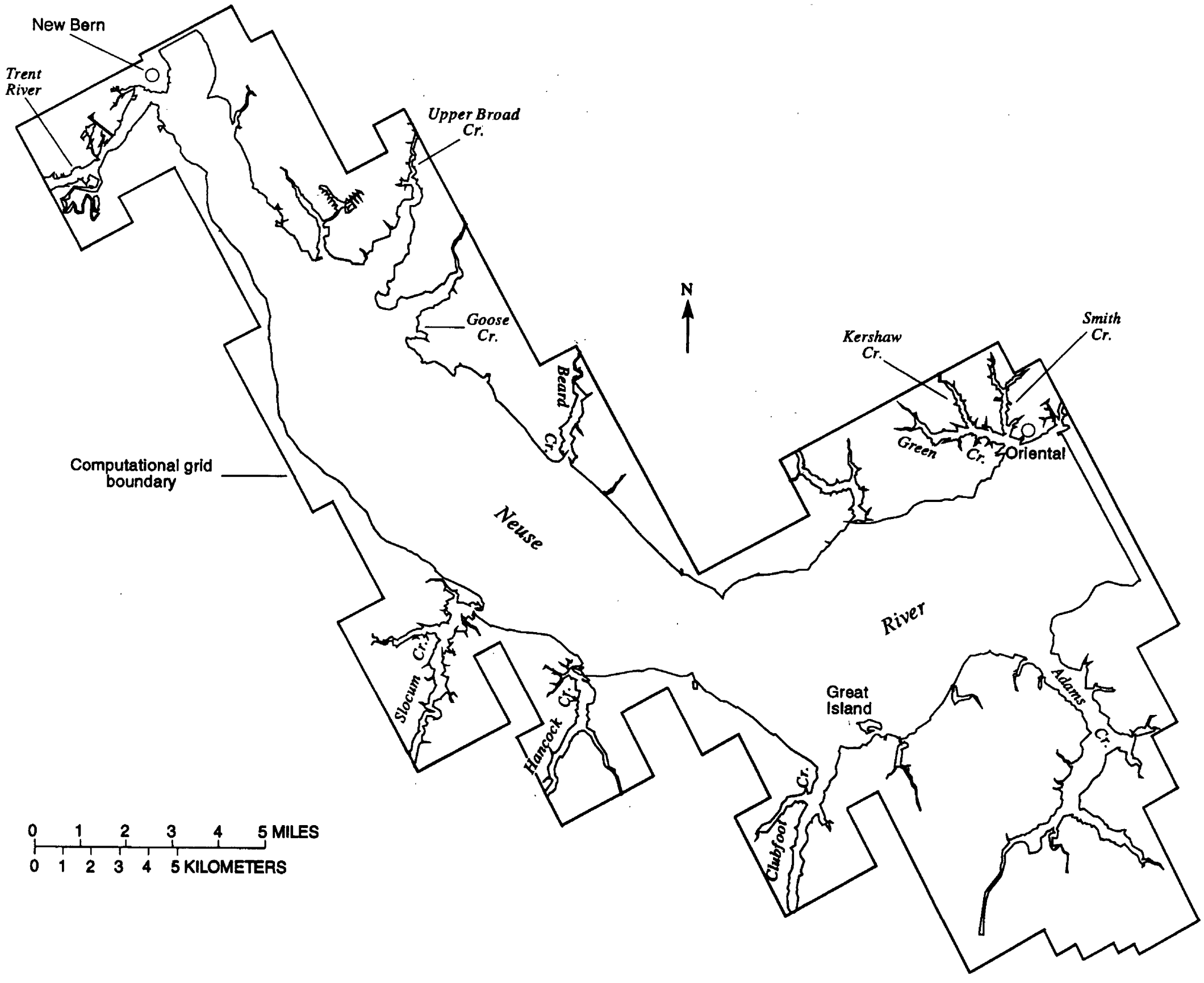

Figure 13. Computational domain for Neuse River model.

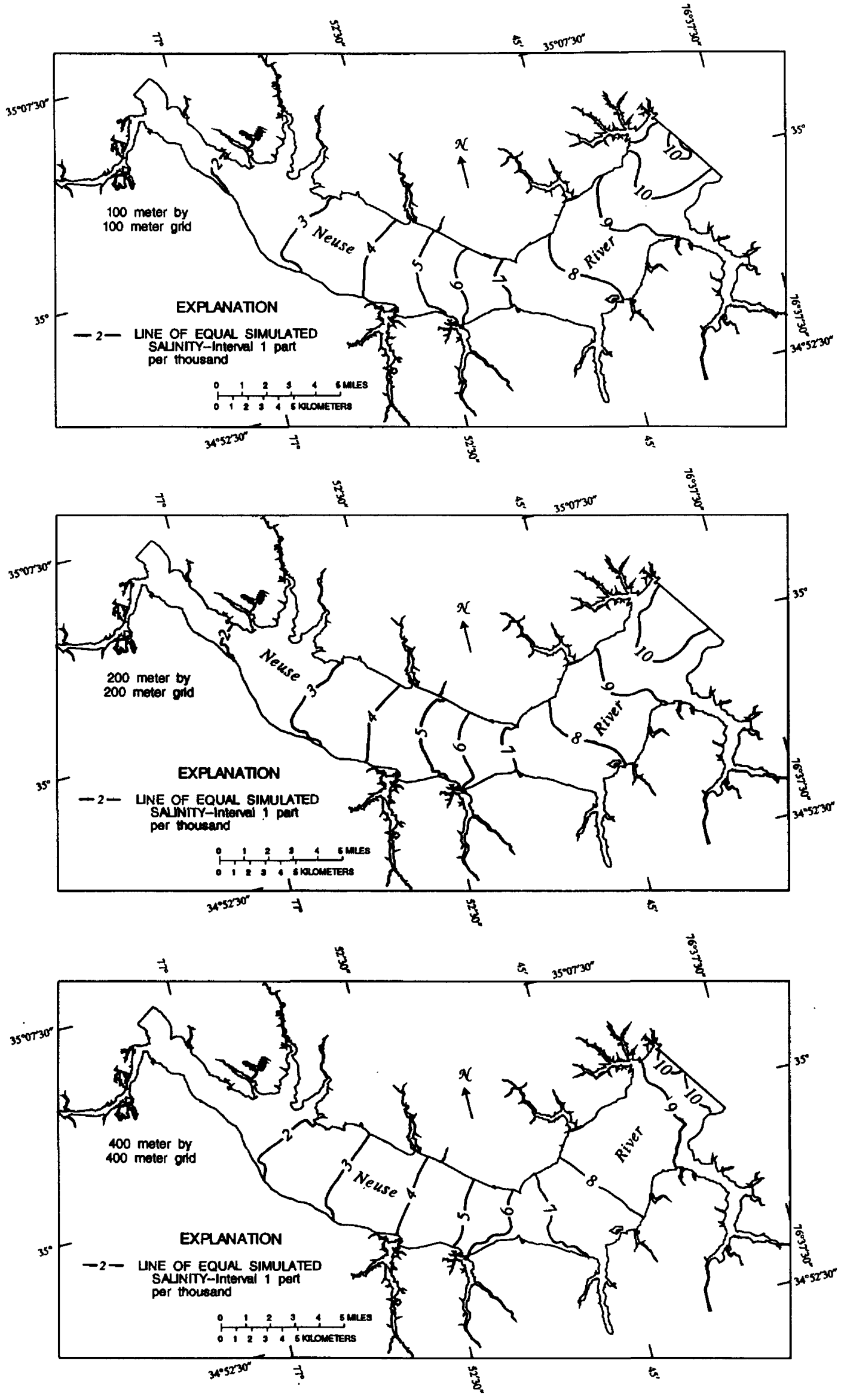

Figure 14. Lines of equal simulated salinity in the Neuse River 59.33 hours after start of simulation for three computational grid sizes.

transport processes but which are not otherwise resolved, can be simulated with spatially detailed grids. Because SIMSYS2D requires that flow channels be at least two computational cells wide, the smaller grid size also permits simulation of flow and transport into and out of more of the tributary streams and embayments along the estuary.

Results from simulations with the 200-m grid provide very good spatial resolution of the hydrodynamics in the Neuse River estuary. Because of the relatively small differences in simulated results for the 100-m and 200-m grids, and to minimize computational time based on the total number of computational cells in the model domain, the 200-m x 200-m grid size was selected for the Neuse River estuary model.

For the 200-m grid, there are 5,801 active computational cells bounded by the Neuse River shoreline; at a level water-surface elevation of 0.0 m throughout the Neuse River, the total water volume in the modeled area is 7.313×10^8 m^3. Water level, velocity, and salinity are computed for each of these cells during model simulations. Additional computational cells lie between the shoreline and the boundary of the model (fig. 13), but these cells generally do not enter into the computations.

Based on model results from the Pamlico River model (Bales and Robbins, 1995), a computational time step of 1.0 minute was used. Tests with the Pamlico River model (Bales and Robbins, 1995) indicated simulated salinities were essentially the same for time steps of 3.0, 1.0, and 0.5 minutes. Simulated mean flows using 0.5- and 1.0-minute time steps also were essentially the same. Consequently, a 1-minute time step was used.

Boundary Conditions

Information on boundary conditions is required at each computational step throughout a simulation. Boundaries of the Neuse River estuary model include the channel bottom, the shoreline and tributary streams, the water surface, a downstream (or eastern) open-water boundary, and an upstream (or western) open-water boundary near New Bern. A description of the assumptions and data used to describe conditions at each boundary follows.

Bottom Boundary

The channel bottom is assumed to be an impermeable boundary that prevents discharge of ground water to the estuary within the model domain and loss of water from the estuary to the ground-water system. Streams and estuaries in eastern North Carolina are typically discharge areas for ground water (Winner and Coble, 1989). Ground-water flow through the estuary streambed is probably small relative to the total flow in the estuary.

The channel bottom is assumed to be immobile. In the Neuse River estuary, fine-grained sediments typically occupy the main channel of the estuary, and sands are confined to the nearshore region (Wells, 1989; Wells and Kim, 1991). The large, mobile, sand bedforms that occur in alluvial streams and open seas do not exist in the Neuse River, and the assumption of an immobile channel bottom is reasonable under most conditions.

The channel bottom is assumed to cause resistance to the flow and thereby extracts energy from the mean flow. Resistance increases as the roughness of the bottom material increases. A resistance coefficient, η, analogous to Manning's n, was assigned to each computational cell. (Manning's n applies to steady-flow conditions only.) The resistance coefficient, which is an empirical value that cannot be directly measured, can vary from cell to cell throughout the model domain. The resistance coefficient is adjusted during model calibration, and bottom boundary conditions subsequently remain constant throughout the remainder of the simulations.

Several formulations for the bottom stress term (eqs 4 and 5) have been proposed and used in two-dimensional, vertically hydrodynamic models. The value of the resistance coefficient used in any given estuarine hydrodynamic model is somewhat dependent on the formulation of the bottom stress term in the model. Moreover, the resistance coefficient is directly dependent on the configuration of the channel bottom, as well as the material that forms the bottom. Nevertheless, resistance coefficient values applied in other studies were used as a general guide in selecting appropriate values for the Neuse River estuary model.

Some examples of previously used resistance coefficients in vertically integrated hydrodynamic models include the following: (1) 0.015 to 0.030 for Stefansson Sound, Alaska (Hamilton, 1992); (2) 0.017 to 0.033 for Singapore Strait (Shankar and others, 1992); (3) 0.018 to 0.035 for Masonboro Inlet, North Carolina (Masch and Brandes, 1975); (4) 0.02 for Pamlico Sound (Amein and Airan, 1976); (5) 0.0235 for Tampa Bay, Florida (Goodwin, 1987); (6) 0.0264 for Boston Harbor (Signell and Butman, 1992); (7) 0.028 for Long Island Sound and adjacent waters (Beauchamp and Spaulding, 1978); (8) 0.030 for Providence River, Rhode Island (Mendelsohn and Swanson, 1992); and (9) 0.030 for Cleveland Bay, Australia (King, 1992). During application of an earlier version of SIMSYS2D, Leendertse (1972) used resistance coefficient values of between 0.026 and 0.034 in a study of Jamaica Bay, New York.

Based on the Pamlico River model calibration (Bales and Robbins, 1995), a resistance coefficient value of 0.028 initially was assigned to all computational cells in the Neuse River estuary model. The resistance coefficient was varied between 0.025 and 0.030 during model calibration and testing. The model also offers the option of increasing the resistance at the open-water boundaries to improve model performance. Resistance was increased slightly at the open-water boundaries, but no change in simulated results was noted.

Shoreline and Tributary Streams

The shoreline is defined as a boundary across which there is no flow. The exact position of the shoreline can change during a model simulation because of flooding or drying of computational grid cells in response to water-level changes.

A "leak test" was performed to ensure that there were no unintentional openings in the shoreline boundary through which flow could leave the model domain. The test was performed by (1) prescribing an initially level water surface throughout the estuary, (2) assuming that water level at the upstream and downstream open boundaries did not vary from the initial conditions, (3) assuming that no salt was in the estuary or at the boundaries, and (4) assuming there was no wind at the water surface. For the assumed conditions, flow should be generated within the model domain only if there were openings in the shoreline. No leaks were observed.

Boundary conditions also are required for computation of flow adjacent to the shoreline. Computation of the component of flow perpendicular to the shoreline requires the assumption that the gradient of velocity perpendicular to the shoreline is zero. For computation of the component of flow parallel to the shoreline, the velocity at the shoreline and the differential of the velocity at the shoreline are assumed to be zero. Additional information and examples on computation of flow adjacent to closed boundaries are given by Leendertse (1987).

Tributary streams were treated as closed-end embayments. Water and salt movement into and out of these streams was simulated by the model, but no additional freshwater was added to the estuary through these tributaries. For most months, the freshwater inflow volume from tributary streams is small relative to inflow from the Neuse River (fig. 7; table 8). Moreover, the inflow volume of tributary streams is quite small relative to the total volume of the Neuse River estuary. Tests with the Pamlico River model (Bales and Robbins, 1995) showed that simulated circulation patterns were unaffected by the additions of tributary inflows; similar results would be expected in the Neuse River estuary.

If the Neuse River estuary model is subsequently used for simulation of water-quality processes, constituent loadings from tributary streams should be included in the model. This would be done by treating the tributary streams as open-water boundaries and prescribing a time series of water level (or flow), salinity, and constituent concentrations at the upstream, open-water boundary of the tributary streams.

Open-Water Boundaries

Time series of observed water level and salinity are required at the open-water boundaries. (The salinity boundary data are used in the computations only for the condition of flow into the model domain.) The upstream (western) water-level boundary data were measured at site WL1, and the downstream (eastern) water-level boundary data were taken from measurements at site WL4 (fig. 3). Upstream salinity boundary data were taken from measurements at site S2. Site S1 was in operation only briefly, and insufficient data were available for simulations (Garrett and Bales, 1991). Downstream salinity boundary data were based on measurements at site S4.

Data from site S5 were available only intermittently (fig. 4). Observed near-surface salinity from site S2 was applied at the upstream open-water boundary because of its distance from the boundary, and near-surface and near-bottom salinities at site S4 were averaged to provide a vertical mean salinity for the downstream boundary condition. Boundary conditions at the computational interval are linearly interpolated from data observed at 15-minute intervals.

Assumptions about velocities at the boundary are required for the condition of flow into the model domain. The longitudinal gradient of the velocity component perpendicular to the boundary is assumed to be zero. Likewise, the second derivative of the velocity, which is just inside and perpendicular to the boundary, is assumed to be zero. Finally, for the component of flow parallel to the open boundary, the advection terms in the momentum equations (eqs 4 and 5) are assumed to be zero, which indicates that flow is perpendicular to the boundary at the boundary.

These assumptions are generally required for the solution of a system of nonlinear, boundary-value equations, such as those solved by this numerical model. Moreover, the magnitude of each of these velocity terms assumed to be zero at or near the boundary is typically quite small. Consequently, these assumptions should have a negligible effect on the simulation results, and the effects should be confined to the region very near the boundary. Additional information on computations near open-water boundaries, along with examples, is given by Leendertse (1987).

Because the Neuse River estuary makes approximately a 90-degree bend near Minnesott Beach, it was possible to orient the computational grid to ensure that flow at each boundary was perpendicular to the boundary. The *y*-axis of the computational grid was oriented at an angle of 146° east of north, or along the longitudinal axis of the western segment of the study reach (upstream from Minnesott Beach). The *x*-axis was oriented at an angle of 56° east of north, or along the longitudinal axis of the eastern segment of the study reach.

Water-Surface Boundary

The "rigid lid" assumption is used in the description of the water surface. That is, the water surface in each computational cell moves vertically, but no deformation of the level water surface within the cell occurs. The rigid lid assumption implies that high-frequency, wind-generated waves are not included in the model. Inputs from precipitation and losses from evaporation are neglected for the relatively short simulation periods used in this investigation.

Momentum is transferred to the estuary by wind blowing over the water surface. Wind speed and direction measured at site W1 were used for the water-surface boundary condition. It was assumed that the wind speed and direction were spatially invariant over the entire model domain but that the wind was unsteady. Wind-speed and direction data at the computational interval are linearly interpolated from the data observed at 60-minute intervals.

Initial Conditions

Initial velocity, water-level, and salinity conditions must be described for each computational cell prior to model simulations. The velocity in each computational cell was assumed to be zero at the beginning of each simulation. The water surface was assumed to be initially level throughout the model domain. The initial water level was set equal to the average of the observed water level at sites WL1 and WL4 (fig. 3) at the beginning of the simulation. The upstream and downstream boundary water levels were measured at sites WL1 and WL4, respectively.

Initial salinity concentrations were determined from measured data at sites S2, S3, S4, and S5 (fig. 3) (when available). Initial values for computational cells between the three or four measurement sites were linearly interpolated from the mean of the observed near-surface and near-bottom salinities. For some simulations, observed salinity did not vary linearly along the longitudinal axis of the estuary, so some adjustment of the linearly interpolated initial values was required. The initial salinity conditions did not include lateral variations in salinity. As expected, model results during the first several days of simulation are very sensitive to estimated initial conditions.

The model can also be restarted using previous simulation results for water level, velocity, and constituent concentration in each computational cell as initial conditions for a subsequent simulation. When the model is restarted in this manner, the initial water surface need not be level.

Model Parameters and Options

Five model parameters must be chosen prior to model simulations: (1) C_d, the wind-stress coefficient; (2) α, which is used in the adjustment of the resistance coefficient; (3) k', the unadjusted horizontal momentum mixing coefficient; (4) D_i, the isotropic mass-dispersion coefficient; and (5) D_c, a coefficient that relates mass dispersion to flow properties. Because these parameters are empirical representations of a physical process, the parameters were not known with certainty and, thus, required some adjustment and testing during the calibration process.

The wind-stress coefficient seems to be a complex function of the roughness of the air-water interface, the fetch, the stability of the air mass above the water, the relative temperatures of the air and water, and the topography of the land upwind of the water body (Watanabe and others, 1983). Some sophisticated formulations are available for the computation of the wind-stress coefficient, and two of the most widely used are those of Garratt (1977) and Large and Pond (1981), both of which are based on measurements in the ocean. The wind-stress coefficient is often assumed to be constant for estuarine model applications, which is the approach taken for the Neuse River estuary model. A value of 0.001 was initially selected for C_d. This is in general agreement with coefficient values suggested by Wu (1969). For example, according to Wu, $C_d = 0.001$ for a wind speed of 4 m/s, and $C_d = 0.0015$ for a wind speed of 9 m/s. In other applications, Schmalz (1985) used $C_d = 0.001$ in a two-dimensional, vertically averaged model of the Mississippi Sound; Leendertse and Gritton (1971) and Goodwin (1987) used a value of 0.0008; and Svendsen and others (1992) used $C_d = 0.0012$.

The term α is used to relate the resistance coefficient to the strength of the horizontal salinity gradients and to the direction of flow. In the Neuse River estuary, flow velocities are generally low, and horizontal salinity gradients are typically small. Consequently, α was set to zero in all Neuse River estuary simulations. Subsequent tests indicated that non-zero values of α made no detectable difference in simulation results.

The parameter k' is used in the computation of the horizontal exchange of momentum. Horizontal momentum exchange, or mixing, depends primarily on the combined effects of spatial variations in the longitudinal and lateral velocities (Ridderinkhof and Zimmerman, 1990). Consequently, for models with spatially detailed computational grids (such as the Neuse River estuary model), currents which dominate horizontal mixing are directly computed by the model, and the so-called horizontal diffusion term becomes relatively small in comparison to other terms in the momentum equation. In fact, Signell and Butman (1992) neglected horizontal momentum exchange in an application of a two-dimensional, vertically averaged model of Boston Harbor, which used 200-m x 200-m computational-grid cells. Ridderinkhof and Zimmerman (1990) used a value of $k_x = k_y = 7$ square meters per second (m^2/s) in a two-dimensional, vertically averaged model with 500-m x 500-m computational cells.

Based on results from the Pamlico River model (Bales and Robbins, 1995), a value of $k' = 10$ m^2/s was initially used for the Neuse River estuary. Tests with a simplified model (Bales and Robbins, 1995) demonstrated that the correct simulation of lateral currents and eddies was fairly sensitive to the selected value of k'.

As with horizontal mixing of momentum, horizontal mass exchange is well represented in the spatially detailed Neuse River estuary model. Hence, there was less need to focus on calibrating the model to D_i and D_c because the processes represented by the parameters were small relative to the other terms in the transport equation (eq 6). Initially, D_i was set at 20 m^2/s, and D_c was set at 14 m^2/s, which was near the value given by Elder (1959). For the velocities and depths typically in the Neuse River estuary, D_f (which is computed from D_c) was much smaller than D_i. Tests with the Neuse River estuary model demonstrated that model results were relatively insensitive to changes in these two parameters.

The air density, latitude of the estuary, and kinematic viscosity of water are easily defined for the Neuse River estuary, assuming that air and water temperatures do not vary significantly during the simulation period. The other parameters previously described are known with less certainty and can require some adjustment during model calibration.

The orientation of the coordinate system must be specified by the user. As previously discussed, at long open boundaries, the governing equations are solved by assuming that the velocity parallel and adjacent to the boundary is zero, and that the gradient

of velocity perpendicular to the boundary is zero. In order to improve model performance near the open boundaries, the x-axis is usually aligned with the longitudinal axis of the estuary so that the y-axis is parallel to the downstream boundary. In the Neuse River estuary model, the y-axis is aligned with the longitudinal axis of the upper reach of the estuary, and the x-axis is aligned with the longitudinal axis of the lower reach of the estuary.

The model includes three primary user-specified options. The user can specify the type and frequency of model output. The numerical scheme for solution of the advective terms in equations 4 and 5 can also be selected. Options include (1) omitting the advective terms; (2) using the Arakawa method (1966), which results in the conservation of vorticity and squared vorticity in the simulation; and (3) using the Leendertse (1987) method, which is computationally more simple than the Arakawa method, but does not conserve vorticity. The Arakawa method is used in this application. The third user-specified option defines the procedure used to integrate the continuity (eq 1) and momentum (eqs 4 and 5) equations. Options define the time level at which the approximation of velocity and water-level terms are made in the finite-difference equations, as well as the spatial representation of these terms. The option recommended by Leendertse (1987), in which the velocity terms become essentially centered in time, was used in this application.

SIMULATION OF HYDRODYNAMICS AND SOLUTE TRANSPORT

Prior to calibration and validation of the Neuse River model, simulations were made for simplified conditions. Following these preliminary simulations, the Neuse River model was calibrated using data collected during June 1-24, 1991. Model validation was conducted using data from October 24, 1989, to November 3, 1989, when current meters were in place, and during September 1-30, 1991. The sensitivity of simulated results to small changes in various model parameters was documented. The model was then applied to simulate flow rates, circulation patterns, salinity distributions, and transport for several different forcing conditions. Finally, simulated model results from the Neuse River model were compared to results from the Pamlico River model for the same simulation period.

Preliminary Simulations

Preliminary simulations were made for the Neuse River model to evaluate model characteristics and the response of the Neuse River estuary to different forcings. First, the model was run with three and two open-water boundaries to determine the effect on circulation patterns within the estuary. Second, the model was run with and without salinity to evaluate some effects of baroclinic forcing on transport throughout the estuary. Third, wind applied over the estuary surface was varied to characterize the effects of wind on transport. And finally, the model was run with varying adjustments to the downstream water-level gage height (at site WL4) to assess sensitivity of model results to gage height at site WL4.

Open-Water Boundaries

Neuse River model simulations were made for 30 days with three and two open-water boundaries. The first simulation was made with open-water boundaries located near New Bern, Oriental, and in the mouth of the Trent River (fig. 3). Measured time-varying water-level data available at New Bern and Oriental were applied as the boundary conditions at the respective open-water boundaries. Measured time-varying water-level data from New Bern also was applied to the open-water boundary at the mouth of the Trent River because no recorded data were available at this location. The second simulation was made with open-water boundaries only near New Bern and Oriental with the model grid expanded to allow for movement and storage of water in the Trent River arm, now treated as a closed-end embayment. Simulated results indicated that the presence of the third open-water boundary had a limited, localized effect on flow patterns in the estuary. At the downstream end of the study reach, far from the influence of the third open-water boundary, the range in flow changed by less than 1 percent, with mean flow for the simulation period changing less than 10 percent. In the Trent River arm of the study reach, nearest the influence of the third open-water boundary, mean flow changed from 33 m^3/s upstream to essentially zero. However, the total range in flow changed only about 5 percent, indicating little change in the ability to simulate transport of water into and out of the Trent River arm. Therefore, subsequent simulations were made with two open-water boundaries because of the lack of

observed water levels at the mouth of the Trent River, and because of the limited effect of the third open-water boundary on overall circulation patterns in the estuary.

Salinity

To characterize some of the effects of baroclinic forcing on circulation and transport throughout the estuary, simulations were made for a 30-day period with and without salinity. There was little change in the range of flows between simulations made with and without salinity gradient. However, mean flow for the period was greatly influenced by the presence of salinity. Mean flow at each open-water boundary was in the downstream direction for the freshwater condition. With the addition of salinity and an average downstream-salinity gradient of about 0.2 part per thousand per kilometer (ppt/km) present for the simulation, the direction of mean flow at each open-water boundary was upstream. Therefore, inclusion of salinity and proper simulation of the longitudinal salinity gradient are major factors in determining overall circulation and transport throughout the estuary.

Wind

Simulations were made for a 24-day period in June 1991 using wind data from site W1 (at the Cherry Point Marine Corps Air Station) and site W2 (near the Pungo River) to evaluate the effects of wind on transport throughout the estuary. Winds at the two sites were generally from the same direction, with the predominant direction being from the south-southwest. Although the strongest winds (upper quartile) at site W1 were from the south-southwest, the strongest winds at site W2 were from the north-northeast. Also, mean wind speeds were nearly three times greater at site W2 (located over water) than at site W1 (located over land). The greater wind speeds and directional differences were evident in the simulated results. Directional differences in wind affected the mean transport throughout the estuary where strong winds from the north-northeast increased mean transport in the upstream direction by 44 percent at the downstream open-water boundary and 78 percent at the upstream open-water boundary. Increased wind speeds affected transport range with the range increasing about 3 percent at the downstream boundary and 12 percent at the upstream boundary. Because directional data seemed to play a key role in simulation processes, wind data measured at the nearer site W1 were used in subsequent simulations.

Water-Level Gage Height

In order to assess the sensitivity of model results to gage height, preliminary simulations were made with varying adjustments to the gage height at site WL4. A series of simulations was made for a 30-day period in May 1991. The model was run first with no gage-height adjustment, and then with a negative 1- and 2-cm adjustment in the gage height. The range of flows was unaffected by the gage-height adjustment, but the mean flow was greatly affected by the gage height (table 10). For the period, a lowering of the site WL4 gage height by only 1 cm resulted in an increase in the mean flow of more than 100 m^3/s. The change in mean direction of flow from upstream to downstream also affected the movement of salt through the estuary (table 10).

Table 10. Effects of gage height at Neuse River site WL4 on simulated flows and salinity for May 1-30, 1991

[m^3/s, cubic meters per second; cm, centimeter; ppt, parts per thousand]

Site WL4 gage height adjustment (cm)	Flow (m^3/s; positive downstream)		Mean salinity at site S3 (ppt)
	Upstream boundsry	Downstream boundary	
0	-128	-115	10.0
-1	7	6	8.3
-2	129	143	6.6

Calibration of Neuse River Model

The model was calibrated by adjusting model parameters and the downstream gage height for June 1-24, 1991. Mean water levels applied at the upstream and downstream boundaries were 0.301 m and 0.290 m, respectively, for the calibration period. These values are higher than the mean water levels recorded at sites WL1 and WL4 for the entire data-collection period (table 2) and higher than the monthly mean water level for June during the data-collection period (table 3). Highest water levels during the calibration period occurred between June 4 and June 8, and also near the end of the simulation (fig. 15).

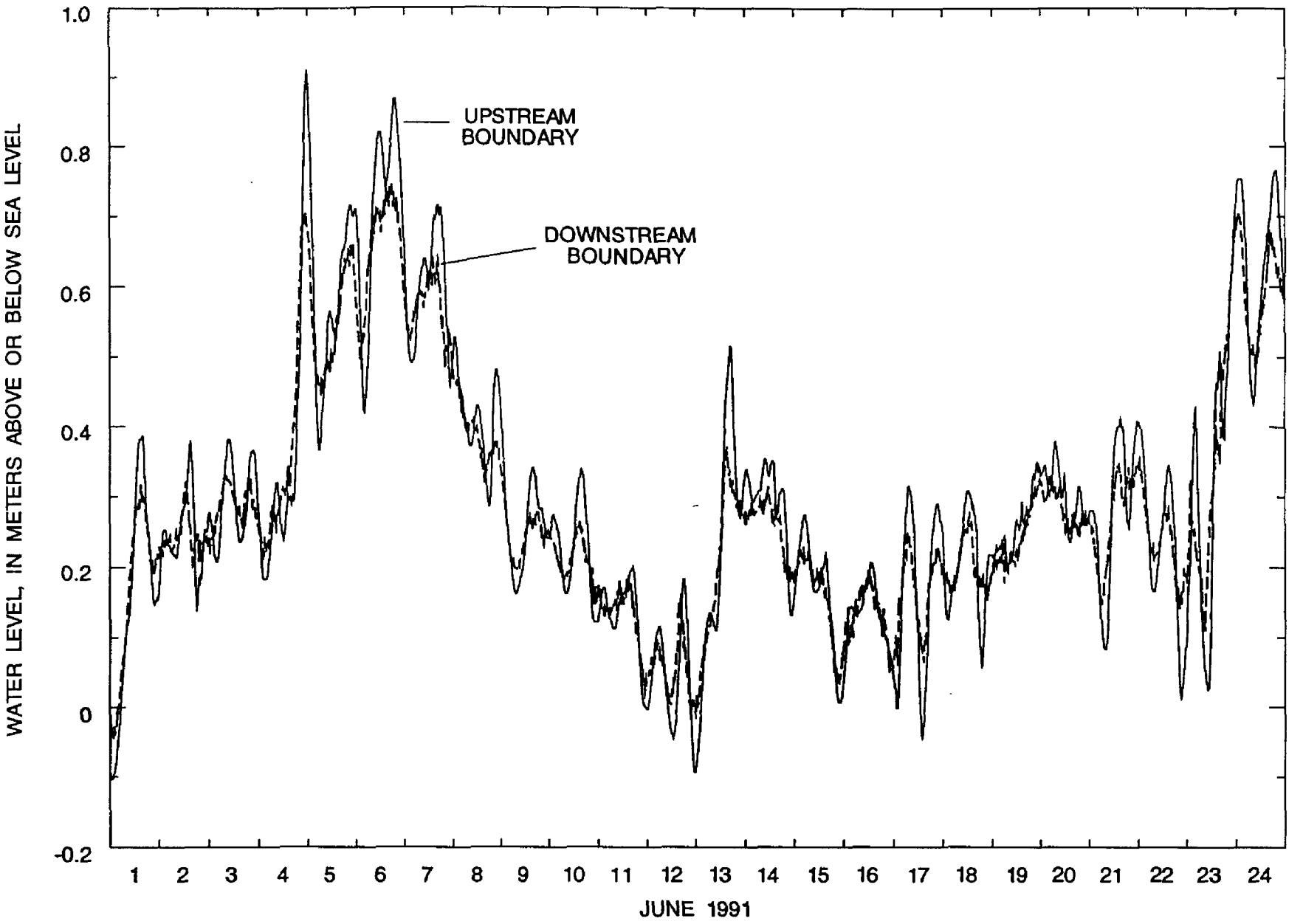

Figure 15. Water levels at model boundaries in the Neuse River for calibration period.

Mean salinity at the upstream and downstream boundaries for the calibration period was 8.0 ppt and 13.3 ppt, respectively. The near-surface salinity at site S2 and the average of near-surface and near-bottom salinity at site S4, which were applied as boundary conditions during the calibration period, were somewhat greater than salinity usually observed at these locations during June 1989-92. Monthly mean near-surface salinities at sites S2 and S4 for the month of June 1989-92 were 5.5 and 10.3 ppt, respectively, and near-bottom values were 7.9 ppt and 12.5 ppt, respectively (table 5). There was some stratification at site S2 from about June 1-4, and again during June 20-23 (fig. 16). The maximum difference between near-surface and near-bottom salinities at site S2 was about 10 ppt during this calibration period, in comparison with a monthly mean value of 2.6 ppt for June during 1989-92. Some stratification was present at site S4, as well as nearly tidal variation in near-bottom salinity for selected periods, which coincided with the presence of southerly winds. As suggested earlier (fig. 6), the high salinity with periodic variations at site S4 could be the result of transport from the ocean through the Intracoastal Waterway and up into Adams Creek (fig. 16). Wind measured at site W1 was primarily from the south-southwest (fig. 17) during the calibration period, which is typical for June (table 7). However, during June 4-8 and June 23-24, wind blew from the east-northeast, which corresponded to periods of higher water levels.

The model was calibrated by adjusting model parameters and the gage height at site WL4, and by comparing (1) simulated and observed water levels, (2) simulated and observed salinities, and (3) simulated mean flow at the upstream boundary and flow at site F1, (fig. 1) adjusted for the intervening drainage

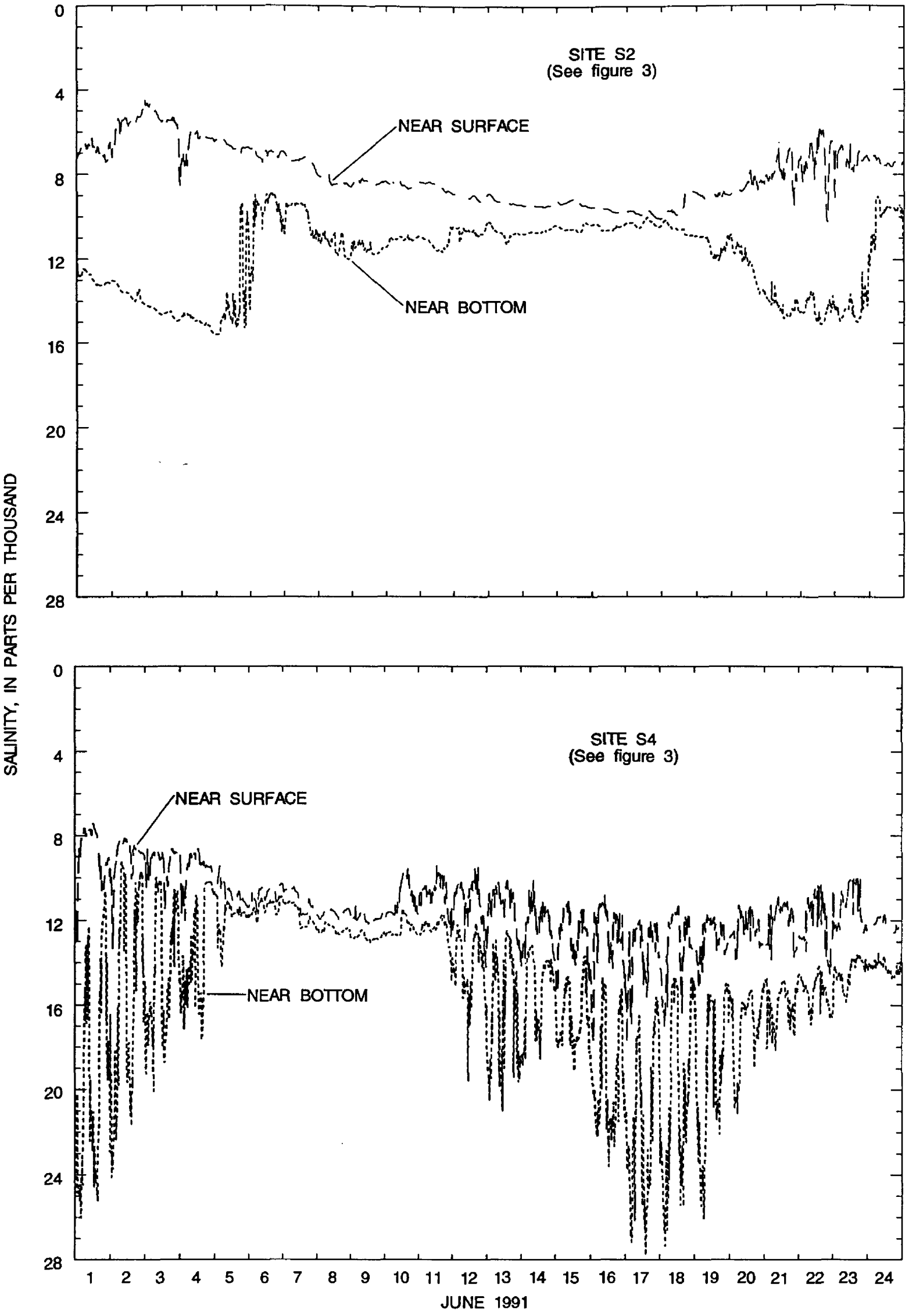

Figure 16. Near-surface and near-bottom salinity at model boundaries in the Neuse River for calibration period.

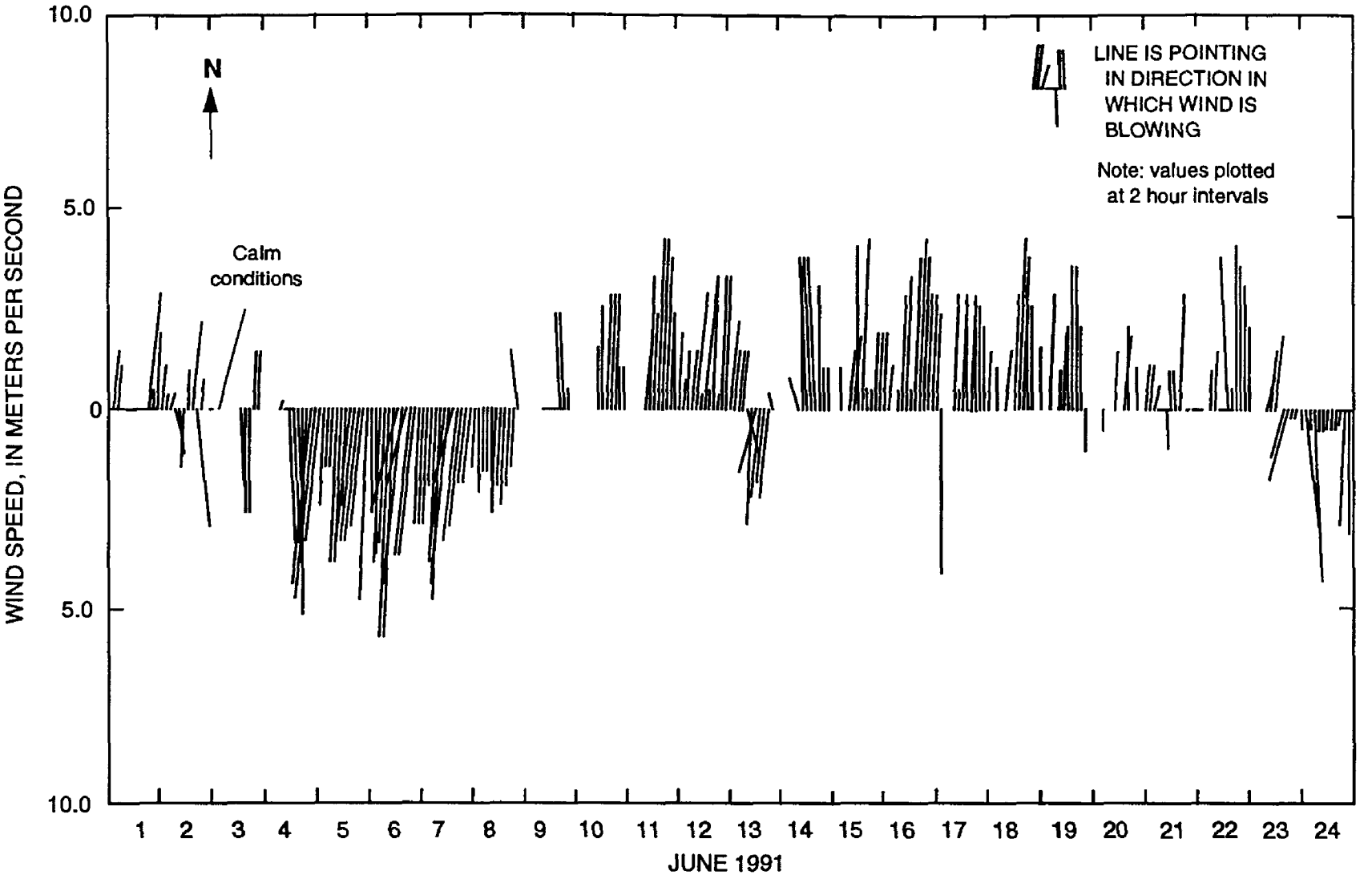

Figure 17. Wind speed and direction at site W1 in the Neuse River for model calibration period.

area. The following model parameters provided the best agreement between observed and simulated data: (1) $\eta = 0.028$ (resistance coefficient); (2) $C_d = 0.001$ (wind-stress coefficient); (3) $k' = 10$ m^2/s (unadjusted horizontal momentum mixing coefficient); (4) $D_i = 20$ m^2/s (isotropic mass-dispersion coefficient); and (5) $D_c = 14$ m^2/s (coefficient relating mass dispersion to flow properties).

Adjustment to the downstream gage height also was required during the calibration. The adjustments made during model simulations were small relative to adjustments made in the record during data collection. Preliminary simulations indicated that small changes to the gage height at site WL4 (fig. 3) resulted in large changes in mean flow during the simulation period (table 10). An adjustment of -3 cm to the gage height at site WL4 was used for the calibration period, resulting in a simulated mean flow at the upstream boundary of 56 m^3/s compared to a drainage area adjusted flow of 52 m^3/s at site F1.

The mean difference between simulated and observed water levels at site WL3 was -0.6 cm (the negative value indicates that observed values exceeded simulated values), and the root mean square (RMS) value was 2.4 cm. These values are about 3 percent and 11 percent, respectively, of the mean daily water-level range for June.

The absolute value of the mean difference between simulated and observed salinities at site S3 for the entire calibration period was less than 0.1 ppt with an RMS value of 1.2 ppt. The mean differences in simulated and observed values and the RMS values are less than the observed monthly mean of the difference between near-bottom and near-surface daily mean salinity for June. Salinity was slightly over-predicted during the early part of the simulation and slightly under-predicted during the latter part of the simulation (fig. 18).

Daily variations in simulated salinities were not as large as observed values. At least part of the smaller simulated variations could be because the downstream model salinity boundary condition is an average of near-surface and near-bottom observed salinities. Averaging these values tended to reduce some of the

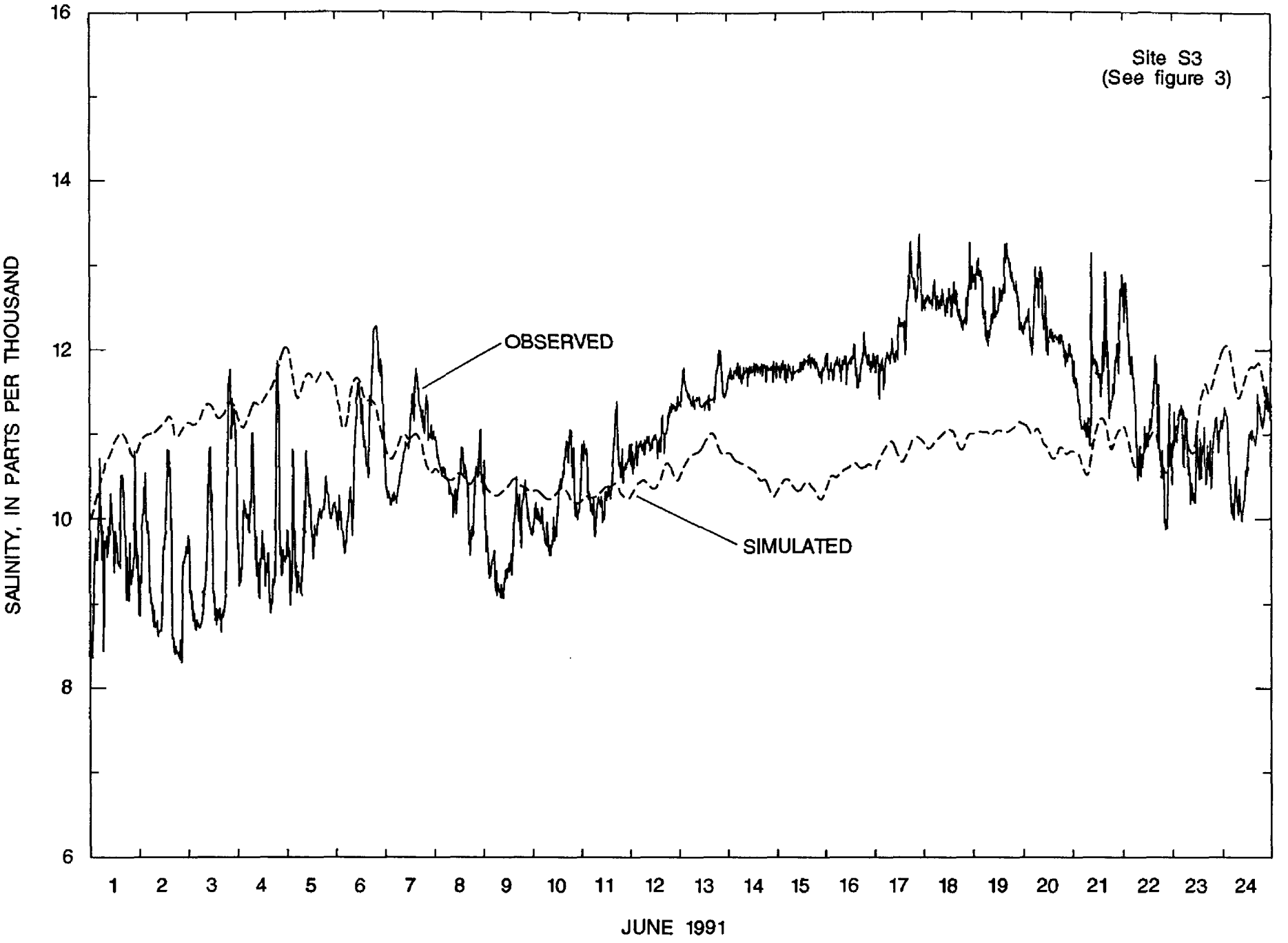

Figure 18. Simulated and observed salinity at site S3 in the Neuse River for model calibration period.

natural variation in the boundary salinity, which in turn resulted in less variation in simulated results.

Validation of Neuse River Model

Model validation is the process used to evaluate a model by testing it with observed data that were not used in the calibration procedure. The model was validated using data collected during two separate periods. Simulations were made for October 24 through November 3, 1989, which included the time when recording current meters were moored in the estuary. The model also was validated using data for September 1991.

1989 Validation Period

Boundary conditions for the October 24-November 3, 1989, validation period were treated the same as for the model calibration period, with two exceptions. First, because salinity data were unavailable at sites S4 and S5 for this period, the average of salinity data measured by recording current meters V5 through V10 (fig. 3) was used as the downstream salinity boundary condition. Second, an inspection of the water-level record and preliminary simulation indicated that a constant adjustment of -1 cm was applied to the gage height at site WL4.

The mean observed water levels for the 1989 validation period at the upstream and downstream boundaries were 0.437 m and 0.425 m, respectively.

These values were higher than the monthly mean for October or November (table 3), when monthly mean water levels were 0.328 m and 0.261 m at site WL1 in October and November, respectively, and 0.347 m and 0.270 m at site WL4 in October and November, respectively. Water levels were fairly uniform throughout the simulation period (fig. 19).

Observed salinity at the upstream boundary (site S2 near surface) ranged from 2.9 to 5.6 ppt (fig. 20), with a mean value of 3.9 ppt, which was lower than the average for October or November (table 5). Observed salinity at the downstream boundary ranged from 9.7 to 11.5 ppt during the 1989 validation period (fig. 20); and the mean salinity during the period was 10.8 ppt, which was higher than the mean values recorded for October. There was some stratification near the upstream boundary for much of the simulation period (fig. 20), but differences between near-surface and near-bottom salinities were never more than 2 ppt and averaged 1.2 ppt. Wind speeds during the period were less than 3 m/s about 50 percent of the time, with a maximum recorded speed of 5.6 m/s. Wind was from the north to northeast nearly 80 percent of the time (fig. 21).

Throughout the 11-day validation period, mean and RMS values of the difference between simulated and observed water levels were less than or equal to 3.0 cm (table 11), which is less than 20 percent of the mean daily water-level range for October and November (table 3). Observed salinity data at the interior checkpoint were only available for the first 2.3 days of the simulation. During this time, the mean and RMS values of the difference between simulated and observed salinity were less than the respective difference between near-bottom and near-surface salinity recorded in October at site S3 (table 6).

Simulated vertical mean velocities were more laterally uniform than observed point velocities at the mid-estuary section. Mean simulated velocities at the mid-estuary section also were more nearly aligned with the longitudinal axis of the upper part of the estuary than were observed velocities (sites V2, V3, and V4; figs. 9 and 22). As previously indicated, the meters may have been farther downstream than assumed (figs. 9 and 22; table 12). The mean difference between simulated vertical mean and the observed point velocities at the mid-estuary section were -1.2 cm/s at site V2, -3.0 cm/s at site V3, and -6.1 cm/s at site V4. Observed point velocities were generally underpredicted (table 12).

Table 11. Results of model validation for 1989 and 1991 validation periods
[cm, centimeter; ppt, parts per thousand]

Site (fig. 3)	1989 validation period		1991 validation period	
	Simulated minus observed		Simulated minus observed	
	Mean value	Root mean square velue	Mean value	Root mean square value
WL3—Water level (cm)	-2.6	2.9	-0.1	3.2
S3—Salinity (ppt)	.3	.5	.3	3.1

At the downstream measurement section (sites V5, V6, V7, V8, V9, and V10), simulated vertical mean velocities exhibited the lateral non-uniformity and the cross-channel flow (fig. 22) seen in the observed record (fig. 9), with best agreement occurring in the deeper sections on the north side of the estuary. Mean simulated and observed magnitudes were in better agreement than at the mid-estuary section, and there was no tendency toward over or under prediction. The mean difference between observed point and simulated vertical mean velocities for the 11-day period was less than or equal to 3 cm/s at all six downstream measurement sites.

Current measured at a single point in the water column can be markedly different from the vertical mean current at that location. Moreover, during periods when near-surface currents are downstream and near-bottom currents are upstream (which can occur in the Neuse River), a point velocity measured near the channel bottom is likely to be greater than the vertical mean current.

Differences of as much as 6 ppt existed between simultaneously measured near-surface and near-bottom salinities during the October 24-November 3, 1989, validation period. Consequently, it is not surprising that the vertically averaged simulated velocities were generally less than measured point velocities, particularly at the mid-estuary section where top-to-bottom salinity differences were greater

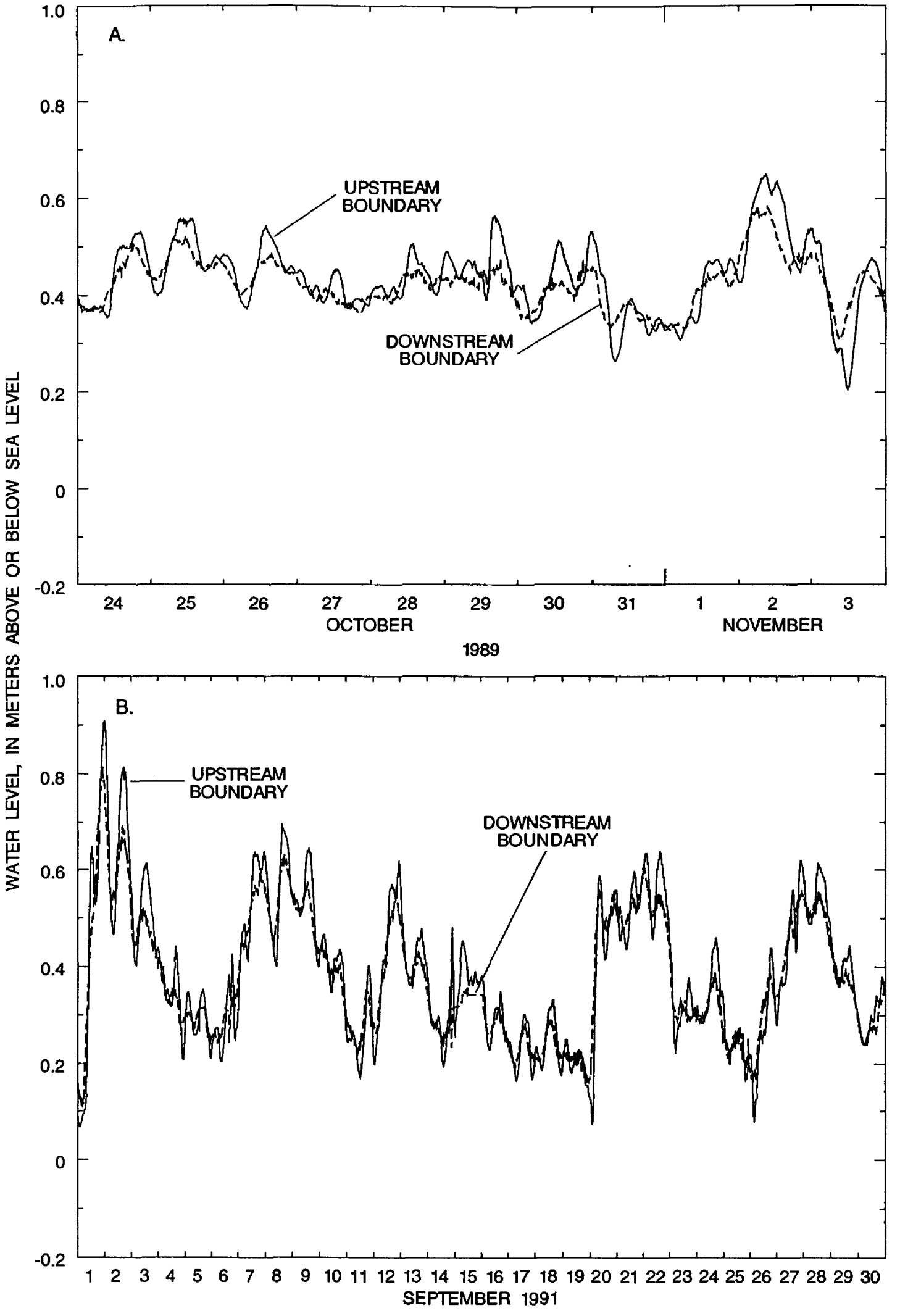

Figure 19. Observed water levels at upstream and downstream boundaries in the Neuse River for two validation periods: (A) October 24-November 3, 1989, and (B) September 1-30, 1991.

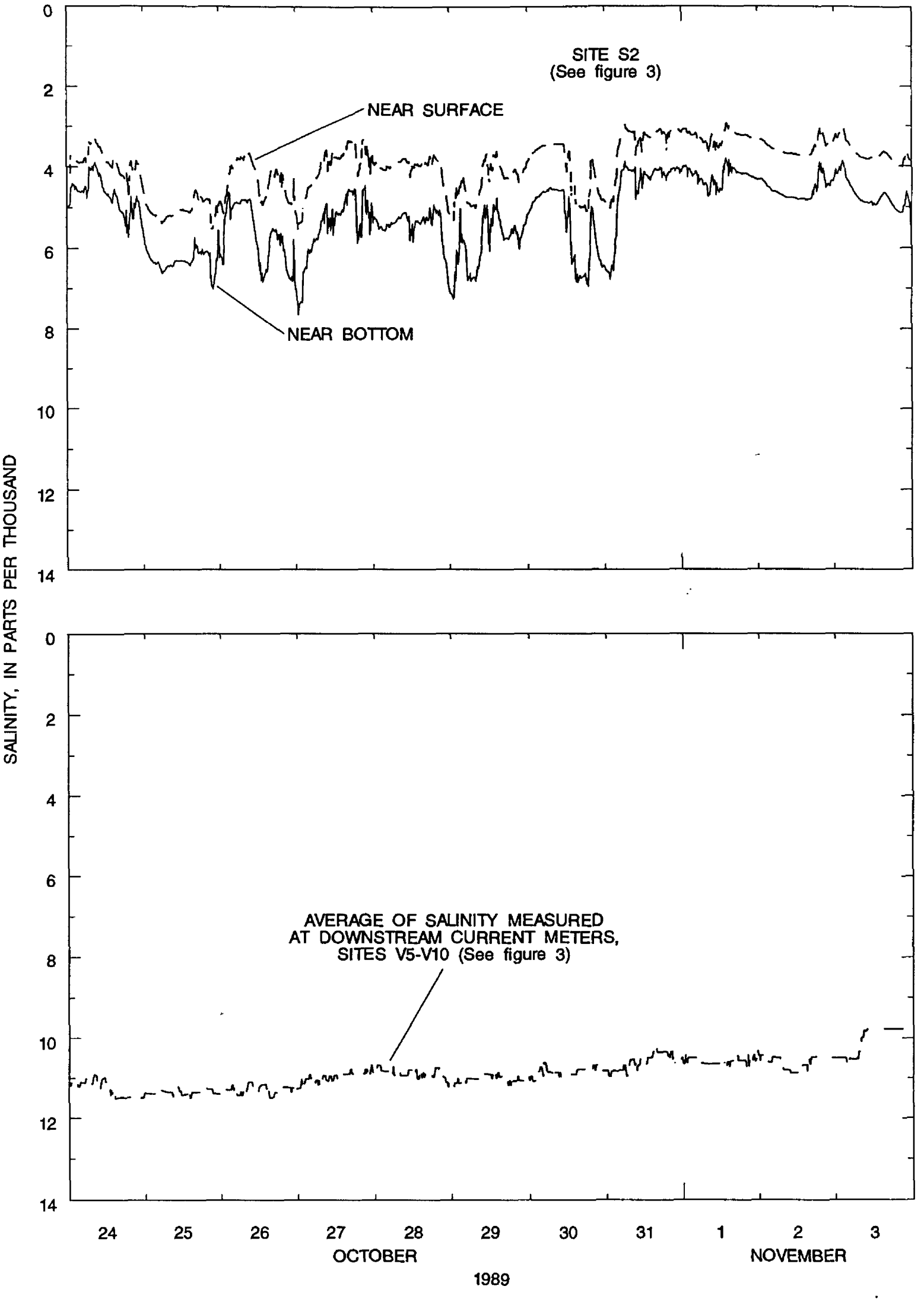

Figure 20. Observed salinity at site S2 and downstream current meters in the Neuse River during October 24-November 3, 1989.

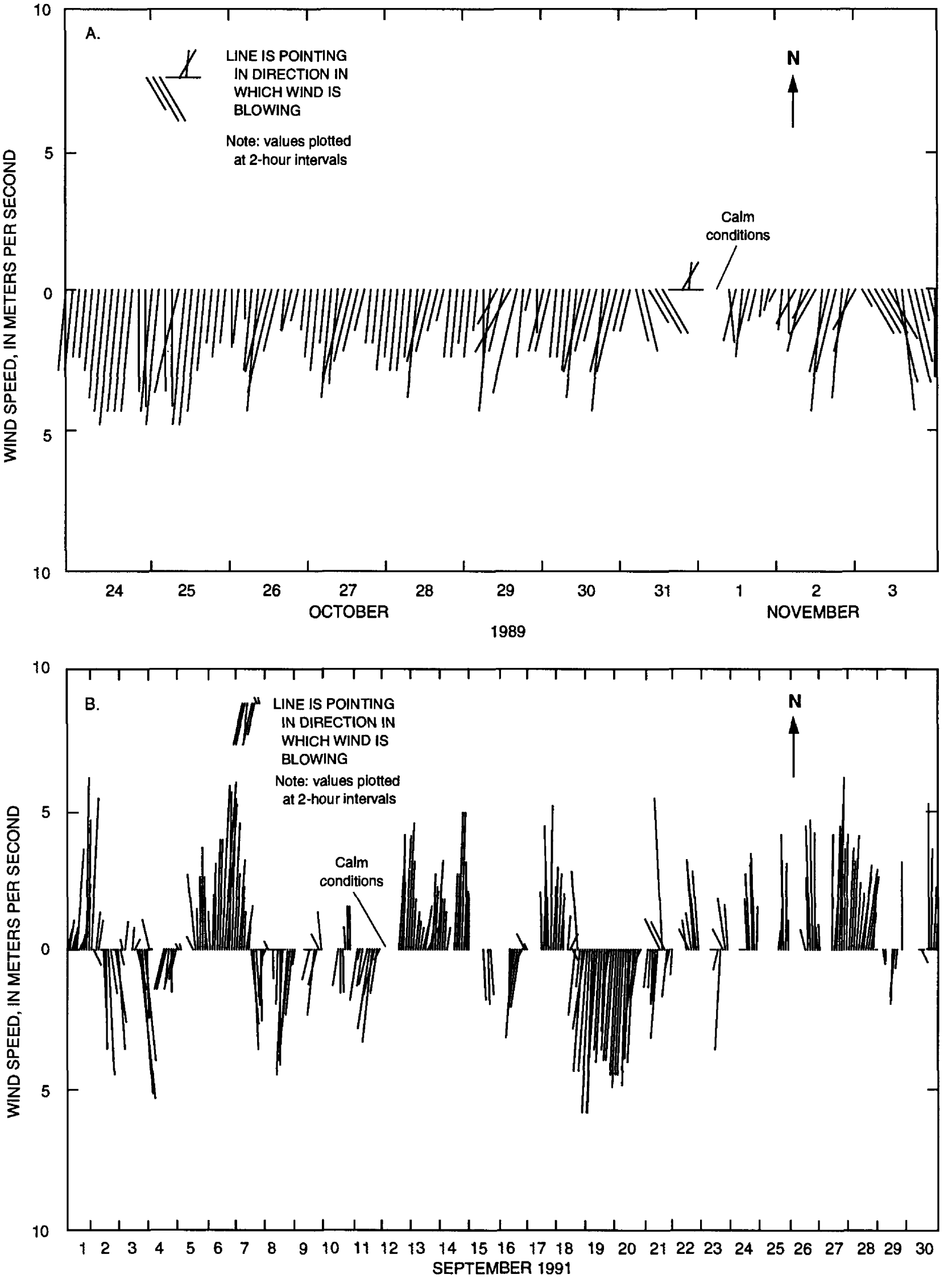

Figure 21. Wind speed and direction measured at Neuse River site W1 during (A) October 24-November 3, 1989, and (B) September 1-30, 1991.

Table 12. Summary of simulated and observed velocities at 10 sites in the Neuse River estuary during October 24-November 3, 1989

[Upstream and downstream current direction shown in figure 8; cm/s, centimeters per second; ---, no data]

Site (fig. 3)		Downstream current				Upstream current			
		Velocity (cm/s)			Direction (degrees E of N)	Velocity (cm/s)			Direction (degrees E of N)
		Mean	Median	Maximum	Mean	Mean	Median	Maximum	Mean
V1	Observed	---	---	---	---	---	---	---	---
	Simulated	9.9	8.2	34.3	144	9.7	8.5	38.8	326
V2	Observed	4.9	5.0	12.0	100	6.0	6.0	16.0	285
	Simulated	4.2	3.1	15.1	77	4.5	3.8	13.7	268
V3	Observed	7.6	7.0	19.0	42	6.1	5.0	19.0	228
	Simulated	3.7	3.0	14.4	98	3.5	2.9	10.3	269
V4	Observed	9.9	9.0	31.0	61	8.0	7.0	19.0	278
	Simulated	3.8	3.7	11.4	124	2.2	1.9	6.6	288
V5	Observed	5.5	4.0	21.0	85	5.2	4.0	18.0	227
	Simulated	5.4	5.2	18.9	96	5.2	4.5	18.2	223
V6	Observed	11.0	10.0	27.0	68	8.8	9.0	17.0	247
	Simulated	6.8	6.9	18.9	122	8.2	7.1	22.1	248
V7	Observed	5.6	5.0	16.0	124	6.2	5.0	20.0	253
	Simulated	8.1	7.4	22.9	103	8.9	8.0	24.0	260
V8	Observed	4.5	4.0	17.0	126	5.0	4.0	18.0	282
	Simulated	7.5	7.1	18.0	104	6.3	5.9	13.2	212
V9	Observed	4.1	3.0	16.0	119	6.2	5.0	25.0	280
	Simulated	7.6	7.3	15.8	103	5.8	5.9	10.6	186
V10	Observed	4.3	4.0	10.0	173	6.2	6.0	11.0	272
	Simulated	5.9	5.8	13.6	70	3.9	3.9	8.7	229

than near the mouth of the estuary. As a final comparison, the mean simulated inflow was 85 m^3/s at site WL1 compared to a drainage area adjusted value of 143 m^3/s.

1991 Validation Period

Boundary conditions for the September 1-30, 1991, validation period were treated as described for the model calibration, except a -2 cm adjustment was applied to the gage height at site WL4. Observed mean daily water levels at the upstream and downstream boundaries during this period were 0.390 m and 0.379 m, respectively (fig. 19). These values are slightly higher than the average mean September water levels at the sites (table 3). Mean salinity during this period was 5.7 ppt at the upstream boundary and 11.1 ppt at the downstream boundary. These values are somewhat lower than that recorded in September at the upstream end of the estuary and slightly higher than the mean salinity value recorded in September at the downstream end of the estuary (table 5). Top-to-bottom salinity differences were as much as 8 ppt at site S2 during the period (fig. 23).

The wind speed measured at site W1 averaged about 2.3 m/s for the simulation period (fig. 21). Winds blew from the north-northeast about 40 percent of the time and were strongest from this direction, with magnitudes in excess of 3.6 m/s more than 50 percent of the time. Strong northerly winds corresponded to periods of increased water levels and seemed to promote mixing in the lower part of the estuary.

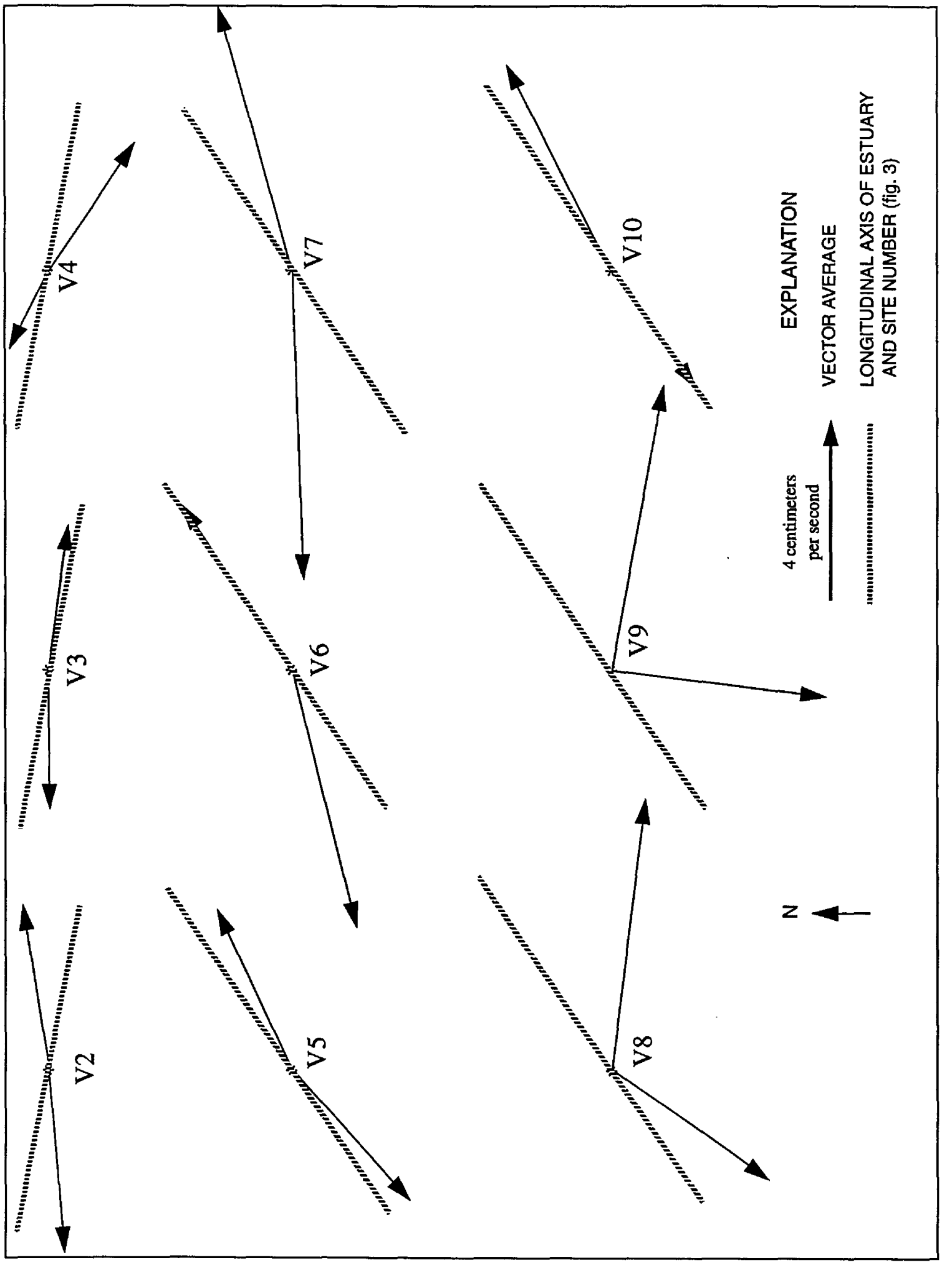

Figure 22. Upstream and downstream vector averages of simulated current data at each meter location in the Neuse River for October 24-November 3, 1989.

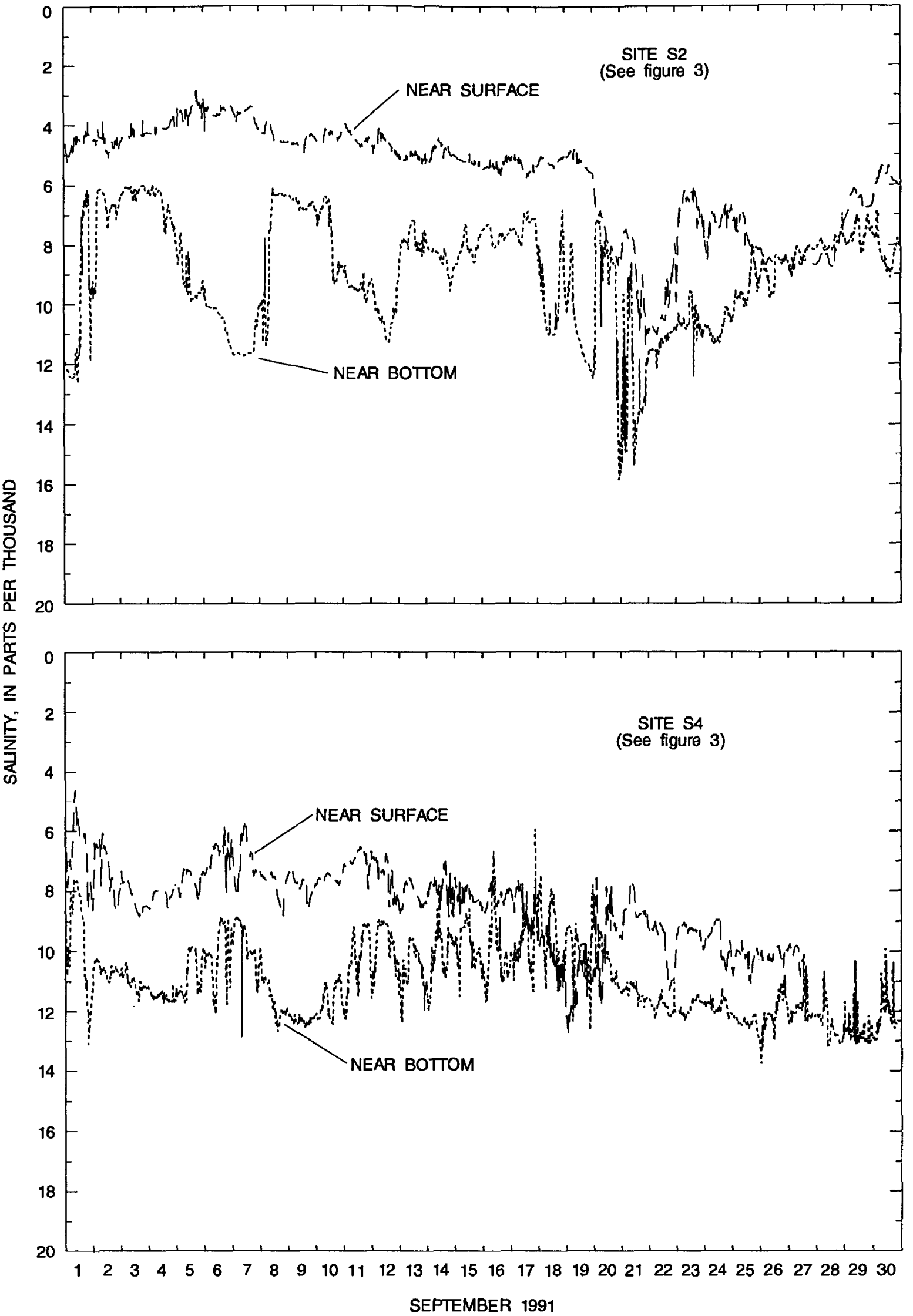

Figure 23. Near-surface and near-bottom salinity at Neuse River sites S2 and S4 during September 1-30, 1991.

For the 30-day simulation period, mean and RMS values of the difference between simulated and observed water levels ranged from 0.5 to 15 percent of the mean daily water-level range for September (tables 11 and 3). The mean difference between simulated and observed salinity was less than the mean difference between near-bottom and near-surface salinity recorded in September for the 1989-92 data-collection period (tables 11 and 6); however, the RMS value of the difference between simulated and observed salinity was nearly 4 times the observed difference for September. The greatest difference between simulated and observed salinities occurred near the end of the simulation when water levels rose rapidly over a short period, and the top-to-bottom salinity difference in the lower part of the estuary increased (fig. 24).

In summary, the model was calibrated and validated for (1) water levels ranging from -0.104 m to 0.908 m, (2) salinities ranging from 2.8 ppt to 22.0 ppt, (3) and wind speeds ranging from calm to 9 m/s. The model was tested for stratified and unstratified conditions. The mean difference between simulated and observed water levels was less than 3 cm. The mean difference between simulated and observed salinities at the interior checkpoint differed by less than 1 ppt. Daily variations in simulated salinities typically were not as great as observed variations. The magnitudes of simulated velocities were in agreement with observations at the downstream measurement section, but simulated magnitudes were generally less than observed values at the mid-estuary section.

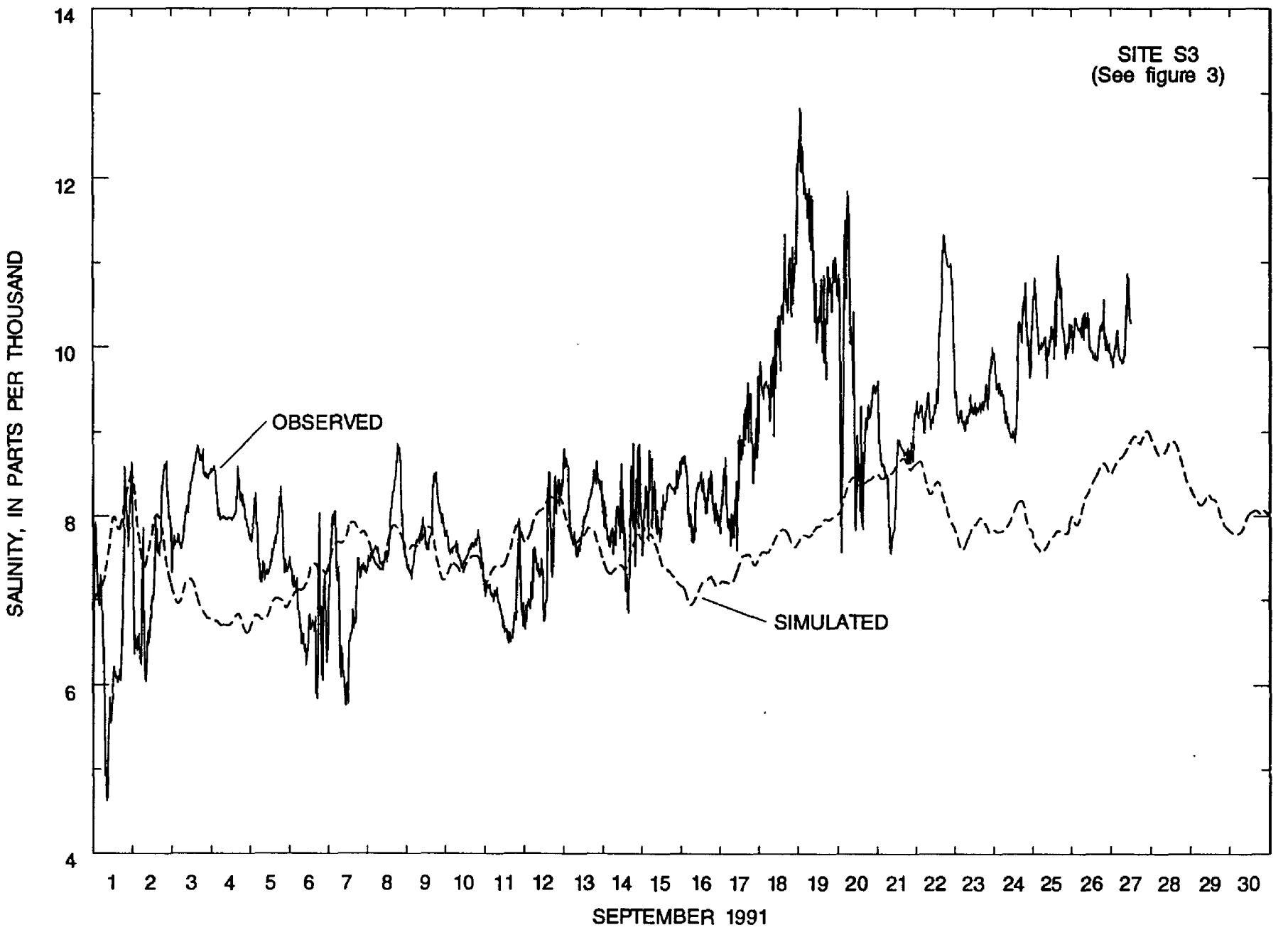

Figure 24. Simulated and observed salinity at site S3 in the Neuse River during September 1-30, 1991.

Sensitivity Analysis

The sensitivity of model results to changes in model parameters was analyzed. Model parameters that were included in the analysis were (1) C_d, the wind-stress coefficient; (2) η, the resistance coefficient; (3) k', the unadjusted horizontal mixing coefficient; and (4) D_i, the isotropic mass-dispersion coefficient, which is used in the computation of the longitudinal mass-mixing coefficient. The parameter D_c was not included in the analysis because the effect of D_c on the magnitude of the longitudinal mass-mixing coefficient was generally minor relative to D_i. Results from a simulation run for May 1-21, 1991, with the calibrated model parameters were used as the basis for comparison in the model parameter sensitivity analysis. The effects of small changes in the downstream gage height on simulated flows were previously described.

Wind-stress coefficient values of 0.0005 and 0.0015 were used for comparison with results from the calibrated model, in which a value of $C_d = 0.001$ was used. Wind speed during the period averaged about 2.5 m/s, and the wind direction was oriented with the longitudinal axis of the lower part of the estuary for much of the period. The changes in C_d had a relatively significant effect on mean simulated flow in the estuary. Net flow during the period changed from 6 m^3/s ($C_d = 0.0005$) to 29 m^3/s ($C_d = 0.0015$) near the upstream boundary and from 27 m^3/s ($C_d = 0.0005$) to 49 m^3/s ($C_d = 0.0015$) at the downstream boundary. The range of flow and mean velocities were less sensitive to changes in C_d than were flow magnitudes, and salinity was insensitive to changes in C_d.

Results from simulations using the calibrated model, May 1-21, 1991, boundary data, and resistance coefficient values of 0.025 and 0.030 were compared with results using a resistance coefficient of 0.028. Both the range in flow (difference between the maximum upstream and maximum downstream flow) and velocity decreased as the resistance coefficient increased. The flow range decreased between about 11 percent at the upstream section and 6 percent at the downstream section as the resistance coefficient was increased from 0.025 to 0.030. Simulated maximum velocities decreased an average of about 9 percent with the change in resistance coefficient from 0.025 to 0.030.

Values of the unadjusted horizontal momentum mixing coefficient, k', of 0 m^2/s and 100 m^2/s were used in simulations for comparison with results from the calibrated model in which $k' = 10$ m^2/s. Flow magnitude was essentially unchanged by the changes in k'; however, circulation patterns in some areas of the estuary were affected by the changes in k'. Spatial variations in velocity direction and magnitude were slightly lower for $k' = 100$ m^2/s than for $k' = 10$ m^2/s, but the changes were observed primarily in the tributary streams, such as Adams Creek, rather than in the mainstem of the estuary.

Results of simulations using an isotropic mass-dispersion coefficient, D_i, of 5 m^2/s and of 60 m^2/s were compared with results from the calibrated model with $D_i = 20$ m^2/s. The mean simulated salinities at sites S2, S3, and S5 for the simulation period showed little differences (less than 0.5 ppt) for the three values of D_i; however, the spatial salinity distribution was sensitive to the value of D_i (fig. 25). Because of the greater mixing produced by the higher value of D_i, the lateral distribution of salinity was more uniform for $D_i = 60$ m^2/s than for the lower values of D_i. The larger value of D_i also resulted in higher salinity in the upper reach of the estuary (fig. 25). Although detailed spatial distributions of salinity are not available for the May 1-21, 1991, simulation period, strong lateral-salinity gradients were often observed in the Neuse River, as previously discussed. Additional field studies, which might include dye tracking, could provide information for better documentation of horizontal mixing of mass in the Neuse River.

Sensitivity of the model to varying boundary conditions, including the effect of a lateral water-level gradient at the downstream boundary and freshwater inflow from tributary streams, was analyzed by Bales and Robbins (1995). In the Pamlico River model, an average water-level gradient of 2 cm applied at the downstream boundary affected circulation patterns within the lower 2 km of the estuary. Similarly, the inclusion of freshwater inflow from tributary streams through the addition of two more open-water boundaries resulted in only very localized effects near the mouths of these tributaries with circulation patterns in the main channel remaining essentially unchanged (Bales and Robbins, 1995). Similar results can be expected for the Neuse River estuary model.

Model Application

The calibrated model was applied to the Neuse River to simulate flow, circulation, and salinity

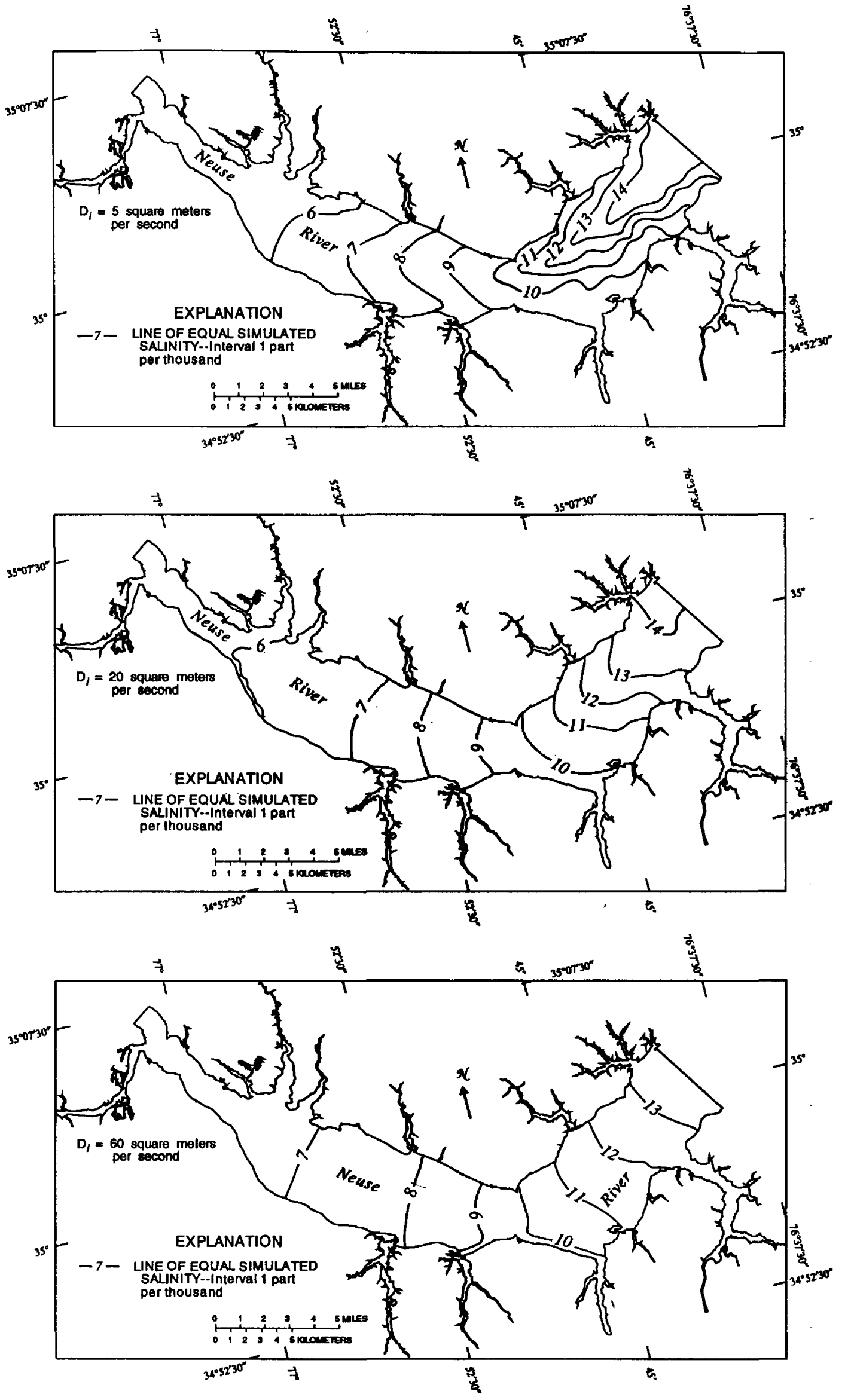

Figure 25. Lines of equal simulated salinity in the Neuse River for May 17, 1991, at 0215 using the calibrated model and three values of the isotropic mass-dispersion coefficient, D_i.

distributions. Circulation patterns are shown using vector plots, particle tracking, and dye transport. Simulated results from the Neuse River model also were compared with results from the Pamlico River model for the same simulation period.

Flow Computation

Flows were simulated for the calibration period, June 1-24, 1991; the two validation periods, October 24-November 3, 1989, and September 1-30, 1991; and for May 1-30, 1991. Maximum instantaneous simulated flow for June 1-24, 1991, ranged from (1) 960 m^3/s upstream to 1,260 m^3/s downstream near New Bern, (2) 3,660 m^3/s upstream to 3,830 m^3/s downstream at mid-estuary, and (3) 6,360 m^3/s upstream to 6,180 m^3/s downstream near the downstream boundary. Daily-flow reversals occurred at all three sections. Mean flow for the entire simulation period was 56 m^3/s downstream near New Bern (about 40 percent of the daily mean freshwater inflow at New Bern) and 12 m^3/s upstream at the downstream boundary (table 13; fig. 26). The net movement of water into the estuary during the simulation period resulted in an increase in water levels of more than 60 cm from the beginning to the end of the simulation (fig. 15). Mean flows for the remaining three simulation periods ranged from 17 m^3/s to 85 m^3/s downstream near the upper end of the estuary, and from 1 m^3/s upstream to 80 m^3/s downstream at the lower end of the estuary.

The computed mean flow can be sensitive to the time for which the mean is determined. For example, for June 1-24, 1991, the mean simulated flow at the downstream section is -12 m^3/s, but for June 1-23, 1991, the mean simulated flow is -47 m^3/s. This sensitivity to averaging period reflects the dynamic nature of the flows in the Neuse River. Furthermore, periods of several consecutive days during which mean flow is in the upstream direction are not unrealistic. Giese and others (1985) estimated that the tidal influence extended about 25 km upstream of the upstream open-water boundary.

These simulations of flow in the Neuse River demonstrate the large variations in flow magnitude that can occur during a day, as well as variations in the mean flow for different periods. Flow is also highly nonuniform throughout the estuary as reflected in daily maximum and minimum flows at the upstream and downstream sections (table 13). Finally, flow simulations such as these can be useful in determining instantaneous and mean constituent loadings throughout the estuary.

Circulation Patterns

One of the results of each model simulation is a time sequence of velocity magnitude and direction for each computational cell. Plots of these vectors can be used to examine detailed circulation patterns in areas of interest. As an example of the temporal and spatial complexities of circulation in the Neuse River, figures 27-30 illustrate simulated velocity vectors for selected times corresponding to three water-level conditions during the October 24-November 3, 1989, simulation.

At 1530, on November 2, 1989, when water levels were falling and the difference from upstream to downstream was approximately 9 cm (fig. 27), simulated flow throughout the estuary was generally in the downstream direction (figs. 28A, 29A, and 30A). Currents were greatest in the upper reaches of the estuary and in the narrow section in the middle reach of the estuary. Fairly strong recirculation eddies also were present near irregularities in shoreline topography (for example, near Clubfoot Creek and Great Island in the lower part of the estuary).

At 1350, on November 3, 1989, when water levels were rising and downstream water levels exceeded upstream water levels by 10 cm (fig. 27), simulated flow was generally in the upstream direction (figs. 28B, 29B, and 30B). Similar to the November 2 pattern (figs. 28A, 29A, and 30A), currents were greatest in the upper reach of the estuary and in the narrow section mid-estuary. Strong recirculation eddies also were present, which resulted in areas of bidirectional flow near the shoreline between Hancock and Slocum Creeks in the mid-estuary section.

Circulation patterns were more complex on October 28, 1989, at 0200, when upstream and downstream water levels were nearly equal (fig. 27). Current patterns were generally upstream in the uppermost reaches of the estuary, but large areas of zero velocity also were present (figs. 28C, 29C, and 30C). Complex circulation patterns and greater lateral differences also were present in the middle and lower reaches of the estuary.

A simulated particle having no mass and infinitesimal diameter was released at the center of the computational grid at each of four locations in the

Table 13. Simulated daily maximum downstream and daily maximum upstream flows at three Neuse River cross sections for June 1-24, 1991

[m^3/s, cubic meters per second; negative flow is upstream (west)]

Date	Daily maximum downstream flow (m^3/s)			Daily maximum upstream flow (m^3/s)		
	Upstream section	Mid-estuary section	Downstream section	Upstream section	Mid-estuary section	Downstream section
June 1	715	1,570	2,690	-681	-1,990	-3,000
2	409	2,530	3,610	-497	-1,520	-2,130
3	455	1,600	2,410	-547	-1,540	-2,210
4	1,260	1,850	2,040	-705	-3,660	-6,080
5	1,100	3,830	6,180	-563	-1,880	-2,780
6	1,180	3,010	4,310	-408	-3,370	-5,300
7	1,050	2,880	4,160	-427	-1,670	-2,270
8	758	2,050	3,050	-289	-1,440	-1,700
9	671	2,160	3,030	-444	-1,140	-1,670
10	664	1,880	2,380	-545	-1,050	-1,620
11	258	1,590	2,370	-483	-1,130	-1,380
12	111	2,050	3,240	-474	-2,520	-4,320
13	1,030	2,880	3,490	-555	-2,010	-3,680
14	719	1,760	2,260	-285	-926	-1,030
15	310	1,200	2,360	-521	-1,670	-2,750
16	239	998	1,590	-714	-1,880	-2,960
17	527	2,010	3,140	-960	-2,380	-3,874
18	411	1,940	2,920	-743	-1,810	-2,070
19	538	601	1,040	-437	-663	-1,280
20	460	1,260	1,720	-234	-943	-1,430
21	591	1,990	2,780	-509	-2,320	-3,420
22	575	1,800	3,010	-913	-2,600	-3,330
23	821	2,780	3,790	-748	-3,520	-6,360
24	1,060	2,780	4,240	-266	-1,400	-2,460
Entire period	1,260	3,830	6,180	-960	-3,660	-6,360

model domain (figs. 31, 32, 33, and 34). Particles were released at the beginning of each of the four simulation periods and were tracked for the duration of the simulation. The resulting particle tracks characterized the transport of materials in the estuary under the hydrodynamic conditions present during each simulation period.

In some cases, there was little net movement of the particles for the duration of the simulation. For example, net movement of particle 1 for June 1-24, 1991 (fig. 31), and September 1-30, 1991 (fig. 33), was less than about 4 km, when simulated mean flow at each open-water boundary was directed into the estuary. For these simulations (figs. 31 and 33), only particle 4, which was released near the downstream boundary, exited the estuary during the September simulation. In other cases, net particle move-ment was much greater, nearly 20 km for particle 1 during May 1-30, 1991 (fig. 34). During these simulations, when mean flow was in the downstream direction at each open-water boundary (figs. 32 and 34), more particles

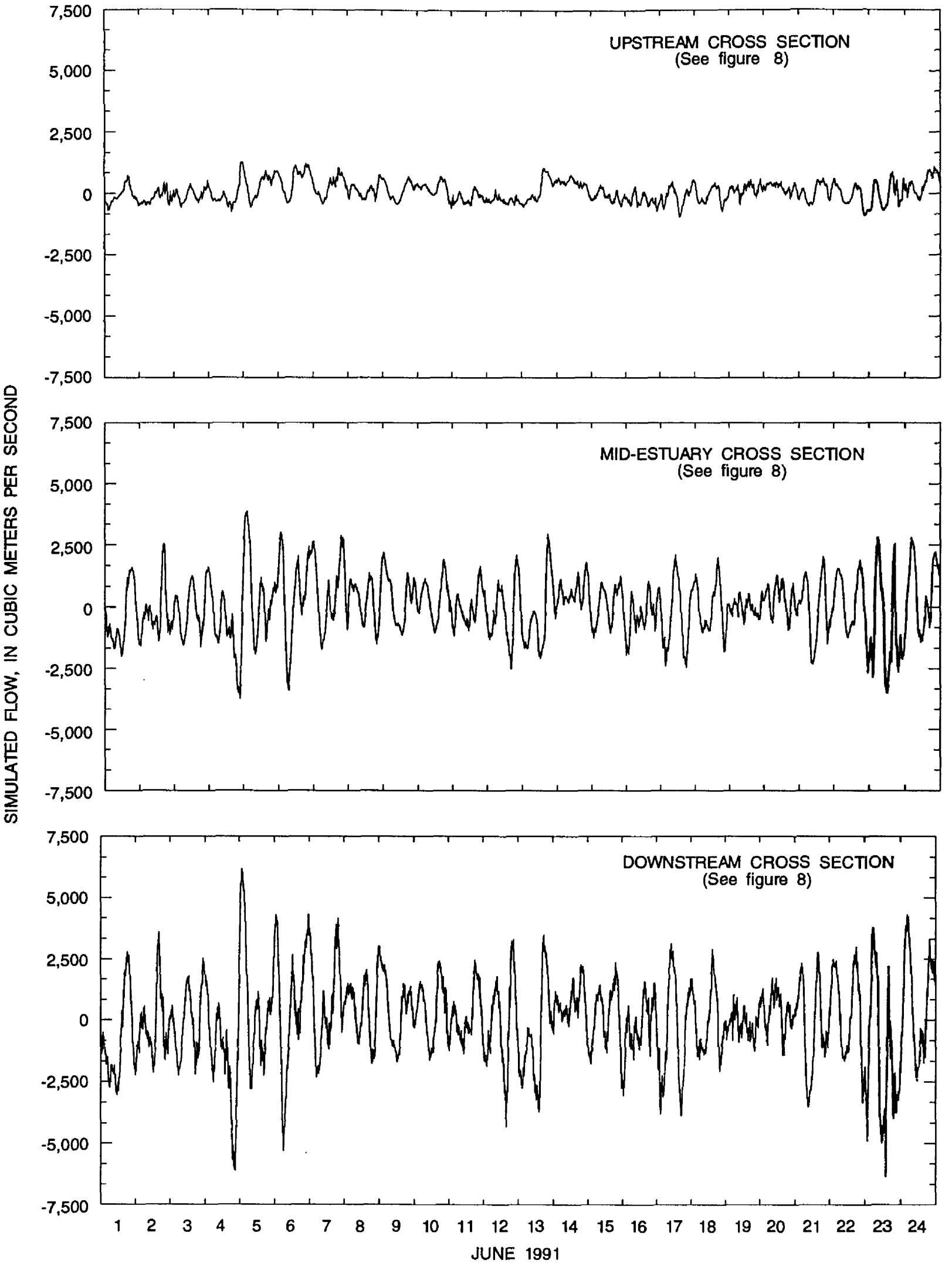

Figure 26. Simulated flow at three cross sections of the Neuse River estuary for June 1-24, 1991.

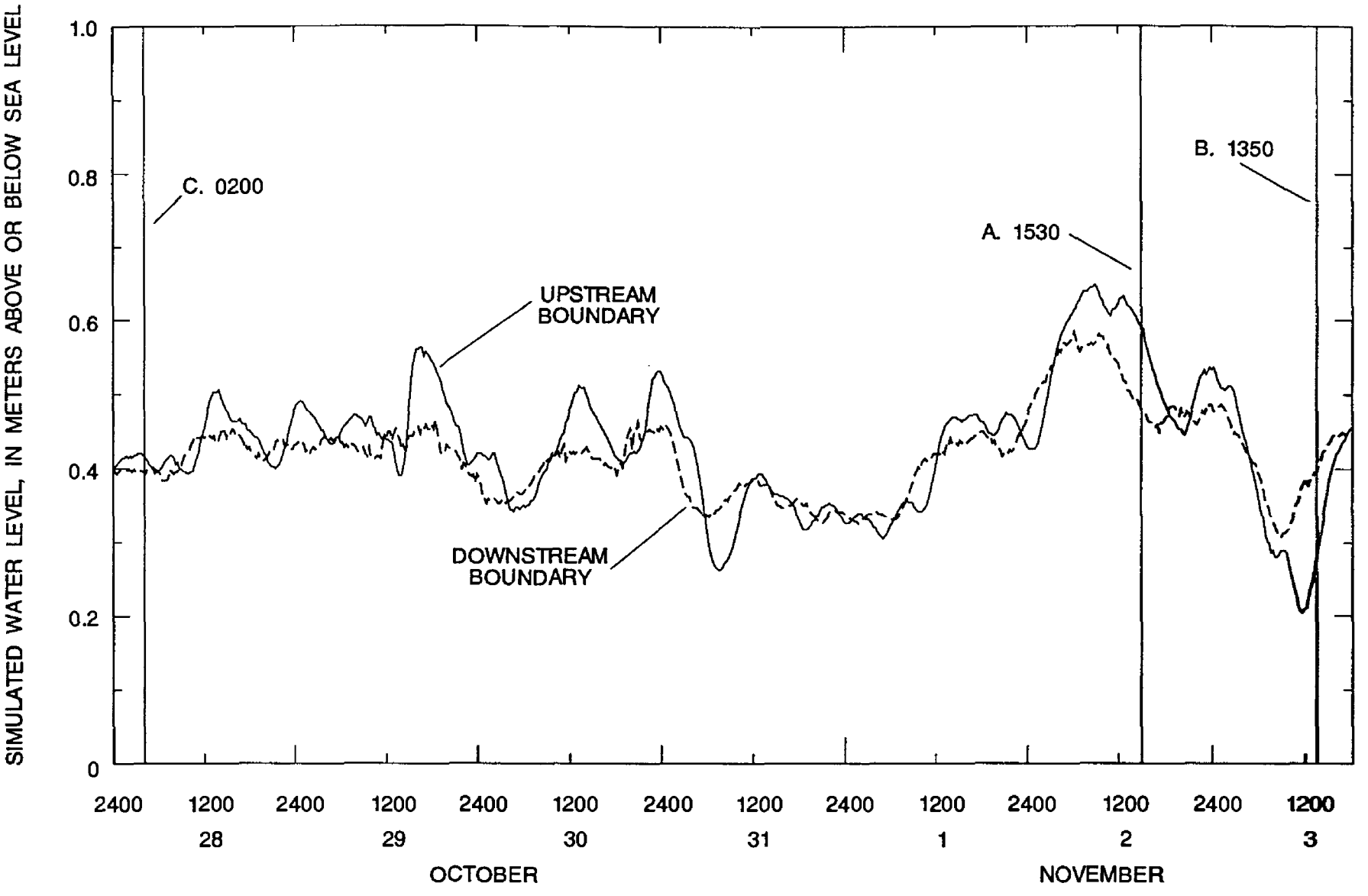

Figure 27. Simulated water levels at Neuse River model boundaries during October 28-November 3, 1989, and selected conditions for (A) November 2 at 1530, (B) November 3 at 1350, and (C) October 28 at 0200.

exited the estuary, particularly when mean flow at the downstream open-water boundary was greater (fig. 34).

These results demonstrate the extreme spatial variation in the flow field at any given time, as well as the large difference in circulation patterns which can occur under different forcing conditions. The results also demonstrate the difficulty in identifying a realistic "flushing time" or "residence time" for materials in the estuary because of the great variations in circulation patterns and resulting transport. In one case, particles released at several locations throughout the estuary did not exit the estuary during a 24-day period, yet under differing conditions all but one particle, released near the upper end of the estuary, exited the estuary during a 30-day period. Similar particle tracks can be generated for any computational cell in the model domain and for any desired flow condition.

Solute Transport

The model is capable of simulating the transport of conservative constituents. To simulate solute transport in the Neuse River and to further characterize circulation patterns, two solute discharges were simulated in the estuary. The first discharge point was on the north side of the estuary near the mouth of Upper Broad Creek (fig. 3), where a flow of 0.1 m^3/s with a source strength of 1,000 ppt was continuously released. The second discharge point was located on the south side of the estuary between Hancock and Slocum Creeks (fig. 3) about 1.5 km into the channel. The flow at the second discharge point was 1.0 m^3/s, and the concentration of the solute in the discharge was also 1,000 ppt.

Solute transport was simulated for May 1-30, 1991. This was a period of near-average water levels and salinity with some stratification, particularly in the upper part of the estuary, with winds from the

A.

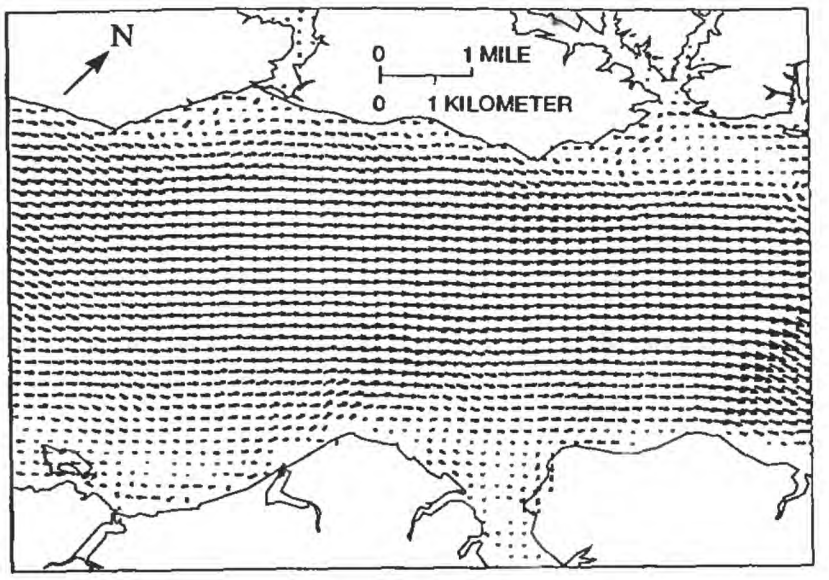

B.

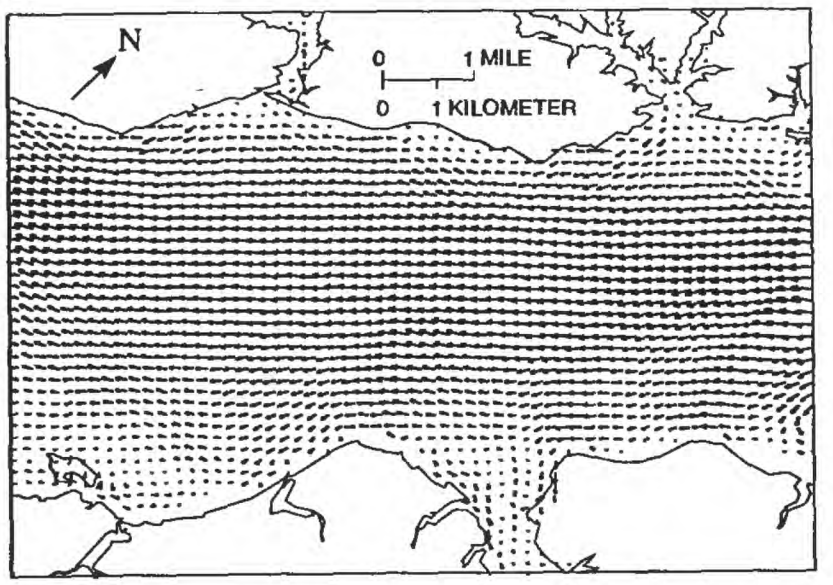

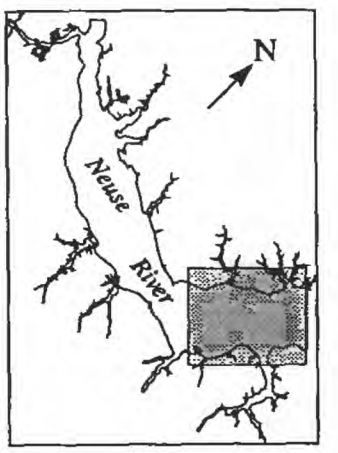

LOWER NEUSE RIVER ESTUARY

EXPLANATION

→ VECTOR--Head points in flow direction. Greater vector length represents greater relative velocity

C.

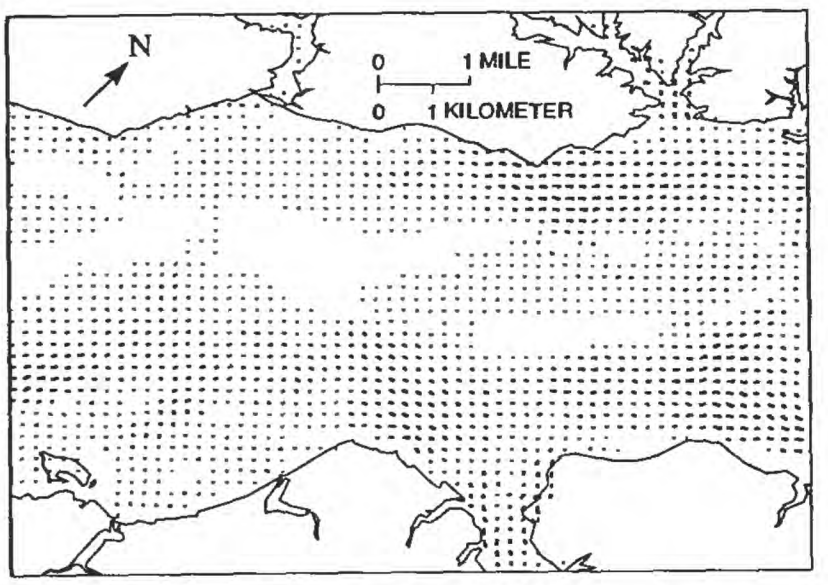

Figure 30. Simulated circulation patterns in the lower Neuse River estuary for 1989: (A) November 2 at 1530, (B) November 3 at 1350, and (C) October 28 at 0200.

A.

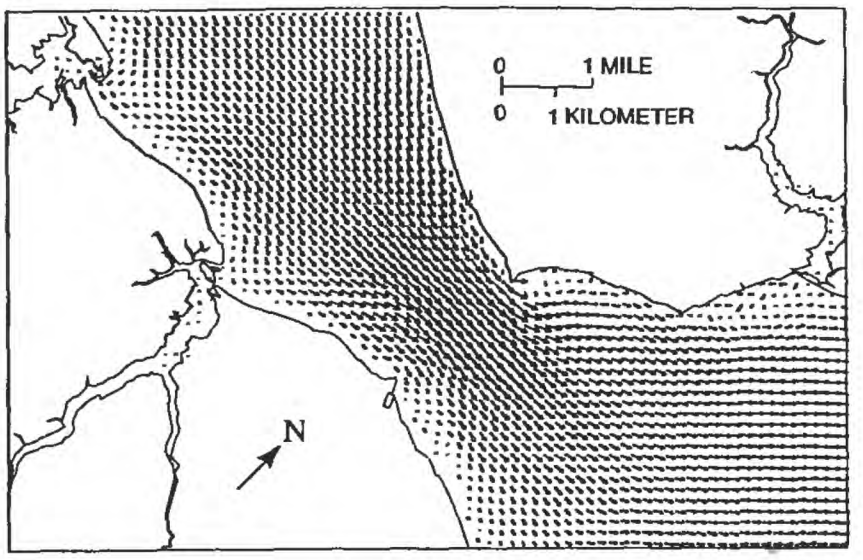

B.

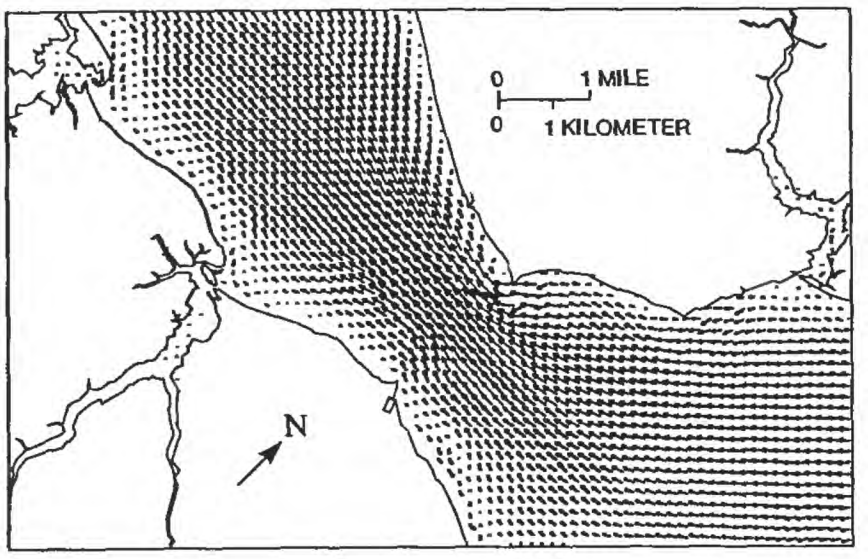

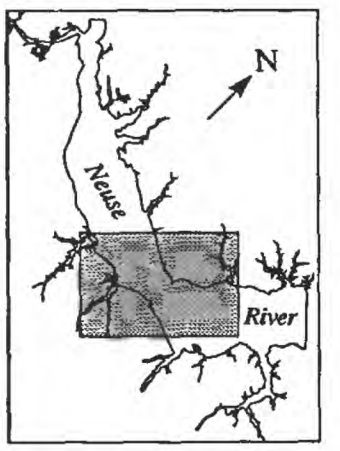

MID-NEUSE RIVER ESTUARY

C.

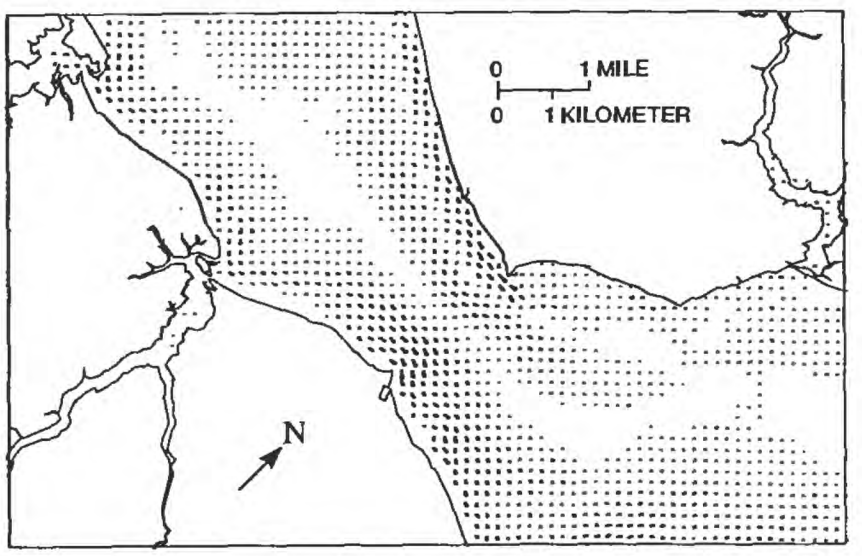

EXPLANATION

→ VECTOR--Head points in flow direction. Greater vector length represents greater relative velocity

Figure 29. Simulated circulation patterns at the mid-Neuse River estuary for 1989: (A) November 2 at 1530, (B) November 3 at 1350, and (C) October 28 at 0200.

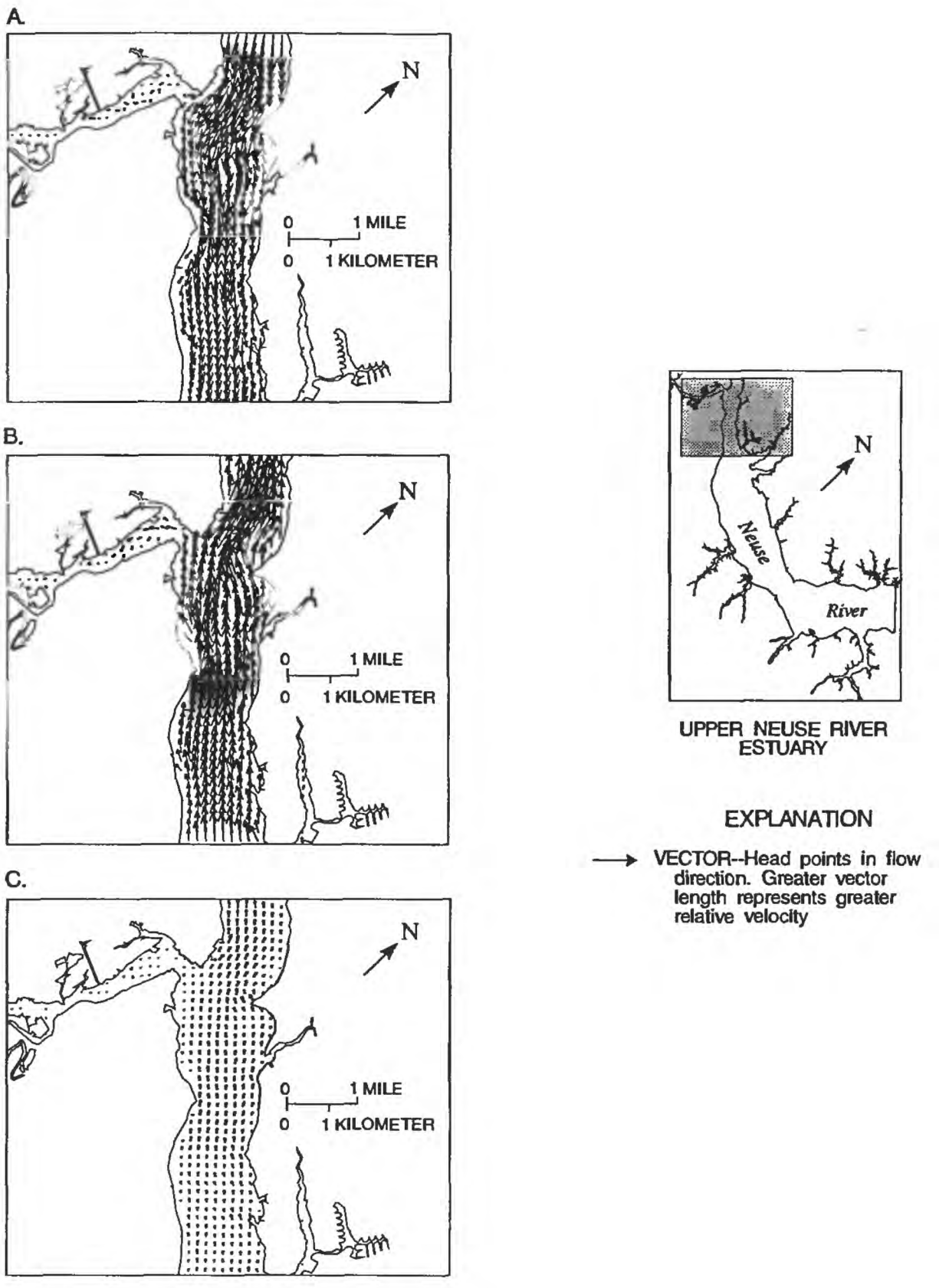

Figure 28. Simulated circulation patterns in the upper Neuse River estuary for 1989: (A) November 2 at 1530, (B) November 3 at 1350, and (C) October 28 at 0200.

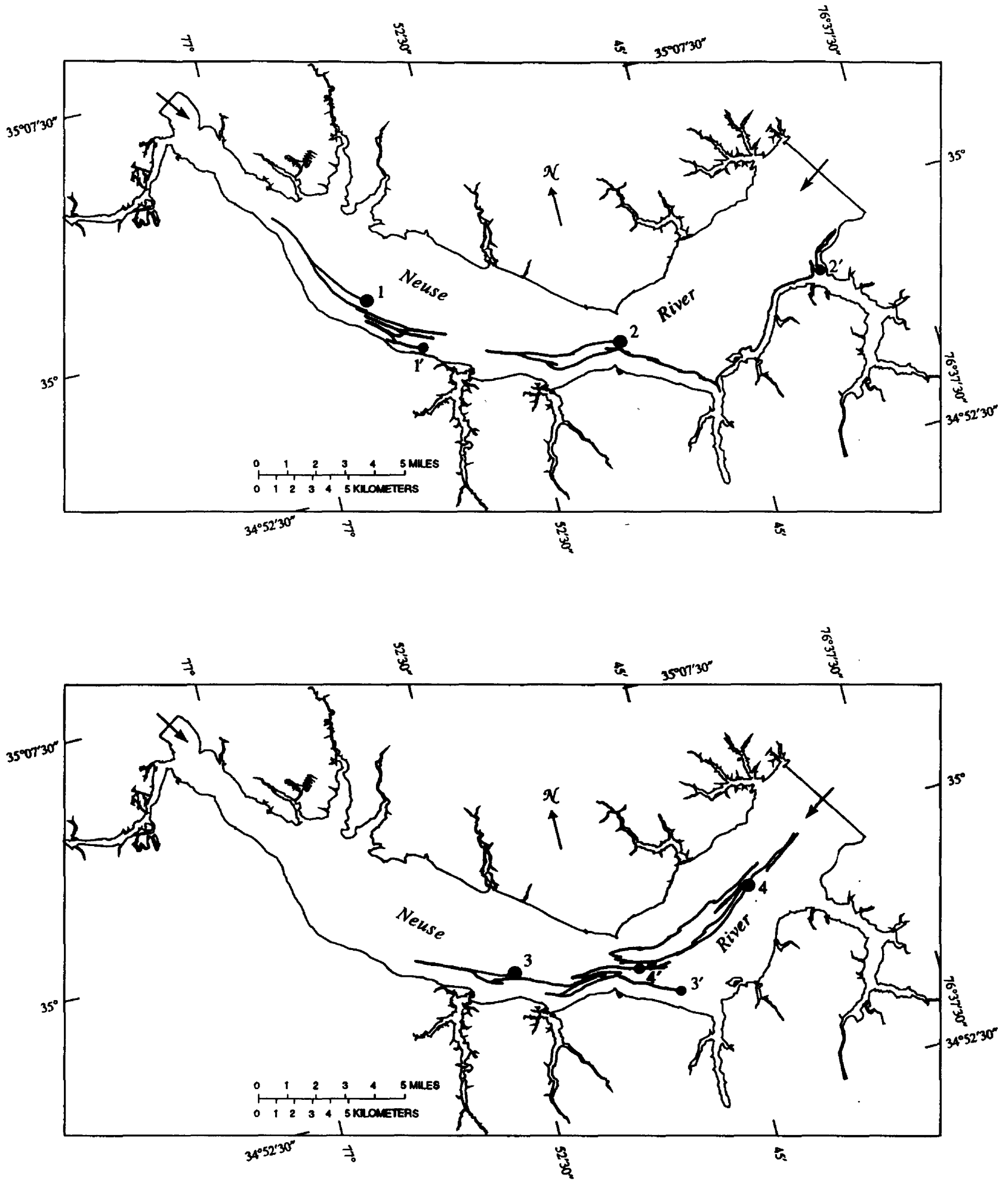

Figure 31. Simulated particle tracks for June 1-24, 1991.

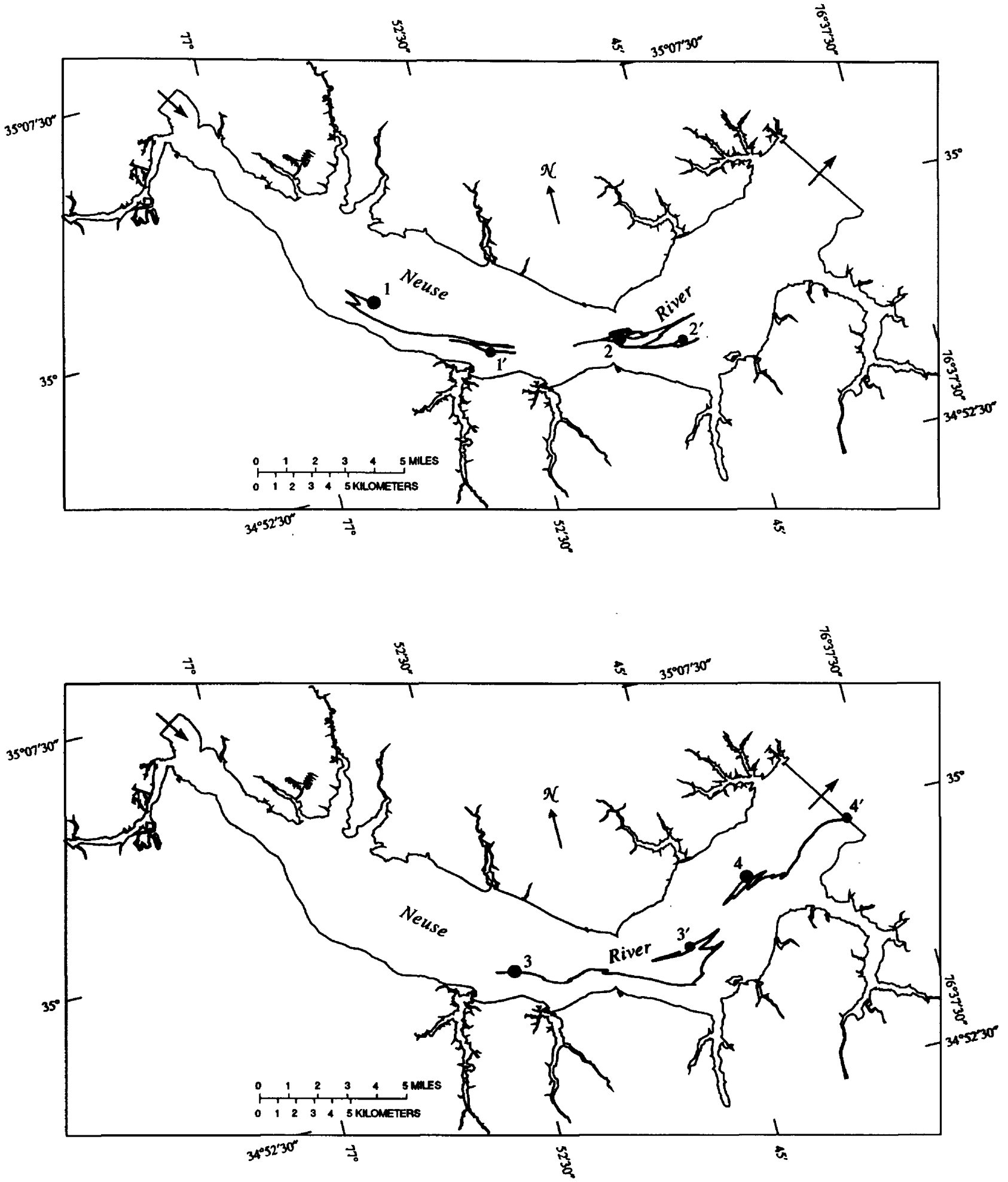

Figure 32. Simulated particle tracks for October 24-November 3, 1989.

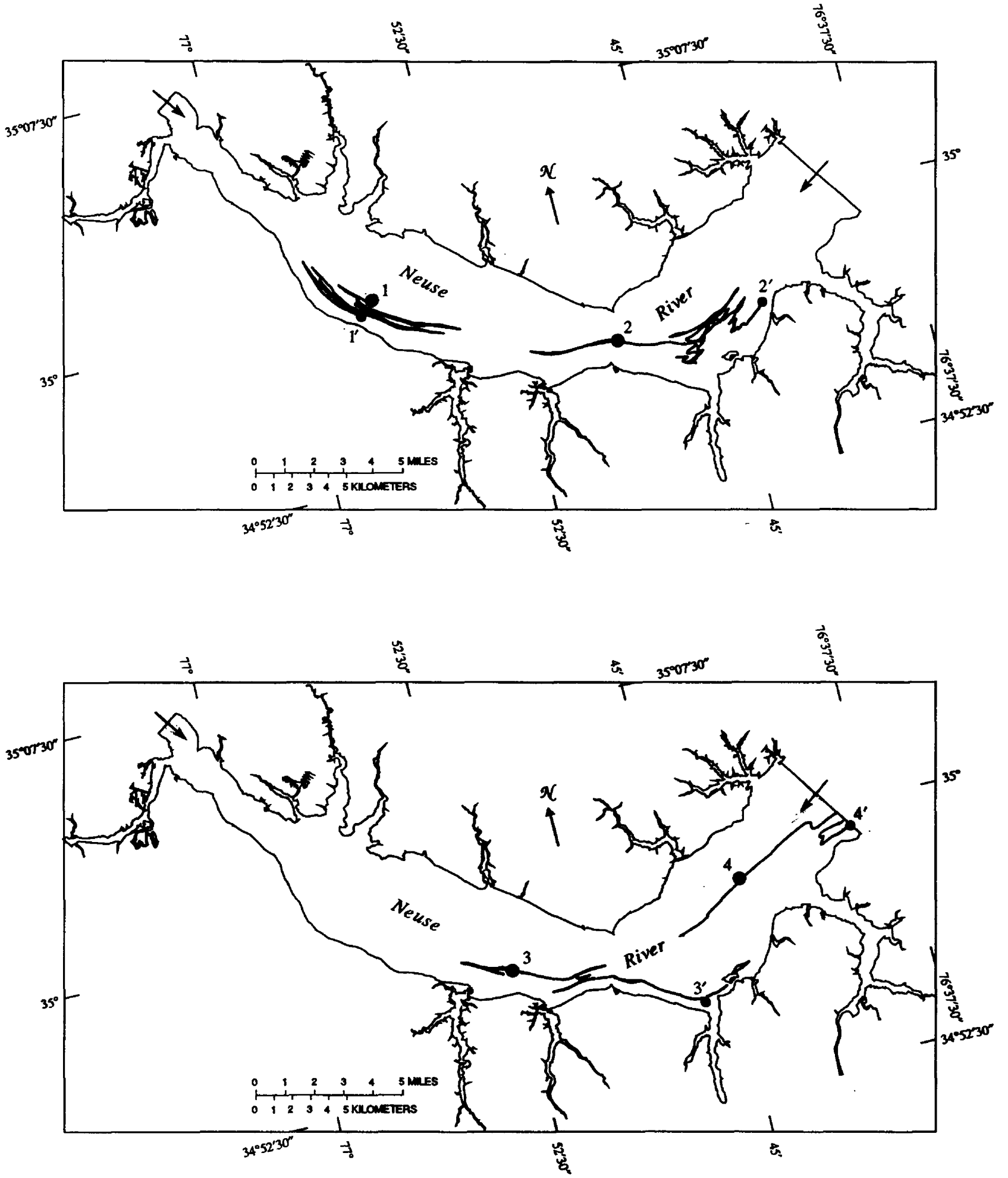

Figure 33. Simulated particle tracks for September 1-30, 1991.

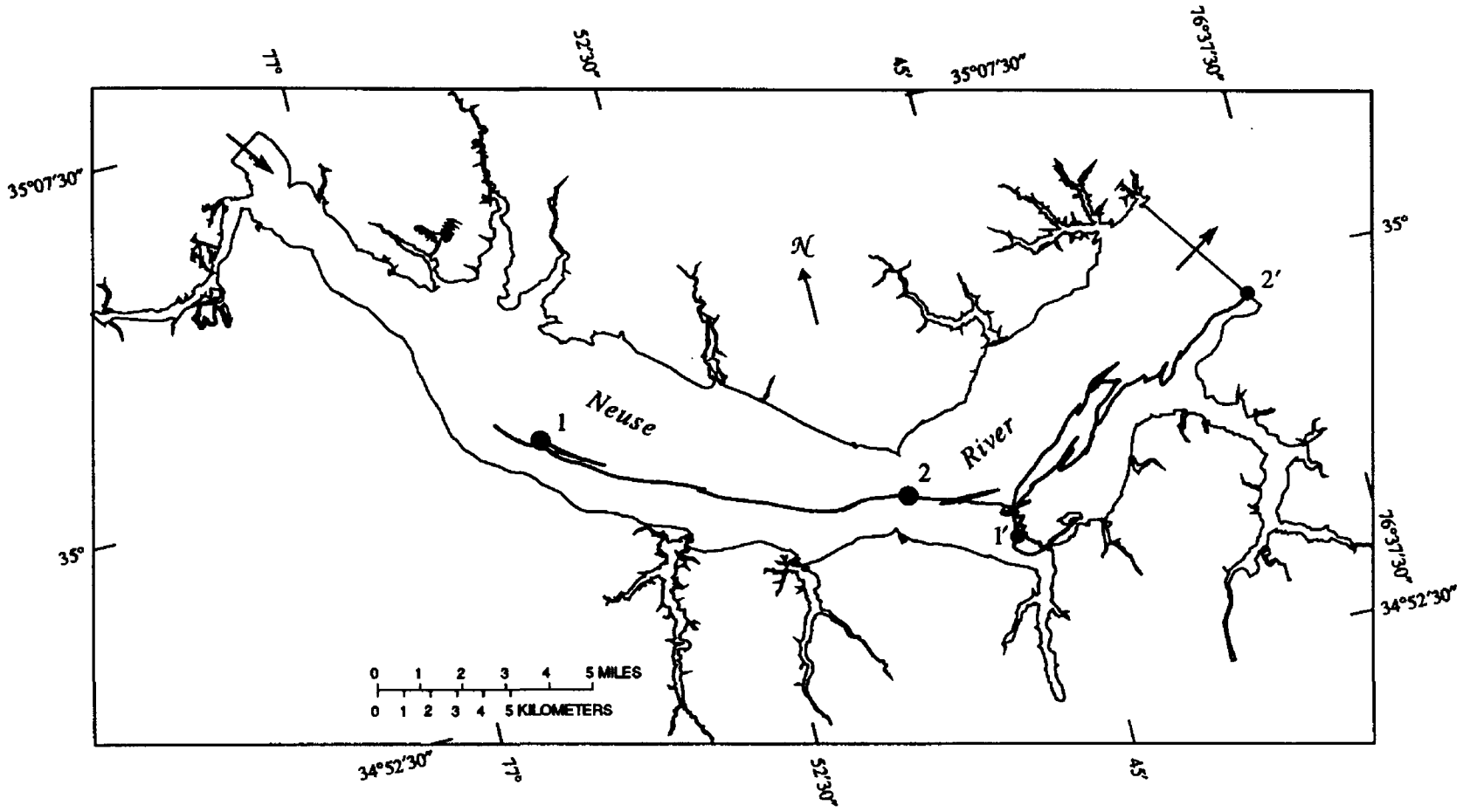

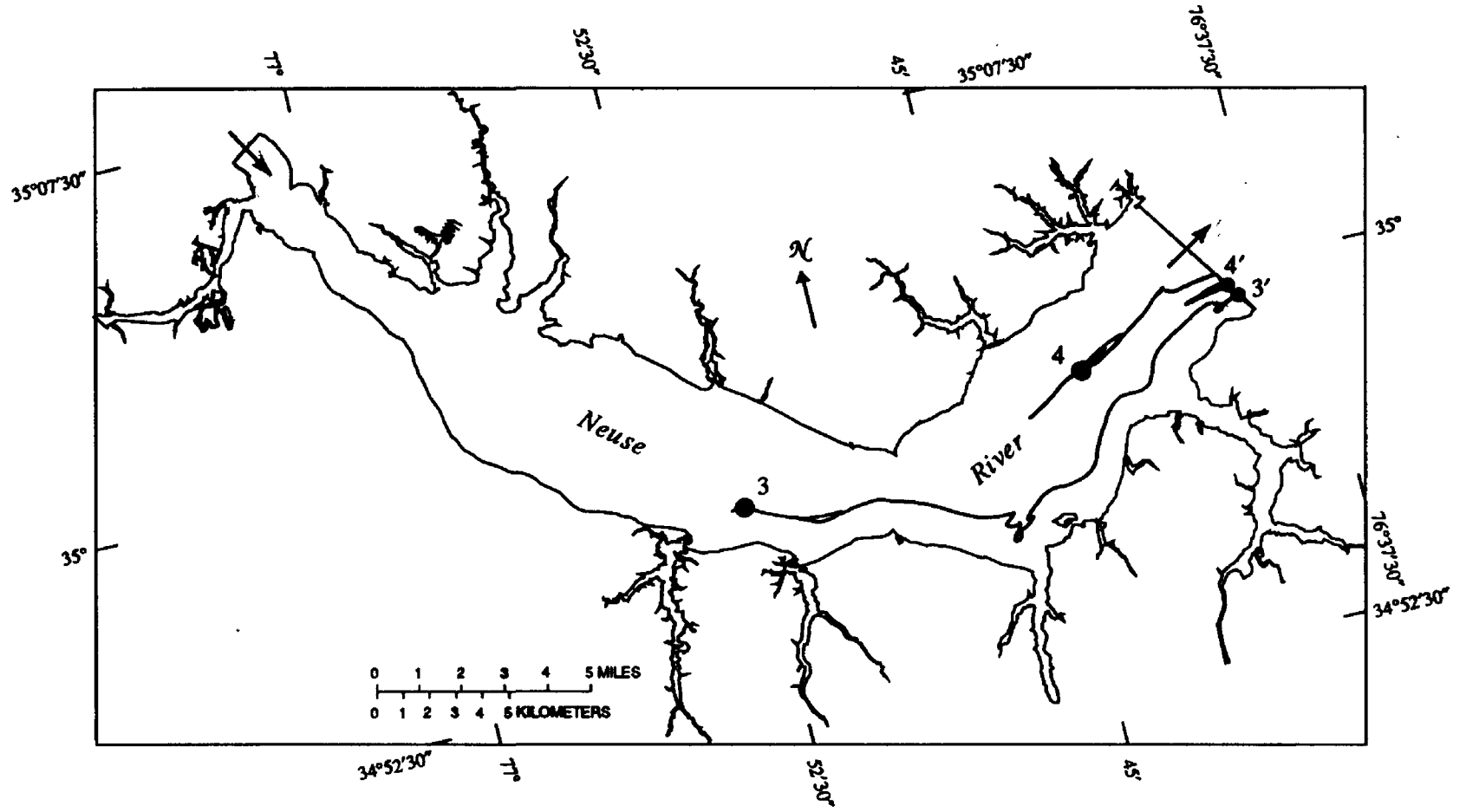

EXPLANATION

PARTICLE TRACK

DIRECTION OF MEAN FLOW ACROSS BOUNDARY FOR SIMULATION PERIOD

1 PARTICLE TRACK START AND NUMBER

1' PARTICLE TRACK END AND NUMBER

Figure 34. Simulated particle tracks for May 1-30, 1991.

south-southeast about 25 percent of the time. Within 3 days, a solute concentration of 1 ppt had nearly crossed the estuary for the mid-estuary release (fig. 35A). After 6 days, the upstream discharge had begun to move out into the main channel of the estuary, and constituent concentrations of 1 ppt were evident almost 13 km downstream from the downstream discharge (fig. 35B). Strong lateral gradients existed near the downstream discharge location 6.1 days after the start of the simulation. Less than 18 hours later, concentration contours took on a much different shape as flow reversed and the constituent was moved upstream from the downstream discharge and back into the tributary at the upstream discharge (fig. 35C).

After 17 days, the constituent was present throughout much of the estuary. Near the release point, the solute was diluted about 100 times from the initial concentration; throughout an 18-km section of the estuary, the solute was diluted about 500 times (fig. 36A). After 23 days, constituent concentrations were similar, with greater concentrations in the upper reach of the estuary (fig. 36B). At the end of 27 days, solute concentrations were much greater in the upper reach of the estuary, and contours took a different shape as flow was again in the upstream direction (fig. 36C). Although the source concentrations were the same, the order of magnitude difference in discharge was evident in the overall constituent contribution to the estuary. Mean flow was in the downstream direction for the simulation period, but maximum upstream flows were 42 percent and 59 percent greater than maximum downstream flows at the mid-estuary and downstream boundary sections, respectively.

The transport of solutes released at other locations in the estuary and under different conditions can be simulated to further characterize mixing and transport. The transport of solutes from continuous and instantaneous (for example, chemical spills) releases can be simulated.

Salinity was simulated for each computational cell at each time step during all simulations. Lines of equal salinity were generated for two periods (October 24-November 3, 1989, and September 1-30, 1991) to show differences in salinity distribution patterns under differing hydrologic conditions. The 1989 period, as previously described, was a period of higher than average water levels and somewhat lower than average salinity, relative to the mean October and November values recorded during the period of data collection. The 1991 period was characterized by somewhat higher than average water levels and near average salinity (slightly lower at the upper end of the estuary and slightly higher at the lower end of the estuary). The 1991 period also showed a greater variation in water level and salinity than the 1989 period (figs. 19, 20, and 23).

For the 1989 period, salinity distributions near the start and end of the simulation, approximately 9 days apart, show a net downstream increase of salinity throughout the estuary (fig. 37). During this period, simulated mean flow was in the downstream direction at the upstream and downstream boundaries. During September 8-17, 1991, however, saltwater moved upstream in the uppermost reaches of the estuary, as indicated by the 5-ppt line that moved more than 9 km to the upper boundary, and by downstream movement in the lower reach of the estuary (fig. 38). This coincided with a period when mean simulated flow at the upstream boundary was in the upstream direction and at the downstream boundary was in the downstream direction.

Lateral differences in salinity were present in all cases shown. The largest gradient occurred near the shore and in the deeper sections of the estuary as a result of the lateral shear in the currents (figs. 28, 29, and 30).

Comparison with Pamlico River Model

To characterize differences between Pamlico and Neuse River circulation and flow for the same set of natural conditions, the models were applied using observed boundary data for June 14-24, 1991 (figs. 39 and 40), including measured wind at site W2. The analysis of one brief period cannot necessarily be extrapolated to a variety of hydrologic conditions, but marked differences in circulation and transport, as detailed below, are apparent in the two estuaries.

Due to their proximity, the Pamlico and Neuse River estuaries display similar physical characteristics. The Pamlico River study area extends about 48 km downstream from Washington, N.C., and increases in width from about 300 m to about 7 km (Bales and Robbins, 1995). The longitudinal axis of the Pamlico River is oriented about 110° east of north and is nearly

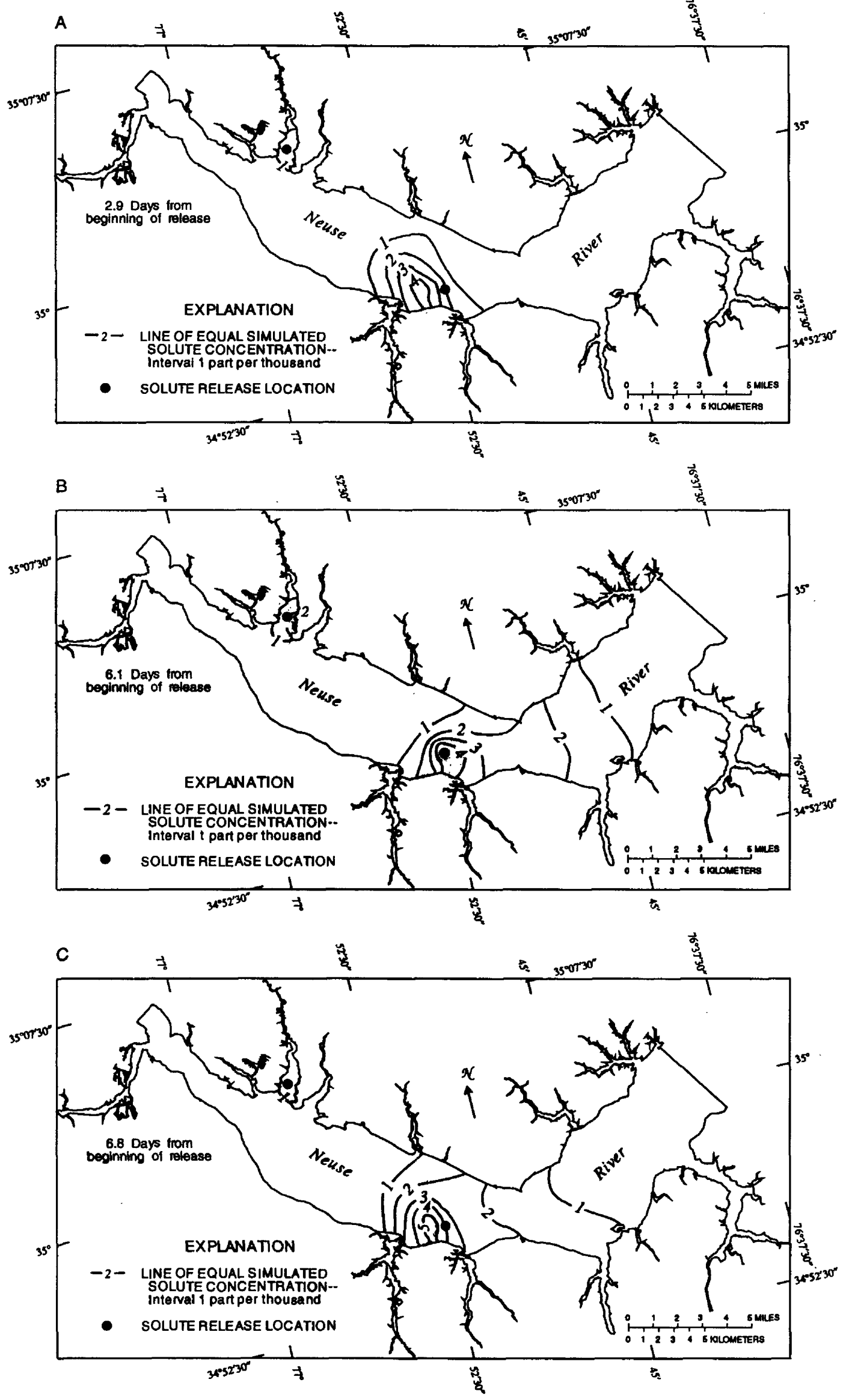

Figure 35. Simulated solute concentration in the Neuse River from two continuous releases at (A) 2.9 days, (B) 6.1 days, and (C) 6.8 days following release on May 1, 1991.

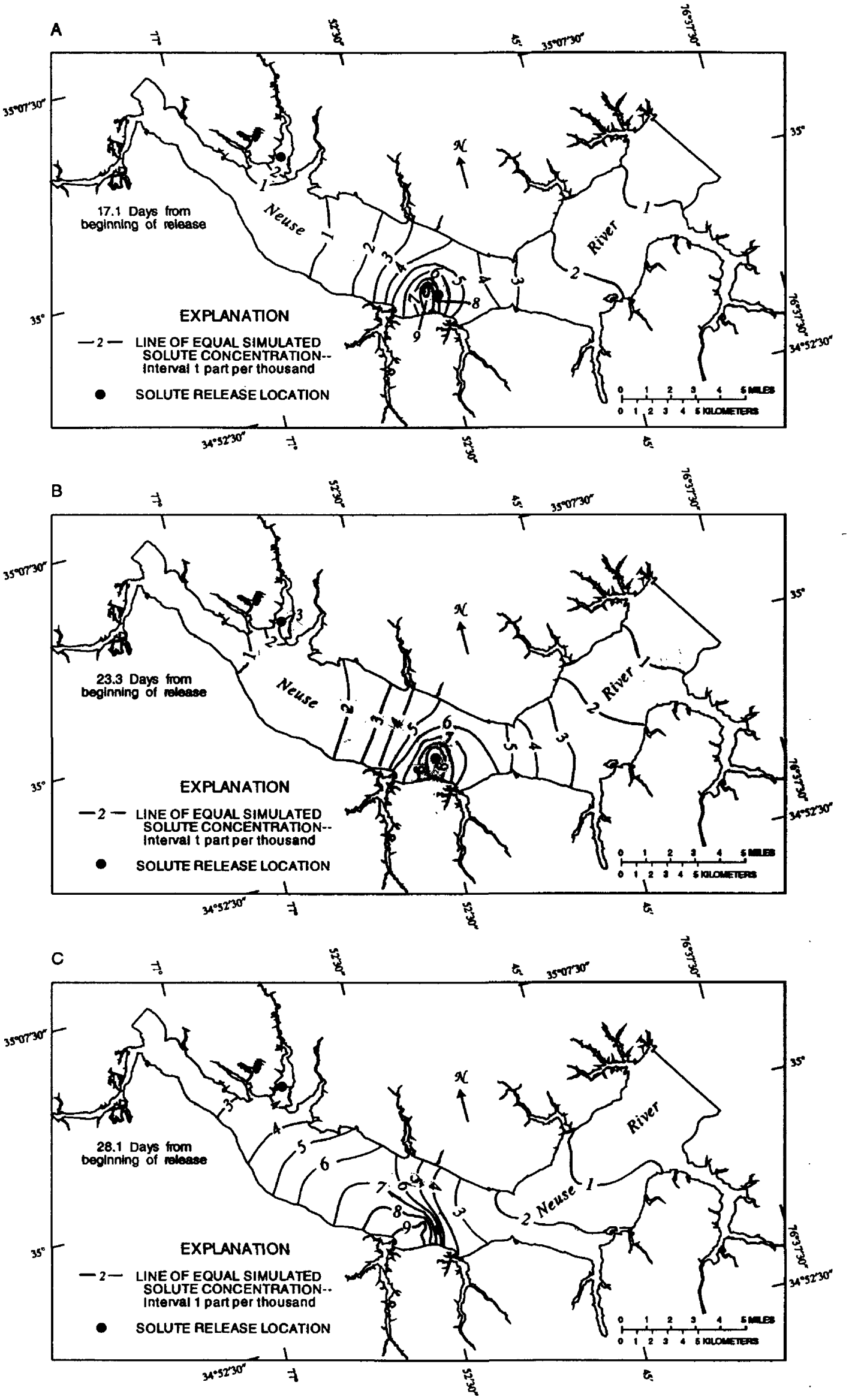

Figure 36. Simulated solute concentration in the Neuse River from two continuous releases at (A) 17.1 days, (B) 23.3 days, and (C) 28.1 days following release on May 1, 1991.

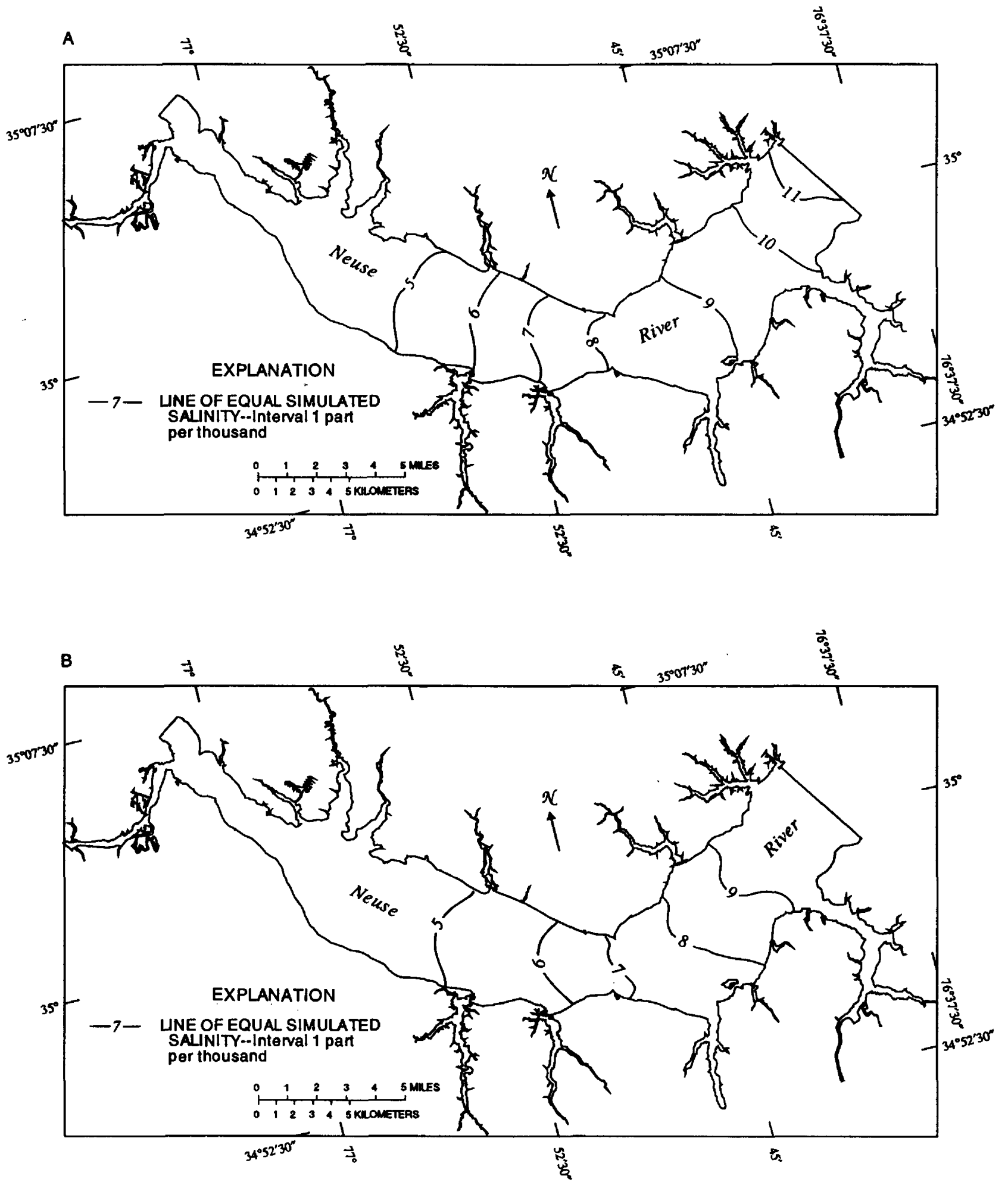

Figure 37. Lines of equal simulated salinity in the Neuse River for (A) October 25, 1989, at 1230 and (B) November 3, 1989, at 2400.

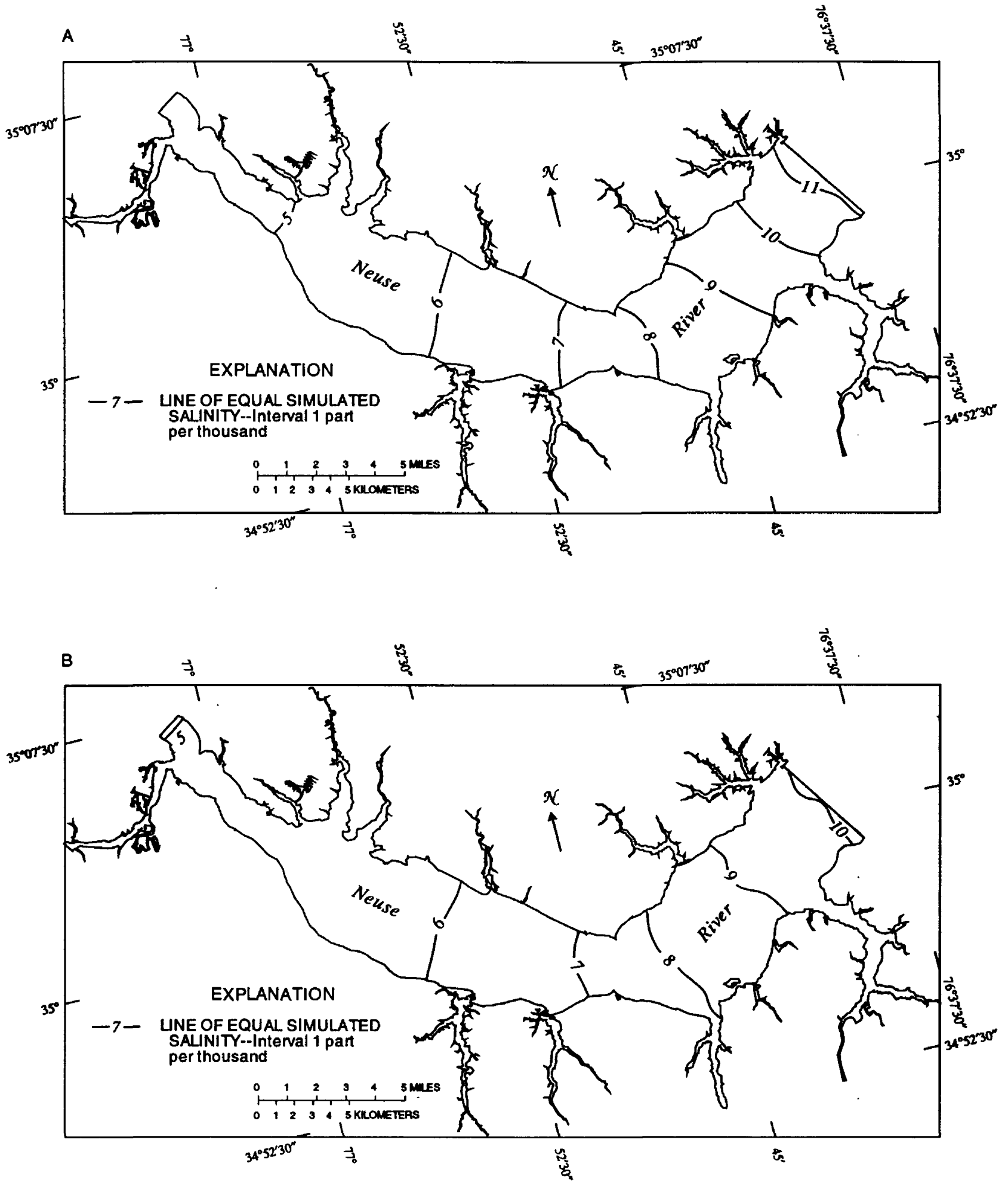

Figure 38. Lines of equal simulated salinity in the Neuse River for (A) September 8, 1991, at 2145 and (B) September 17, 1991, at 2400.

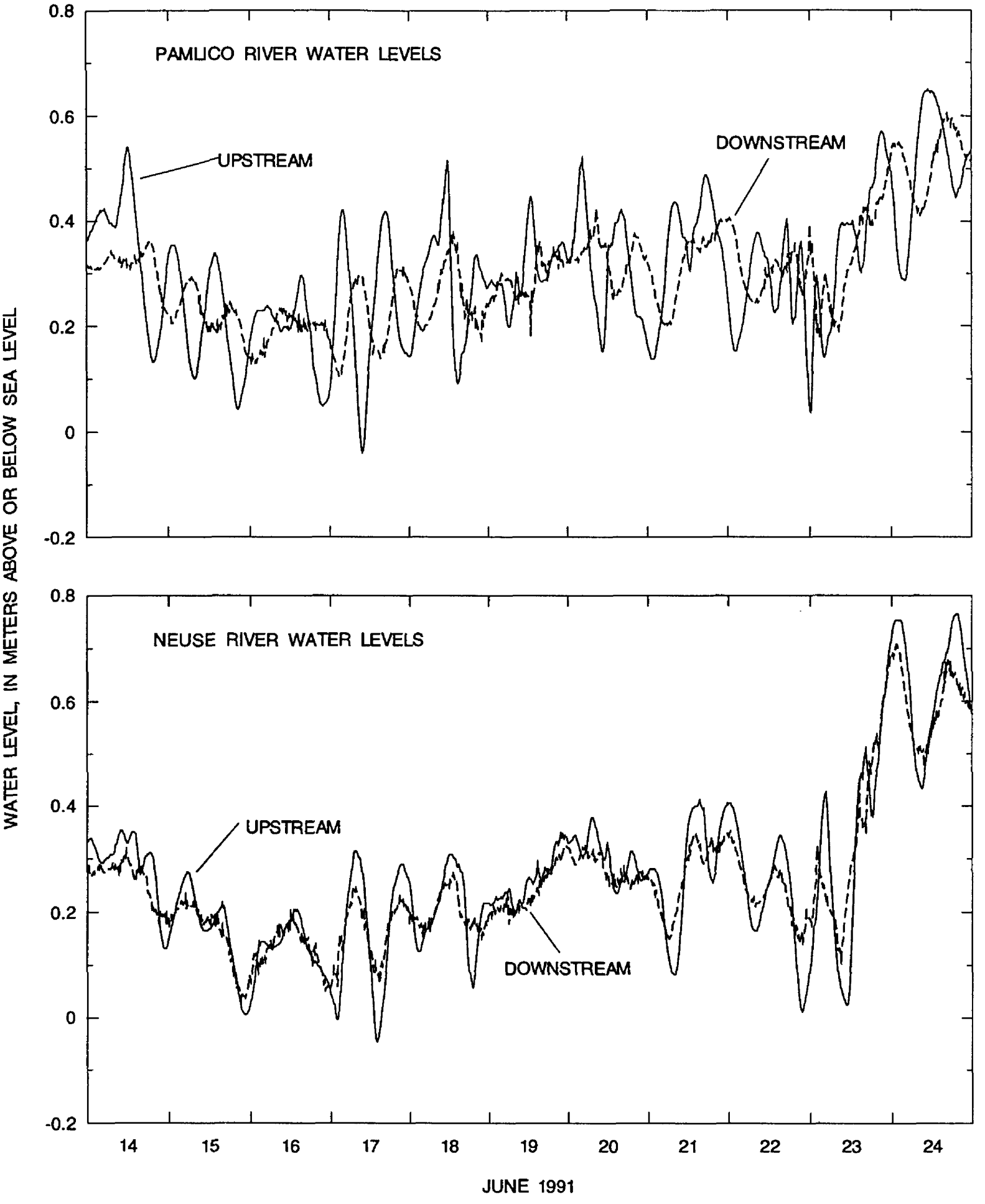

Figure 39. Measured water levels at the Pamlico and Neuse Rivers during June 14-24, 1991.

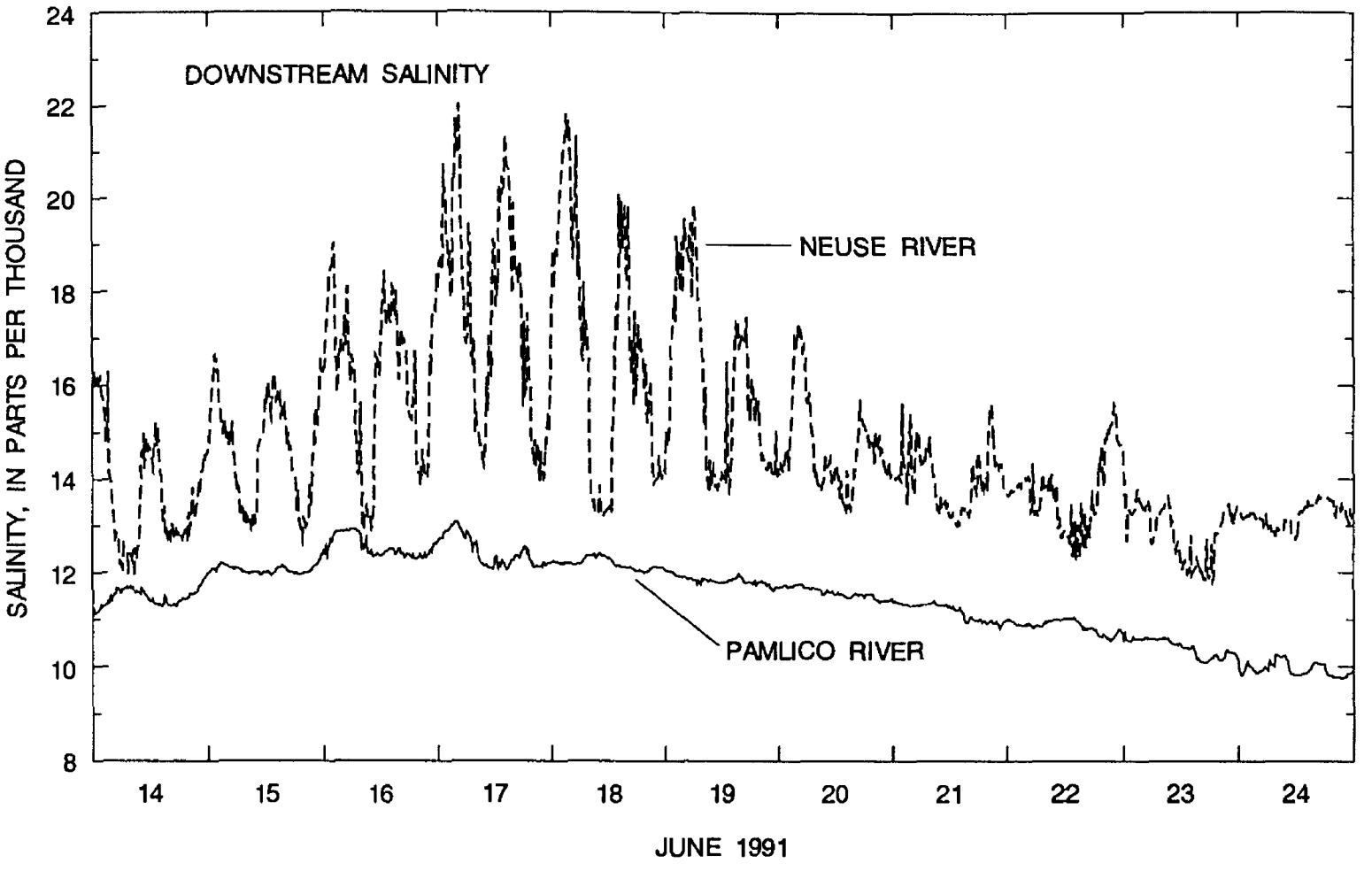

Figure 40. Average of measured downstream near-surface and near-bottom salinities at the Pamlico and Neuse Rivers during June 14-24, 1991.

perpendicular with the longitudinal axis of Pamlico Sound. The Neuse River study area extends about 40 km downstream from New Bern and varies in width from 1.5 km at the upper end to about 6 km at the downstream boundary. The longitudinal axis of the upper reach of the Neuse River estuary is oriented at an angle of about 146° east of north and the downstream reach (approximately perpendicular to the upstream reach) is oriented at an angle of 56° from north and in line with the longitudinal axis of Pamlico Sound. Maximum depths are greater in the Neuse River estuary, nearly 8 m as compared to about 6 m in the Pamlico River estuary. Each model applied the same set of model parameters, as described in the Model Implementation section of this report.

During the simulation period, wind directions were commonly aligned with the longitudinal axis of Pamlico Sound and the lower Neuse River estuary (fig. 41). Water-level fluctuations recorded in the Neuse River estuary were greater than those recorded in the Pamlico River estuary (fig. 39). Water levels at the downstream boundary of the Neuse River ranged from 0.034 to 0.707 m above sea level, whereas, water levels at the downstream boundary of the Pamlico River ranged from 0.104 to 0.604 m above sea level. These differences were magnified at the upper end of each estuary where water levels in the Neuse River ranged from 0.046 m below sea level to 0.765 m above sea level, but water levels in the Pamlico River ranged only from 0.040 m below sea level to 0.649 m above sea level. Water levels in both estuaries increased in response to the strong sustained winds blowing from the northeast along the axis of Pamlico Sound beginning June 23, with a significantly greater increase in water levels occurring in the Neuse River (fig. 39).

The flow and circulation patterns of the Neuse River estuary reflect the effects of greater water-level range and predominant wind patterns. The range in flow simulated at the mouth of the Neuse River estuary was nearly 25 percent greater than the range in flow simulated at the mouth of the Pamlico River estuary. Furthermore, flow in the upstream direction was more than 75 percent greater at the mouth of the Neuse River estuary than at the mouth of the Pamlico River estuary. Simulated instantaneous flow ranged from 6,360 m^3/s upstream to 4,240 m^3/s downstream at the mouth of the Neuse River estuary, and from

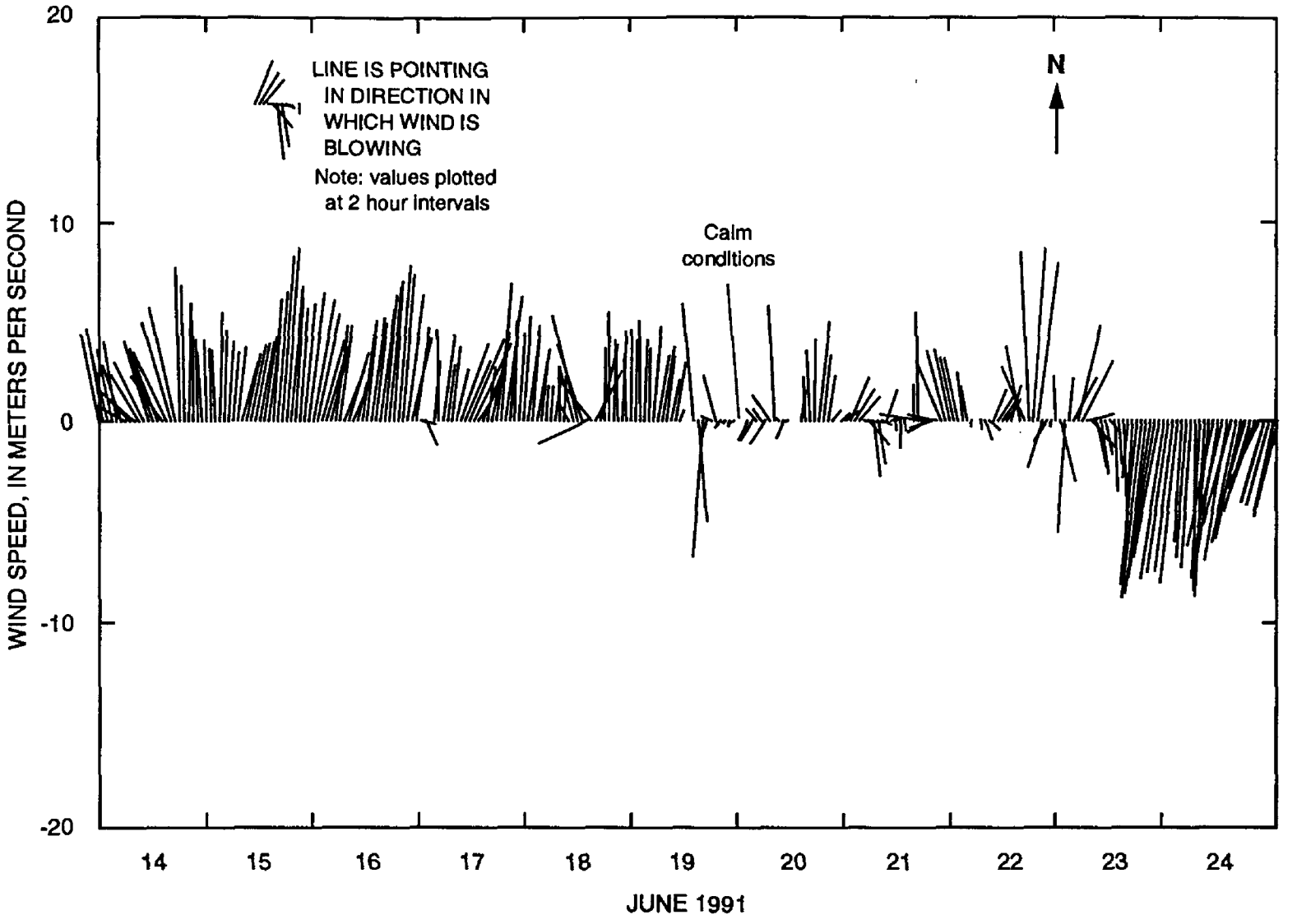

Figure 41. Measured wind speed and direction at Neuse River site W2 during June 14-24, 1991.

3,620 m^3/s upstream to 4,910 m^3/s downstream at the mouth of the Pamlico River estuary. The cumulative flow volume also was greater and more dynamic for the Neuse River than for the Pamlico River (fig. 42). Net movement of water into the estuary was in response to the net increase in water levels for both estuaries.

Simulated currents were generally much greater throughout most of the Neuse River estuary than in the Pamlico River estuary at similar points in the tide cycle. For example, circulation patterns near the middle of each estuary were different when water levels at the upstream boundaries were near a local maximum (fig. 43). In the Neuse River, where upstream and downstream boundary water levels were in phase, currents were predominantly downstream. In the Pamlico River, however, currents were much lower and in the upstream direction, possibly because boundary water levels were out of phase, and the downstream water levels were rising while the upstream water level was peaking. Likewise, circulation patterns near the mouth of each estuary were dissimilar when upstream and downstream water levels were equal and water levels were falling (fig. 44). Velocities were greater in the Neuse River, with the greatest velocities corresponding to the deep channel present just north of the center of the estuary. Bidirectional flow and areas of no movement were present in the Pamlico River, whereas flow in the Neuse River was almost exclusively downstream.

Four particles were tracked from the beginning to the end of the simulation to characterize differences in circulation patterns in time and space (fig. 45). Net movement in each estuary was small, with particles generally moving less than about 8 km. Path lengths, however, were somewhat greater in the Neuse River at the upper end of the estuary, indicating the potential for greater mixing and dispersion of solutes. Of particular interest in both estuaries was the lateral movement of particles. In some cases, particles returned to within a few kilometers of their original position after following a circuitous path for several days.

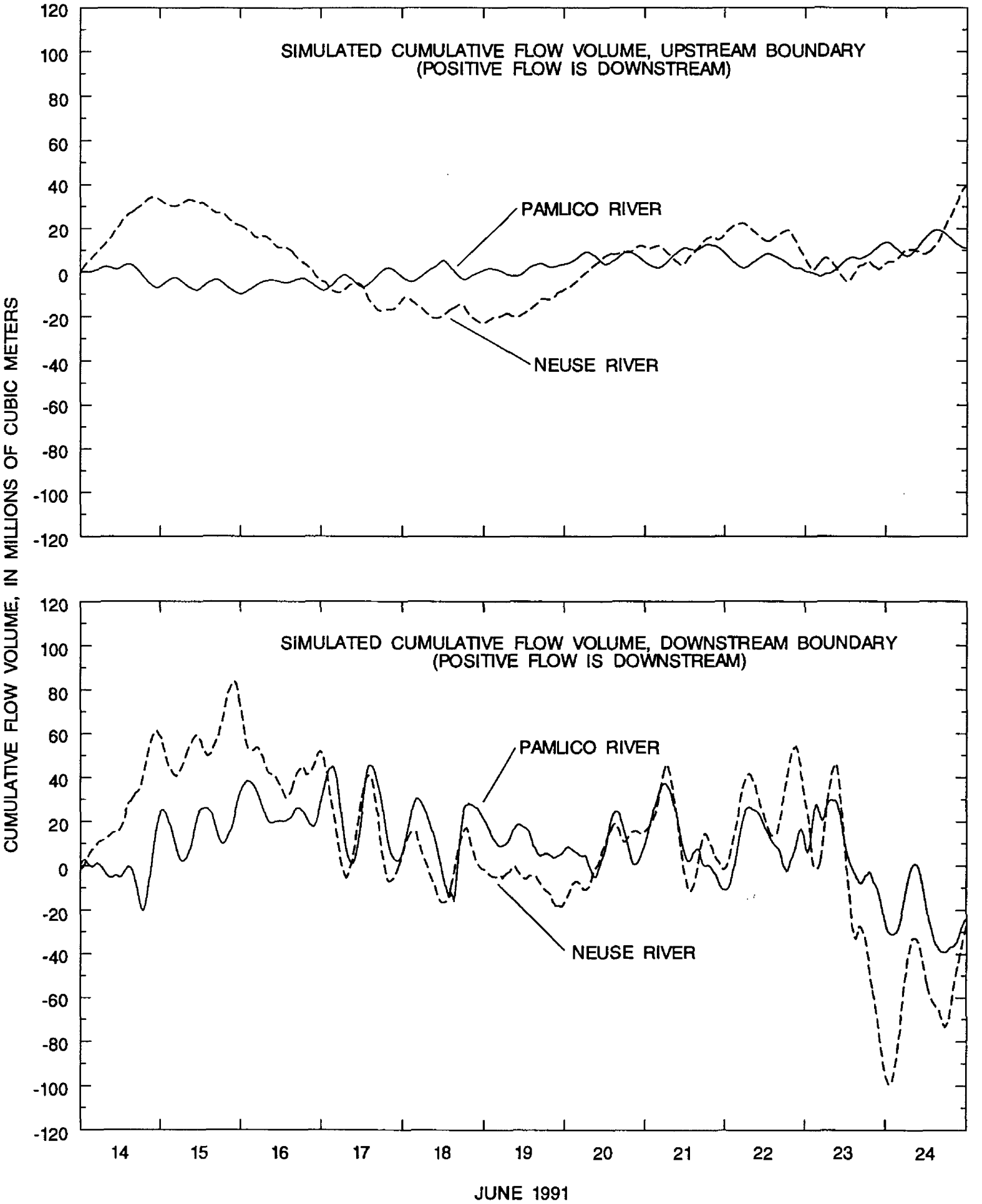

Figure 42. Simulated cumulative flow volume at the upstream and downstream model boundaries for the Pamlico and Neuse Rivers.

A. PAMLICO RIVER

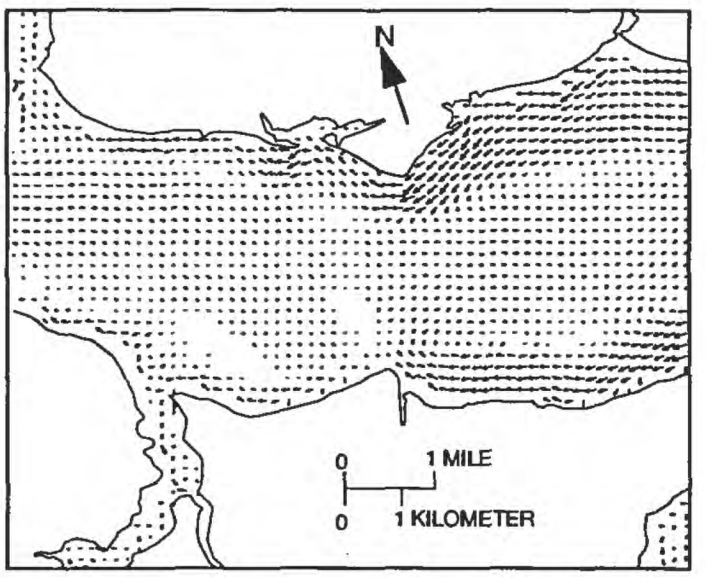

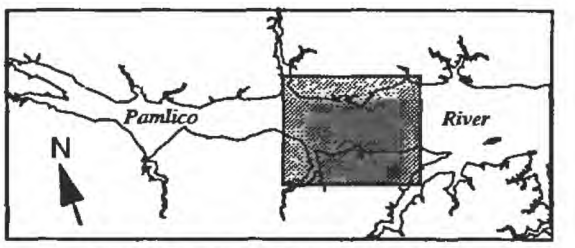

MID-PAMLICO RIVER ESTUARY

EXPLANATION

→ VECTOR--Head points in flow direction. Greater vector length represents greater relative velocity

B. NEUSE RIVER

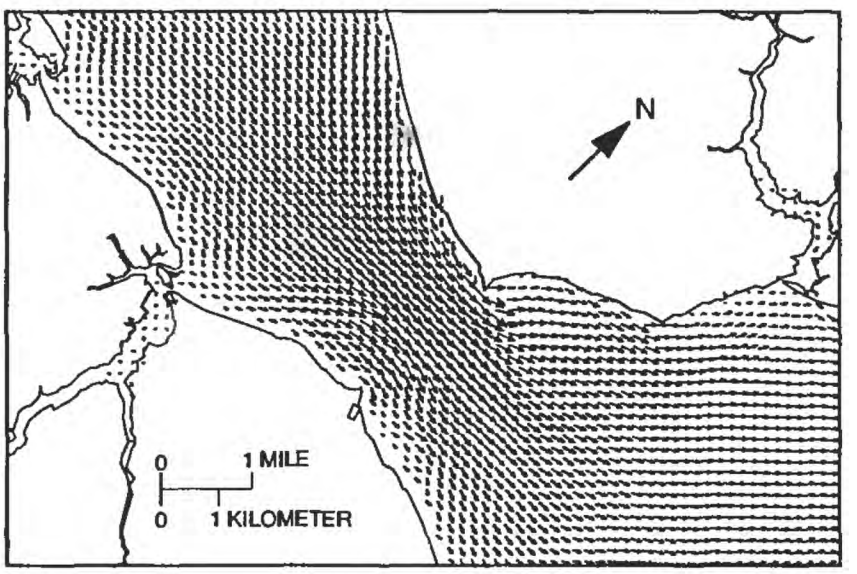

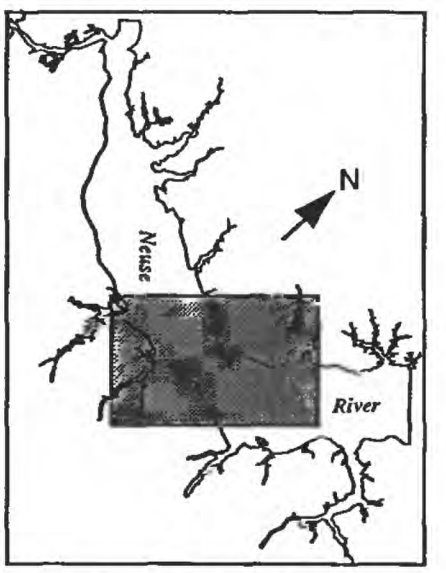

MID-NEUSE RIVER ESTUARY

Figure 43. Simulated circulation patterns near mid-estuary for the (A) Pamlico and (B) Neuse Rivers for high water at the upstream boundary.

A. PAMLICO RIVER

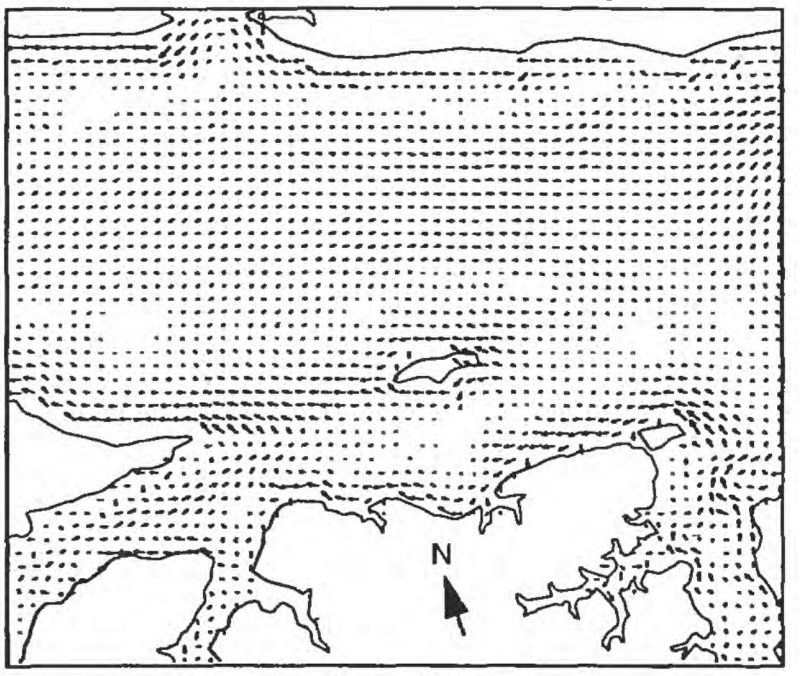

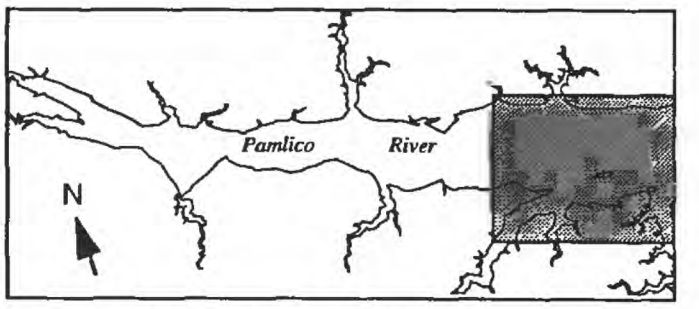

LOWER PAMLICO RIVER ESTUARY

EXPLANATION

→ VECTOR--Head points in flow direction. Greater vector length represents greater relative velocity

B. NEUSE RIVER

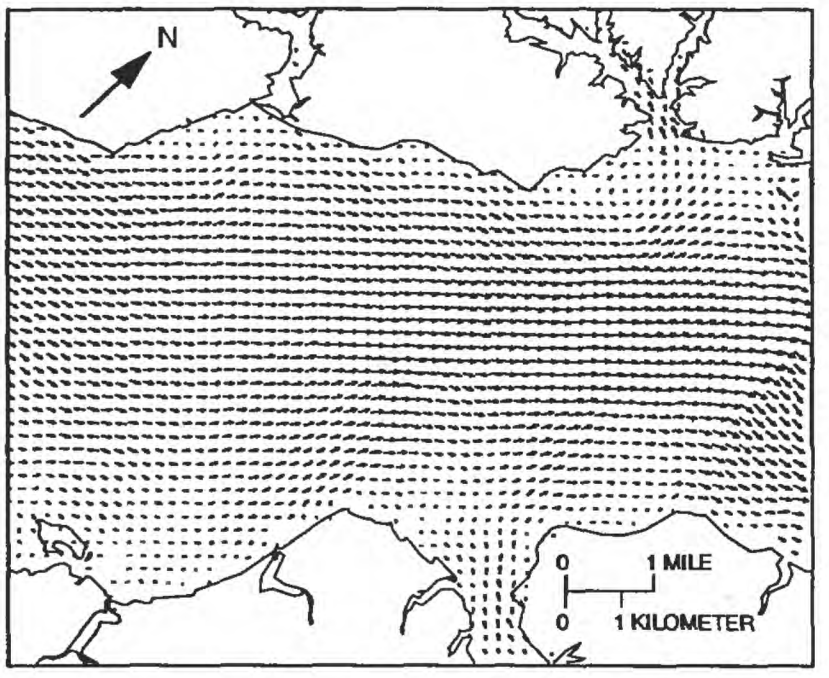

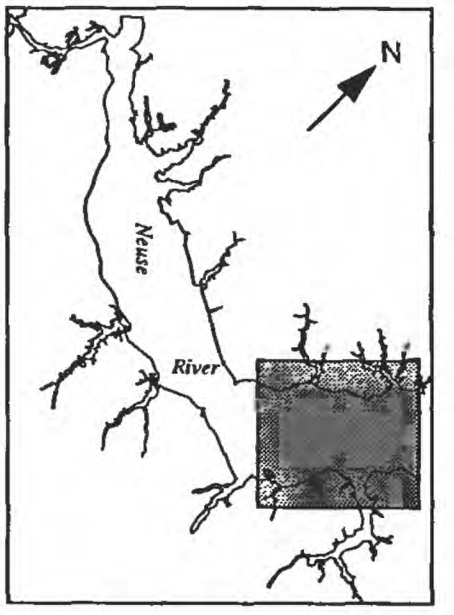

LOWER NEUSE RIVER ESTUARY

Figure 44. Simulated circulation patterns near the downstream boundary for the (A) Pamlico and (B) Neuse Rivers at a time when upstream and downstream water levels were falling.

A. PAMLICO RIVER

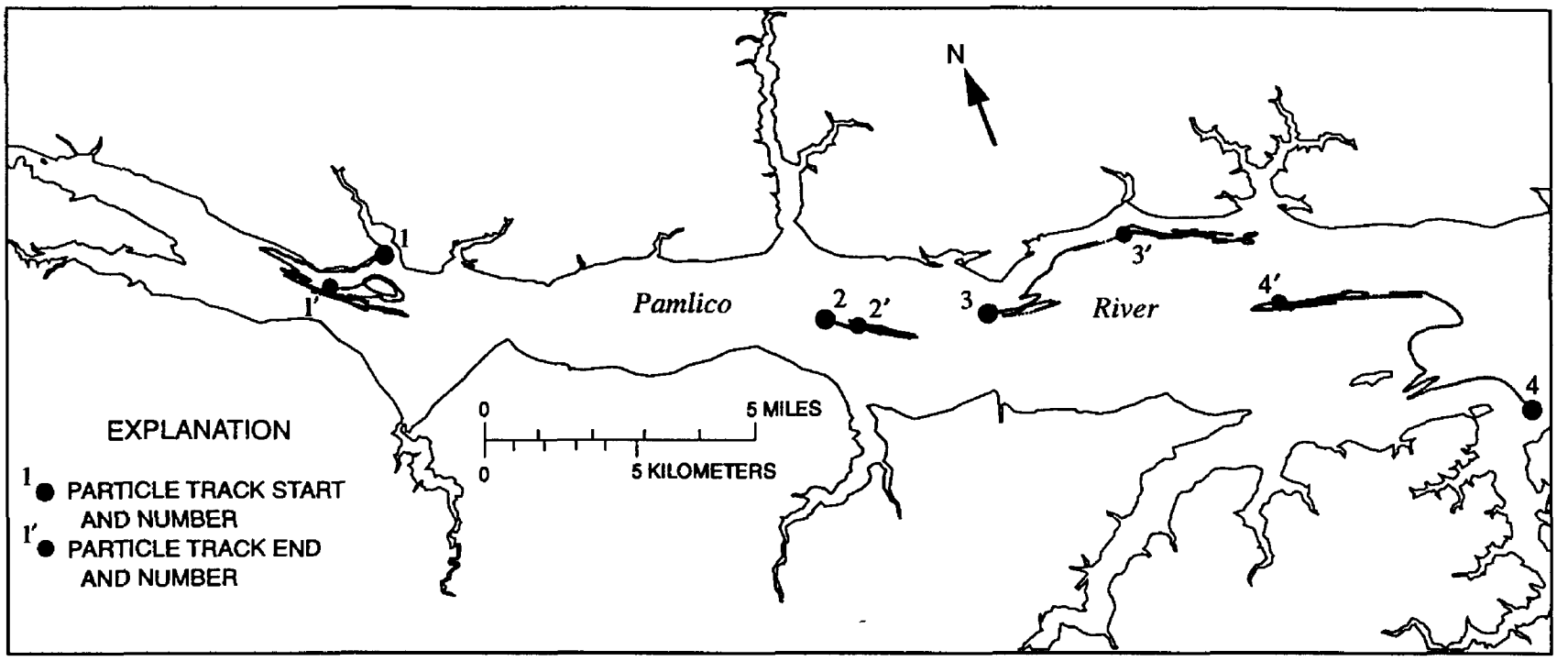

B. NEUSE RIVER

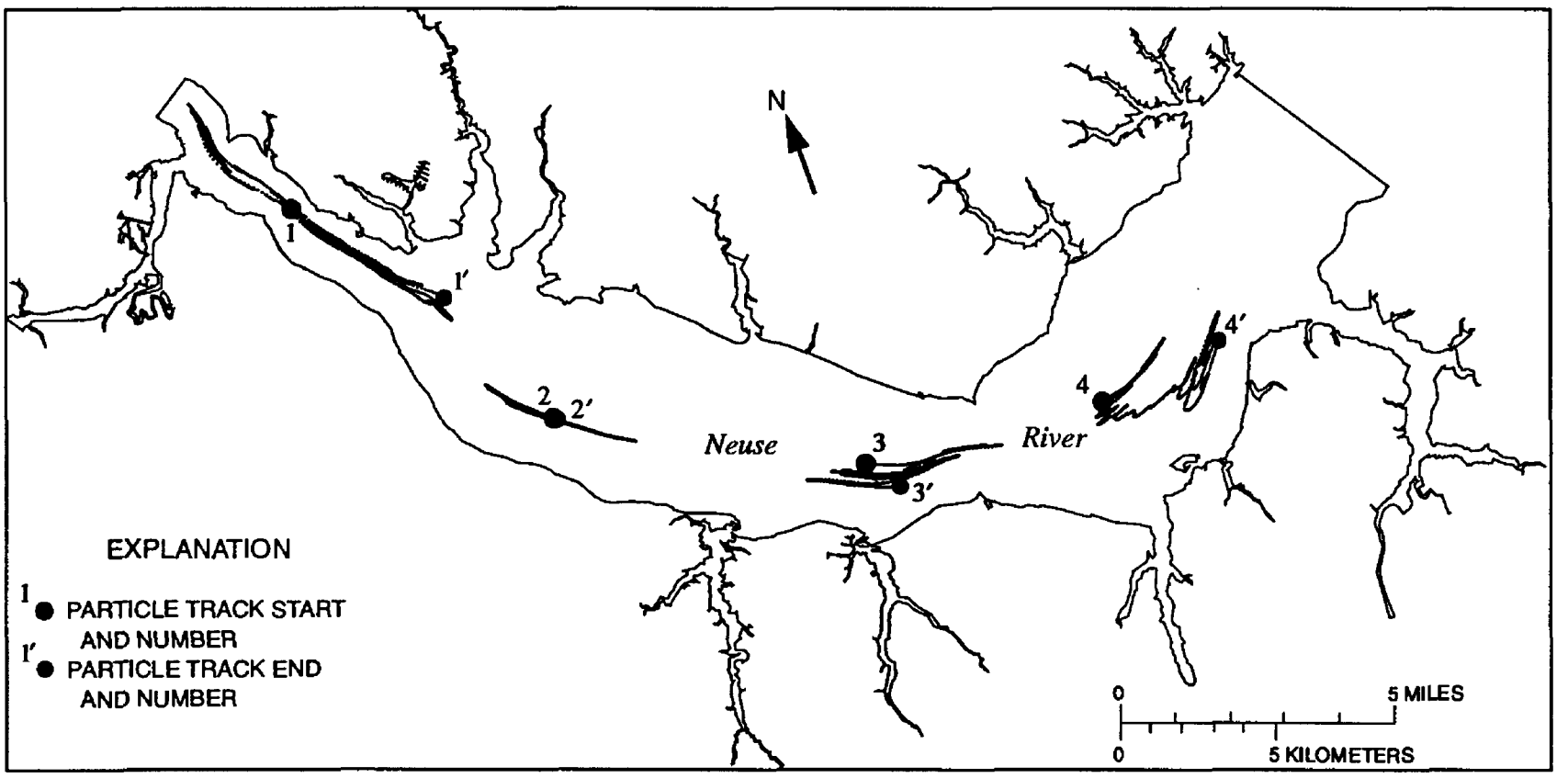

Figure 45. Simulated particle tracks in the (A) Pamlico and (B) Neuse Rivers for selected locations during the simulation period.

Conclusions

Data and model results demonstrate the complexity of the Neuse River estuary flow field. Currents vary temporally (fig. 11; table 9) and spatially. Currents can be simultaneously directed upstream in one segment of the estuary (fig. 28C) and downstream in another segment of the estuary (fig. 29C). Likewise, currents vary laterally. For example, currents can be simultaneously downstream near the shore and upstream near the center of the channel (fig. 29C).

Many of the characteristics of the flow field are related to the topographic features of the estuary. When flow reverses direction, currents near the shore, where depths are small, reverse direction before currents near the center of the channel, where depths and inertia are greater. Shoreline features and the large bend in the estuary also affect circulation patterns. Recirculation eddies form in the lee of points or promentories that extend into the estruary. Currents can often be greater near these topographic features because the flow must accelerate to move the greater distance around these points. Currents also are higher in the narrow section of the estuary near Cherry Point.

A spatially detailed hydrodynamic model is required to simulate the spatial heterogeneity of the Neuse River estuary flow field. The 200-m grid used in this study provides good lateral and longitudinal resolution of circulation, as well as solute transport. However, a spatially detailed three-dimensional model in which flow and transport are coupled is needed if the gravitational circulation in the estuary is to be accurately simulated. The lateral variation should be retained in the model if the effects of individual point- and nonpoint-source controls are to be evaluated.

Transport of solutes in the Neuse River estuary is generally quite slow. Materials can be retained in the estuary for several weeks with little net movement during the period (for example, particle 1, fig. 31). The net transport of a solute is very sensitive to the initial position (release point) of the material. Some particles can undergo a net upstream movement while others undergo a net downstream movement (for example, particles 3 and 4, fig. 31).

Flow rates in the estuary are quite large relative to mean freshwater inflows. Consequently, dilution of materials released to the estuary also can be large, provided the concentration of the released material in the estuary is initially low. For example, the solute released continuously for more than 4 weeks (fig. 36), on the south shore of the estuary, was diluted to less than 1 percent of the initial concentration except near the release point.

Although the model results presented in this report show good agreement with observations, some features of the model can be enhanced to provide additional, or perhaps improved, simulation results. As previously discussed, a three-dimensional model is needed to simulate gravitational circulation, as well as vertical gradients, which govern selected water-quality processes.

Better vertical control is needed at water-level gages to ensure that circulation is forced by accurate water-level gradients. Accurate water-level records are required for future applications of the model. Additionally, relocating the western model boundary upstream and forcing the model with measured flow at the upstream boundary rather than water level should improve results and alleviate the problem associated with internal consistency of water-level records. A sophisticated flow measurement device, such as an ultrasonic velocity meter, would be required to obtain reliable flow records. Also, as previously discussed, inflows from tidal creeks need to be added to the model if water-quality processes in the estuary are to be simulated. These inflows, however, are small relative to flows in the estuary, and the inflows do not affect circulation patterns.

SUMMARY

The physical, chemical, and biological characteristics of the Neuse River estuary, which extends from about Streets Ferry to Pamlico Sound, exhibit extreme spatial and temporal variability. The hydrodynamic processes in natural water bodies are key components of the complex aquatic ecosystem. The proper description of circulation is critical to the understanding and management of water quality, productivity, and distribution and abundance of biota in estuaries. Numerical models provide the capability of (1) describing physical and biochemical processes with high spatial resolution throughout the entire estuary and (2) conducting experiments by evaluating estuarine response to a wide range of imposed conditions. Scientifically credible and effective modeling requires carefully collected field measurements for use in model calibration, validation, and application.

The development of numerical models to characterize water circulation was identified as a high-priority goal of the Albemarle-Pamlico Estuarine Study. To address this need, the U.S. Geological Survey, in cooperation with the Albemarle-Pamlico Estuarine Study of the North Carolina Department of Environment, Health, and Natural Resources, conducted an investigation of hydrodynamics and transport in the Neuse River. The investigation included a detailed field-measurement program and the development and application of a physically realistic model of hydrodynamics and transport. The objectives of the modeling were to (1) provide a spatially detailed description of circulation and solute transport in the estuary, (2) develop the capability to compute bulk-flow rates, and (3) characterize the movement of passive materials in the estuary.

This report documents development and application of a two-dimensional, unsteady hydrodynamic and transport model for a reach of the Neuse River that extends 40 km downstream (east) from the U.S. Highway 17 bridge near New Bern. To provide the required information for the Neuse River estuary hydrodynamic model and to better define the physics of flow in the Neuse River, water level, salinity and water temperature, wind speed and direction, current velocity, and bathymetric data were collected from March 1988 through September 1992. Data from pre-existing, continuous-record streamflow gaging stations and meteorological stations also were available during this period.

During the study period, the mean daily water-level range was 0.186 m at site WL5 at the downstream end of the study reach and 0.292 m at site WL1 at the upstream end of the study reach. Although instantaneous differences in water level of as much as 0.3 m were observed throughout the study reach, the water-surface slope in the Neuse River was generally small, on the order of 10^{-6}.

Mean near-surface salinities ranged from 0.9 ppt at site S1 to 11.4 ppt at site S5, and mean near-bottom salinities ranged from 4.9 ppt at site S1 to 12.9 ppt at site S5. The difference between maximum observed and minimum observed salinity at each site ranged from 9.2 ppt at site S1 to 32.5 ppt at site S4. High salinities also were observed at site S1 at the upstream end of the estuary (9.2 ppt near the surface and 12.0 ppt near the bottom). Likewise, low salinities were observed at the downstream end of the estuary (1.3 ppt near the surface at site S5). Although overall observed variations in salinity were large at each site, daily variations were generally less than 3 ppt.

Winds generally were from the south, southwest, and west during the late spring and summer months. Wind speeds were greatest during the winter months. During December-May, wind speeds were greater than 9 m/s at least 10 percent of the time. Winds were lighter during June and August, with wind speeds less than 4.5 m/s about 37 percent of the time.

The long-term (1983-1992) average annual flow at Kinston, the downstream-most continuous-record streamflow station on the Neuse River, was 74.9 m^3/s. The estimated long-term average annual freshwater flow at New Bern was 124 m^3/s. The estimated annual average freshwater flow at New Bern during the study period ranged from 57 m^3/s in 1988 to 198 m^3/s in 1989.

During the 18-day period when current meters were deployed in the study reach, velocities ranged from a maximum downstream velocity of 48 cm/s to a maximum upstream velocity of 52 cm/s. The highest mean velocity occurred near the south bank at the mid-estuary section and near the north shore at the downstream section. Even at the relatively narrow, mid-estuary section where three meters were moored, there was a marked difference in currents across the estuary. Velocities were generally lower on the north side of the estuary than on the south side at the mid-estuary measurement section. At the downstream end of the study, velocities were greatest in the deepest part of the cross section.

Bathymetric data for the Neuse River estuary were obtained from the National Ocean Survey (NOS). Approximately one million soundings were recorded for the study reach. Additional depth points were digitized from the 1:40,000-scale NOS chart for the Neuse River. The 0-, 1.5-, and 3.0-m elevation contours around the study reach were digitized from 1:24,000-scale USGS topographic maps. Spot elevations that were below the 3.0-m contour also were digitized from the topographic maps to complete the bathymetry data base.

The modeling approach chosen for the Neuse River estuary was based on the objectives of the investigation, the observed physical characteristics of the estuary, and the time and funding constraints of the study. A two-dimensional, vertically averaged modeling approach was selected. This approach

allowed discretization of the estuary into small computational cells to provide spatially detailed information on velocity, circulation, and transport so that longitudinal and lateral movement of materials within the estuary could be simulated. Implementation of the hydrodynamic and transport model for the Neuse River included (1) development of the computational grid, (2) specification of model boundary conditions, (3) identification of initial conditions, and (4) selection of model parameters.

To determine the effects of grid size on model results, convergence testing was conducted prior to model calibration. Simulations of flow and transport in the Neuse River estuary were performed for three computational grid sizes: (1) 100 m x 100 m, (2) 200 m x 200 m, and (3) 400 m x 400 m. Simulated water levels were only slightly affected by changes in grid size. Likewise, the mean and maximum simulated salinity at each site did not change appreciably with grid size. Because of the relatively small differences in simulated results for the 100-m and the 200-m grids, and to minimize computational time based on the total number of computational cells in the model domain, the 200-m x 200-m grid size was selected for the Neuse River model.

Boundaries of the Neuse River model include the channel bottom, the shoreline and tributary streams, the water surface, a downstream (or eastern) open-water boundary, and an upstream (or western) open-water boundary near New Bern. The channel bottom was assumed to be an impermeable and immobile boundary, and was also assumed to cause resistance to the flow and thereby extract energy from the mean flow.

The shoreline is defined as a boundary across which there is no flow. The exact position of the shoreline may change during model simulation because of flooding or drying of computational-grid cells in response to water-level changes. Tributary streams were treated as closed-end embayments in the model.

Time series of observed water level and salinity are required at the open-water boundaries. Measured water levels and salinities were used to provide boundary data for the model. Measured near-surface salinity data were applied as the upstream boundary condition and near-surface and near-bottom salinities were averaged to provide a vertical-mean salinity for the downstream boundary condition. Boundary conditions at the 1-minute computational interval were linearly interpolated from the data collected at 15-minute intervals.

Momentum is transferred to the estuary by wind blowing over the water surface. Measured wind speed and direction were used for the water-surface boundary condition.

Initial velocity, water-level, and salinity conditions must be described for each computational cell prior to model simulations. The velocity in each computational cell is assumed to be zero at the beginning of each simulation. Initial salinity concentrations throughout the model domain were interpolated from measured salinities.

Five model parameters must be chosen prior to model simulations. These parameters include (1) the wind-stress coefficient, (2) a parameter that relates the direction of flow and the salinity gradient to the resistance coefficient, (3) the horizontal momentum mixing coefficient, (4) the isotropic mass-dispersion coefficient, and (5) a coefficient used to compute mass dispersion in the direction of flow.

Prior to calibration and validation of the Neuse River model, simulations were made for simplified conditions to evaluate model characteristics and the response of the Neuse River estuary to different forcings. The effects of additional open-water boundaries, baroclinic forcing, wind applied to the estuary surface, and varying the downstream water-level gage height were all analyzed; baroclinic forcing and gage height adjustment had the greatest effects on simulated transport.

The model was calibrated by adjusting model parameters for a period with complete time-varying data at all boundaries and at interior check points and was validated by using data collected during two separate periods. The model was calibrated and validated for (1) water levels ranging from -0.104 to 0.908 m, (2) salinities ranging from 2.8 to 22.0 ppt, and (3) wind speeds ranging from calm to 9 m/s. The model was tested for stratified and unstratified conditions. Mean simulated water levels minus observed water levels were less than 3 cm. The mean difference between simulated and observed salinities at the interior check point was less than 1 ppt. Daily variations in simulated salinities typically were not as large as observed variations. The magnitudes of simulated velocities were in good agreement with observations at the downstream measurement section, but simulated magnitudes were generally less than observed values at the mid-estuary section.

The sensitivity of model results to changes in model parameters and boundary conditions was analyzed. Simulated model results were most sensitive to the downstream water level and the value of wind-stress coefficient, but they were relatively insensitive to changes in other model parameters.

The calibrated model was applied to the Neuse River to simulate flows, circulation, and solute transport. Flows were simulated for the calibration period (June 1-24, 1991), the two validation periods (October 24-November 3, 1989, and September 1-30, 1991), and for May 1-30, 1991. For the calibration period, instantaneous simulated flows at New Bern ranged from 960 m^3/s upstream to 1,260 m^3/s downstream; flows ranged from 6,360 m^3/s upstream to 6,180 m^3/s downstream at the downstream boundary. The maximum simulated daily mean downstream flow at New Bern during the four simulation periods was 85 m^3/s, or about 68 percent of the estimated long-term daily mean freshwater inflow at New Bern. The simulations demonstrated the large variations in flow magnitude which can occur during a day and the sensitivity to time over which mean flow is determined. Flow also is highly nonuniform throughout the estuary, as reflected in daily maximum flows between upstream and downstream sections.

One of the results of each model simulation was a time sequence of velocity magnitude and direction for each computational cell, which can be used to examine detailed circulation patterns in areas of interest. As an example of the temporal and spatial complexity of circulation in the Neuse River, simulated velocity vectors for selected times corresponding to three water-level conditions during the October 24-November 3, 1989, simulation were presented. Downstream and upstream circulation patterns were simulated for falling and rising water levels, respectively, with recirculation eddies present near shoreline irregularities. More complex circulation patterns were simulated when water levels were nearly equal, resulting in large areas of zero velocity.

Particles were released at the beginning of each of four simulation periods and were tracked for the duration of each simulation. In some cases, there was little net movement of the particles; in other cases, particles moved in excess of 20 km. The results demonstrate the extreme spatial variation in the flow field at any given time, as well as the large difference in circulation patterns that can occur under different forcing conditions. The results also demonstrate the difficulty in identifying a realistic "flushing time" or "residence time" for materials in the estuary because of the great variations in circulation patterns and resulting transport.

The transport of a solute continuously released at two locations was simulated for a 30-day period to exhibit solute transport in the Neuse River and to further characterize circulation patterns. Discharges were located on the north side of the estuary near the mouth of Upper Broad Creek and on the south side of the estuary between Hancock and Slocum Creeks about 1.5 km into the channel. After 17 days of continuous release, the solute was present throughout most of the estuary with a concentration of 100 times dilution (10 ppt) near the source of the downstream discharge and 500 times dilution (2 ppt) present throughout an 18-km reach of the estuary.

Salinity was calculated for each computational cell at each time step during all simulations. Lines of equal salinity were generated for two periods (October 24-November 3, 1989, and September 1-30, 1991) to show differences in salinity distribution patterns under differing hydrologic conditions. For the 1989 period, salinity distributions at the beginning and at the end of the simulation period showed a net downstream movement of salt throughout the estuary. However, during September 8-17, 1991, there was upstream displacement in the uppermost reaches of the estuary and downstream movement in the lower part of the estuary. For all cases shown, lateral differences in salinity were present, with the largest gradients occurring near the shore and in the deeper sections of the estuary as a result of the lateral shear in currents.

Simulated circulation and transport for June 14 -24, 1991, indicate a greater range in transport in the Neuse River estuary than in the Pamlico River estuary, and cumulative transport over the simulation period was greater in the Neuse River. Similarly, particle tracks showed net movement of less than 8 km at each of the four sites in the Pamlico and Neuse Rivers, with particle tracks in the Neuse River showing somewhat greater total movement than those in the Pamlico River. Simulated currents were generally higher in the Neuse River than in the Pamlico River where boundary water levels were out of phase, as compared to the Neuse River where boundary water levels were in phase.

SELECTED REFERENCES

Abbott, M.B., McGowan, A., and Warren, I.R., 1981, Numerical modeling of free-surface flows that are two-dimensional in plan, *in* Fischer, H.B., ed., Transport models for inland and coastal waters: New York, Academic Press, p. 222-283.

Amein, M., and Airan, D.S., 1976, Mathematical modeling of hurricane surge in Pamlico Sound, North Carolina: Raleigh, North Carolina State University, University of North Carolina Sea Grant College Program, Report No. UNC-SG-76-12, 102 p.

Anwar, H.O., 1983, Turbulence measurements in stratified and well-mixed estuarine flows: Journal of Estuarine, Coastal, and Shelf Science, v. 17, p. 243-260.

Anwar, H.O., and Atkins, R., 1980, Turbulence measurements in simulated tidal flow: Journal of the Hydraulics Division, American Society of Civil Engineers, v. 106, no. HY8, p. 1273-1289.

Arakawa, A., 1966, Computational design of long-term numerical integration of the equations of fluid motion: I. Two-dimensional incompressible flow: Journal of Computational Physics, v. 1, no. 1, p. 119-143.

Bales, J.D., and Nelson, T.M., 1988, Bibliography of hydrologic and water-quality investigations conducted in or near the Albemarle Sounds region, North Carolina: U.S. Geological Survey Open-File Report 88-480, 148 p.

Bales, J.D., and Robbins, J.C., 1995, Simulation of hydrodynamics and solute transport in the Pamlico River estuary, North Carolina: U.S. Geological Survey Water-Resources Investigations Report 94-454, 85 p.

Beauchamp, C.H., and Spaulding, M.L., 1978, Tidal circulation in coastal seas, *in* Proceedings of the symposium on verification of mathematical and physical models in hydraulic engineering: New York, American Society of Civil Engineers, p. 518-528.

Bellis, V., O'Connor, M.P., and Riggs, S.R., 1975, Estuarine shoreline erosion in the Albemarle-Pamlico region of North Carolina: Raleigh, North Carolina State University, University of North Carolina Sea Grant College Program, Report No. UNC-SG-75-29, 67 p.

Benque, J., Cunge, J., Fevillet, J., Haugel, A., and Holly, F., 1982, New method for tidal current computation: Journal of the Waterways, Ports, and Coastal Ocean Division, American Society of Civil Engineers, v. 108, p. 396-417.

Chu, W.-S., Liou, J.-Y., and Flenniken, K.D., 1989, Numerical modeling of tide and current in central Puget Sound: Comparison of a three-dimensional and a depth-averaged model: Water Resources Research, v. 25, no. 4, p. 721-734.

Copeland, B.J., Hodson, R.G., Riggs, S.R., and Pendleton, E.C., 1984, The ecology of the Pamlico River, North Carolina—an estuarine profile: Washington, D.C., U.S. Fish and Wildlife Service, Report No. FWS/OBS-82/06, 83 p.

Creager, C.S., Baker, J.P., and North Carolina Division of Environmental Management, 1991, North Carolina's whole basin approach to water quality management—program description: Raleigh, North Carolina Department of Environment, Health, and Natural Resources, Water Quality Section, Report No. 91-08, 54 p.

Ditmars, J.D., Adams, E.E., Bedford, K.W., and Ford, D.E., 1987, Performance evaluation of surface water transport and dispersion models: Journal of Hydraulic Engineering, v. 113, no. 8, p. 961-980.

Douglas, J., 1955, On the numerical integration of $d^2u/dx^2 + d^2u/dy^2 = du/dt$ by implicit methods: Journal of the Society of Industrial Applied Mathematics, v. 3, no. 1, p. 42-65.

Eckert, C., 1958, The equation of state of water and sea water at low temperatures and pressures: American Journal of Science, v. 256, p. 240-250.

Elder, J.W., 1959, The dispersion of marked fluid in turbulent shear flow: Journal of Fluid Mechanics, v. 5, p. 544-560.

Garratt, J.R., 1977, Review of drag coefficients over oceans and continents: Monthly Weather Review, v. 105, p. 915-929.

Garrett, R.G., 1992, Water-quality data from continuously monitored sites in the Pamlico and Neuse River estuaries, North Carolina, 1990-91: U.S. Geological Survey Open-File Report 92-110, 196 p.

Garrett, R.G., and Bales, J.D., 1991, Water-quality data from continuously monitored sites in the Pamlico and Neuse River estuaries, North Carolina, 1989-90: U.S. Geological Survey Open-File Report 91-465, 151 p.

Garvine, R.W., 1985, A simple model of estuarine subtidal fluctuations forced by local and remote wind stress: Journal of Geophysical Research, v. 90, no. C6, p. 11945-11948.

Giese, G.L., and Bales, J.D., 1992, Two-dimensional circulation modeling of the Pamlico River estuary, North Carolina, *in* Spaulding, M.L., Bedford, K., Blumberg, A., Cheng, R., and Swanson, C., eds., Estuarine and coastal modeling: New York, American Society of Civil Engineers, p. 607-619.

Giese, G.L., Eimers, J.L., and Coble, R.W., 1991, Simulation of ground-water flow in the Coastal Plain aquifer system of North Carolina: U.S. Geological Survey Open-File Report 90-372, 178 p.

Giese, G.L., Wilder, H.B., and Parker, G.G., 1985, Hydrology of major estuaries and sounds of North Carolina: U.S. Geological Survey Water-Supply Paper 2221, 108 p.

Goodwin, C.R., 1987, Tidal-flow, circulation, and flushing changes caused by dredge and fill in Tampa Bay, Florida: U.S. Geological Survey Water-Supply Paper 2282, 88 p.

Gordon, C.M., and Dohne, C.F., 1973, Some observations of turbulent flow in a tidal estuary: Journal of Geophysical Research, v. 78, no. 12, p. 1971-1978.

Hamilton, P., 1992, Modeling nearshore currents in the vicinity of the Endicott Causeway, Alaska, *in* Spaulding, M.L., Bedford, K., Blumberg, A., Cheng, R., and Swanson, C., eds., Estuarine and coastal modeling: New York, American Society of Civil Engineers, p. 227-239.

Hardy, A.V., and Hardy, J.D., 1971, Weather and climate in North Carolina: Raleigh, North Carolina State University, Agricultural Experiment Station, Bulletin 396.

Harned, D.A., and Davenport, M.S., 1990, Water-quality trends and basin activities and characteristics for the Albemarle-Pamlico estuarine system, North Carolina and Virginia: U.S. Geological Survey Open-File Report 89-11, 164 p.

Horton, D.B., Kuenzler, E.J., and Woods, W.J., 1967, Current studies in the Pamlico River and estuary of North Carolina: Raleigh, The University of North Carolina Water Resources Research Institute, Report No. 6, 21 p.

Hunter, J.R., and Hearn, C.J., 1987, Lateral and vertical variations in the wind-driven circulation in long, shallow lakes: Journal of Geophysical Research, v. 92, no. C12, p. 13106-13114.

Ippen, A.I., 1966, Estuary and coastline hydrodynamics: New York, McGraw-Hill, Inc., 744 p.

Jarrett, J.T., 1966, A study of the hydrology and hydraulics of Pamlico Sound and their relation to the concentration of substances in the sound: Raleigh, North Carolina State University, Department of Civil Engineering, M.S. thesis, 156 p.

King, B., 1992, A predictive model of the currents in Cleveland Bay, *in* Spaulding, M.L., Bedford, K., Blumberg, A., Cheng, R., and Swanson, C., eds., Estuarine and coastal modeling: New York, American Society of Civil Engineers, p. 746-758.

Knowles, C.E., 1975, Flow dynamics of the Neuse River, North Carolina, for the period 7 August to 14 September, 1973: Raleigh, North Carolina State University, University of North Carolina Sea Grant College Program, Report No. UNC-SG-75-16, 18 p.

Large, W.G., and Pond, S., 1981, Open ocean momentum flux measurements in moderate to strong winds: Journal of Physical Oceanography, v. 11, p. 324-336.

Lean, G.H., and Weare, T.J., 1979, Modeling two-dimensional circulation flow: Journal of the Hydraulics Division, American Society of Civil Engineers, v. 105, no. HY1, p. 17-26.

Leendertse, J.J., 1972, A water-quality simulation model for well mixed estuaries and coastal seas—volume IV, Jamaica Bay tidal flows: Santa Monica, Calif., RAND Corp., Report No. R-1009-NYC.

_____1987, Aspects of SIMSYS2D, a system for two-dimensional flow computation: Santa Monica, Calif., RAND Corp., Report No. R-3572-USGS, 80 p.

Leendertse, J.J., and Gritton, E.C., 1971, A water-quality simulation model for well mixed estuaries and coastal seas—volume III, Jamaica Bay simulation: Santa Monica, Calif., RAND Corp., Report No. R-709-NYC.

Leendertse, J.J., Langerak, A., and de Ras, M.A.M., 1981, Two-dimensional tidal models for the Delta Works, *in* Fischer, H.B., ed., Transport models for inland and coastal waters: New York, Academic Press, p. 408-450.

Lung, W.S., 1988, The role of estuarine modeling in nutrient control: Water Science and Technology, 20 (6/7), p. 243-252.

Masch, F.D., and Brandes, R.J., 1975, Simulation of tidal hydrodynamics—Masonboro Inlet, *in* Proceedings of the symposium on modeling techniques: New York, American Society of Civil Engineers, p. 220-239.

Mendelsohn, D.L., and Swanson, J.C., 1992, Application of a boundary fitted coordinate transport model, *in* Spaulding, M.L., Bedford, K., Blumberg, A., Cheng, R., and Swanson, C., eds., Estuarine and coastal modeling: New York, American Society of Civil Engineers, p. 382-417.

Miller, R.L., Bradford, W.L., and Peters, N.E., 1988, Specific conductance—theoretical considerations and application to analytical quality control: U.S. Geological Survey Water-Supply Paper 2311, 16 p.

North Carolina Department of Natural Resources and Community Development, 1987, Albemarle-Pamlico Estuarine Study work plan: Raleigh, North Carolina Department of Natural Resources and Community Development, 77 p.

_____1989, Tar-Pamlico River basin nutrient sensitive waters designation and nutrient management strategy: Raleigh, North Carolina Department of Natural Resources and Community Development, Division of Environmental Management, Report No. 89-07, 40 p.

North Carolina Division of Environmental Management, 1993, Neuse River basinwide water quality management plan: Raleigh, North Carolina Department of Natural Resources and Community Development, Water Quality Section.

Partch, E.N., and Smith, J.D., 1978, Time dependent mixing in a salt wedge estuary: Journal of Estuarine and Coastal Marine Science, v. 6, p. 3-19.

Peaceman, D.W., and Rachford, H.H., 1955, The numerical solution of parabolic and elliptic differential equations: Journal of the Society of Industrial Applied Mathematics, v. 3, no. 1, p. 28-41.

Pietrafesa, L.J., Janowitz, G.S., Chao, T.-Y., Wiesberg, R.H., Askari, F., and Noble, E., 1986, The physical oceanography of Pamlico Sound: Raleigh, North Carolina State University, University of North Carolina Sea Grant College Program, Working Paper 86-5, 125 p.

Rader, D.N., Loftin, L.K., McGee, B.A., Dorney, J.R., and Clements, T.J., 1987, Surface-water concerns in the Tar-Pamlico River Basin: Raleigh, North Carolina Department of Natural Resources and Community Development, Division of Environmental Management, Report No. 87-04, 113 p.

Ridderinkhof, H., and Zimmerman, J.T.F., 1990, Mixing processes in a numerical model of the Western Dutch Wadden Sea, *in* Cheng, R.T., ed., Residual currents and long-term transport: New York, Springer-Verlag, Coastal and Estuarine Studies, v. 38, p. 194-209.

_____1992, Chaotic stirring in a tidal system: Science, v. 258, p. 1107-1111.

Riggs, S.R., Powers, E.R., Bray, J.T., Stout, P.M., Hamilton, C., Ames, D., Moore, R., Watson, J., Lucas, S., and Williamson, M., 1989, Heavy metal pollutants in organic-rich muds of the Pamlico River estuarine system—their concentration, distribution, and effects upon benthic environments and water quality: Raleigh, North Carolina Department of Environment, Health, and Natural Resources, Albemarle-Pamlico Estuarine Study, Project No. 89-06, 108 p.

Roache, P.J., 1982, Computational fluid dynamics: Albuquerque, N.M., Hermosa Publishers, 446 p.

Rodi, W., 1978, Mathematical modeling of turbulence in estuaries, *in* Nihoul, J.C.J., ed., Hydrodynamics of fjords and estuaries: Amsterdam, Elsevier Scientific Publishing Co., p. 14-26.

_____1987, Examples of calculation methods for flow and mixing in stratified fluids: Journal of Geophysical Research, v. 92, no. C5, p. 5305-5328.

Schaffranek, R.W., and Baltzer, R.A., 1988, A simulation technique for modeling flow on floodplains and in coastal wetlands, *in* Abt, S.R., and Gessler, J., eds., Hydraulic engineering—proceedings of the 1988 national conference: New York, American Society of Civil Engineers, p. 732-739.

Schmalz, R.A., 1985, User guide for WIFM-SAL—a two-dimensional vertically integrated, time-varying estuarine transport model: Vicksburg, Miss., U.S. Army Corps of Engineers, Waterways Experiment Station, Instruction Report EL-85-1, 44 p.

Schwartz, F.J., and Chestnut, A.F., 1973, Hydrographic atlas of North Carolina estuarine and sound waters, 1972: Raleigh, North Carolina State University, University of North Carolina Sea Grant College Program, Report No. UNC-SG-73-12, 132 p.

Shankar, N.J., Cheong, H.F., and Chen, C.T., 1992, Modeling of coastal circulation in Singapore waters—a hybrid approach, *in* Spaulding, M.L., Bedford, K., Blumberg, A., Cheng, R., and Swanson, C., eds., Estuarine and coastal modeling: New York, American Society of Civil Engineers, p. 669-683.

Signell, R.P., 1992, Tide- and wind-driven flushing of Boston Harbor, Massachusetts, *in* Spaulding, M.L., Bedford, K., Blumberg, A., Cheng, R., and Swanson, C., eds., Estuarine and coastal modeling: New York, American Society of Civil Engineers, p. 594-606.

Signell, R.P., and Butman, B., 1992, Modeling tidal exchange and dispersion in Boston Harbor: Journal of Geophysical Research, v. 97, no. C10, p. 15591-15606.

Stanley, D.W., 1988, Water quality in the Pamlico River estuary, 1967-1986—a report to Texasgulf Chemicals Company: Greenville, N.C., East Carolina University, Institute for Coastal and Marine Resources, ICMR Technical Report 88-01, 199 p.

Strickland, A.G., and Bales, J.D., 1993, Simulation of unsteady flow in the Roanoke River from near Oak City to Williamston, North Carolina: U.S. Geological Survey Water-Supply Paper 2408-A, 34 p.

Svendsen, H., Mikki, S.R., and Golmen, L.G., 1992, Frontal dynamics and circulation of the upper layer of a fjord system with complicated topography, *in* Spaulding, M.L., Bedford, K., Blumberg, A., Cheng, R., and Swanson, C., eds., Estuarine and coastal modeling: New York, American Society of Civil Engineers, p. 252-267.

Thomas, W.A., McAnally, W.H., and Letter, J.V., 1990, Generalized computer program system for open-channel flow and sedimentation; TABS system; volume 1: General overview; appendix f: user instructions for RMA-2V, a two-dimensional model for free-surface flows: Vicksburg, Miss., U.S. Army Corps of Engineers, Waterways Experiment Station, 54 p.

Thompson, D.B., 1992, Numerical methods 101—convergence of numerical models, *in* Jennings, M., and Bhowmik, N.G., eds., Hydraulic engineering; saving a threatened resource—in search of solutions: New York, American Society of Civil Engineers, p. 398-403.

Treece, M.W., Jr., 1993, Hydrologic and water-quality data in selected agricultural drainages in Beaufort and Hyde Counties, North Carolina, 1990-92: U.S. Geological Survey Open-File Report 93-78, 96 p.

Treece, M.W., Jr., and Bales, J.D., 1992, Hydrologic and water-quality data in selected agricultural drainages in Beaufort and Hyde Counties, North Carolina, 1988-90: U.S. Geological Survey Open-File Report 92-498, 89 p.

U.S. Geological Survey, 1988-92, Water resources data, North Carolina, water-years 1988-92: U.S. Geological Survey Water-Data Report (published annually).

van Dam, G.C., 1988, Models of dispersion, *in* Kullenberg, G., ed., Pollutant transfer and transport in the sea—volume I: Cleveland, Ohio, CRC Press, p. 91-160.

Watanabe, M., Harleman, D.R.F., and Vasiliev, O.F., 1983, Two- and three-dimensional mathematical models for lakes and reservoirs, *in* Orlob, G.T., ed., Mathematical modeling of water quality—streams, lakes, and reservoirs: New York, John Wiley & Sons, International Series on Applied Systems Analysis, v. 12, p. 274-336.

Weare, T.J., 1979, Errors arising from irregular boundaries in ADI solutions of the shallow-water equations: International Journal for Numerical Methods in Engineering, v. 14, p. 921-931.

Weisberg, K.H., and Pietrafesa, L.J., 1983, Kinematics and correlation of the surface wind field in the South Atlantic Bight: Journal of Geophysical Research, v. 88, no. C8, p. 4593-4610.

Wells, J.T., 1989, A scoping study of the distribution, composition, and dynamics of water-column and bottom sediments—Albemarle-Pamlico estuarine system: Morehead City, N.C., North Carolina Department of Natural Resources and Community Development, Albemarle-Pamlico Estuarine Study, Project No. 89-05, 39 p.

Wells, J.T., and Kim, S.Y., 1991, Trapping and escape of fine-grained sediments: Neuse River estuary, North Carolina, *in* Krause, N.C., Gingerrich, K.J., and Kriebel, D.L., eds., Coastal sediments '91—proceedings of special conference on quantitative approaches to coastal sediment processes: Seattle, Wash., American Society of Civil Engineers, p. 775-788.

Westerink, J.J., and Gray, W.G., 1991, Progress in surface water modeling: Reviews of Geophysics, Supplement, U.S. National Report to International Union of Geodesy and Geophysics, 1987- 90, p. 210-217.

Wilder, H.B., Robinson, T.M., and Lindskov, K.L., 1978, Water resources of northeast North Carolina: U.S. Geological Survey Water Resources Investigations 77-81, 113 p.

Williams, A.B., Posner, G.S., Woods, W.J., and Duebler, E.E., 1967, A hydrographic atlas of larger North Carolina sounds: Morehead City, N.C., University of North Carolina, Institute of Marine Sciences, Report No. UNC-SG-73-02, 129 p.

Winner, M.D., and Coble, R.W., 1989, Hydrogeologic framework of the North Carolina Coastal Plain aquifer system: U.S. Geological Survey Open-File Report 87-690, 155 p.

Woods, W.J., 1969, Current study in the Neuse River and estuary of North Carolina: Raleigh, The University of North Carolina Water Resources Research Institute, Report No. UNC-WRRI-69-13, 35 p.

Wu, J., 1969, Wind stress and surface roughness at air-sea interface: Journal of Geophysical Research, v. 74, no. 2, p. 444-445.

Yeh, H.H., Chu, W.-S., and Dahlberg, O., 1988, Numerical modeling of separation eddies in shallow water: Water Resources Research, v. 24, no. 4, p. 607-614.